Distribution Agreement

In presenting this thesis or dissertation as a partial fulfillment of the requirements for an advanced degree from Emory University, I hereby grant to Emory University and its agents the non-exclusive license to archive, make accessible, and display my thesis or dissertation in whole or in part in all forms of media, now or hereafter known, including display on the world wide web. I understand that I may select some access restrictions as part of the online submission of this thesis or dissertation. I retain all ownership rights to the copyright of the thesis or dissertation. I also retain the right to use in future works (such as articles or books) all or part of this thesis or dissertation.

Signature

_____ _____

Michelle M. Giddens Date

PROTECTIVE ACTIONS OF THE BRAIN-EXPRESSED RECEPTORS GPR37 AND GPR37L1 IN MODELS OF NEUROLOGICAL DISEASE

By

Michelle M. Giddens

Doctor of Philosophy
Division of Biological and Biomedical Science
Neuroscience

_____

Randy A. Hall
Advisor

_____

A
Victor Faundez, MD, PhD

_____

B
Thomas Kukar, PhD

_____

C
Malu Tansey, PhD

_____

D
Stephen Traynelis, PhD

Accepted:

_____

Lisa A. Tedesco, Ph.D.
Dean of the James T. Laney School of Graduate Studies

_____

Date

PROTECTIVE ACTIONS OF THE BRAIN-EXPRESSED RECEPTORS GPR37 AND GPR37L1 IN MODELS OF NEUROLOGICAL DISEASE

By

Michelle M. Giddens

B.S. Worcester State University, 2008

Advisor: Randy A. Hall

An abstract of
A dissertation submitted to the faculty of the
James T. Laney School of Graduate Studies of Emory University
in partial fulfillment of the requirements for the degree of
Doctor of Philosophy
in the Division of Biological and Biomedical Science
Neuroscience
2017

Abstract

PROTECTIVE ACTIONS OF THE BRAIN-EXPRESSED RECEPTORS GPR37 AND GPR37L1 IN MODELS OF NEUROLOGICAL DISEASE

By

Michelle M. Giddens

G protein-coupled receptors (GPCRs) are essential for cellular communication. In the central nervous system, GPCRs serve as the molecular targets for many neurotransmitters, neuropeptides, and neuromodulators. Therefore, it is not surprising that GPCRs are essential for most physiological processes and their dysfunction contributes to the etiology of many disease states and disorders. Furthermore, GPCRs constitute one of the largest classes of drug targets in the body. While the functions of many GPCRs are well characterized, a subset of GPCRs remain poorly understood. These receptors have the potential to increase understanding of basic biology, and/or serve as novel therapeutic targets. Here, we present evidence that GPR37 and GPR37L1, a pair of closely related receptors that are predominantly expressed in the brain, exert protective actions in models of seizure and stroke.

My colleagues and I demonstrated that a variant in *GPR37L1* is associated with a novel human progressive myoclonic epilepsy. We also found that loss of *Gpr37L1* leads to increased seizure susceptibility in two seizure induction models. Additionally, we demonstrated that loss of GPR37 increases seizure susceptibility and loss of both Gpr37 and Gpr37L1 in double knockout (DKO) mice leads to an even more dramatic effect, suggesting loss of both receptors is synergistic.

In separate studies, we demonstrated that expression of GPR37 is dramatically elevated in the penumbra following ischemia, and that loss of GPR37 results in increased infarct volume in a focal cerebral ischemia model. Conversely, GPR37L1 expression was significantly reduced following ischemic insult in WT mice, but not GPR37$^{-/-}$ mice suggesting a compensatory relationship between the two receptors *in vivo*. The results of these studies also demonstrated that loss of GPR37 results in attenuated HIF1α and GFAP expression following ischemia. Finally, astrocytes cultured from *Gpr37*$^{-/-}$ mice were found to be more susceptible to an in vitro model of stroke.

The findings described in this dissertation provide evidence that GPR37 and GPR37L1 function as protective receptors in the central nervous system in seizure models and a cerebral ischemia model. These observations mark GPR37 and GPR37L1 as novel therapeutic targets for the treatment of epilepsy, stroke and other neurological disorders.

PROTECTIVE ACTIONS OF THE BRAIN-EXPRESSED RECEPTORS GPR37 AND GPR37L1 IN MODELS OF NEUROLOGICAL DISEASE

By

Michelle M. Giddens

B.S. Worcester State University, 2008

Advisor: Randy A. Hall

A dissertation submitted to the faculty of the
James T. Laney School of Graduate Studies of Emory University
in partial fulfillment of the requirements for the degree of
Doctor of Philosophy
in the Division of Biological and Biomedical Science
Neuroscience
2017

ACKNOWLEDGEMENTS

Over the past six years I have received support and encouragement from many individuals. I would like to acknowledge and thank my advisor Dr. Randy Hall for his guidance and support. I would also like to thank my dissertation committee of Victor Faundez, Thomas Kukar, Malu Tansey, and Stephen Traynelis for their input, advice and support as I moved from an idea to a completed dissertation.

Additionally, I would like to thank my colleagues in the Hall lab and beyond, and my collaborators, Jennifer Wong, Brilee Smith, Emily Farrow, Becky Meyer, Sharon Owino, Duc Duong, Jason Schroeder, Sarah Soden, Carol Saunders, J.B. LePichon, David Weinshenker, Andrew Escayg, Xiaohuan Gu, Michael Jiang, Shan Ping Yu, Ling Wei, all of whom provided their expertise to help drive the research described in this document.

TABLE OF CONTENTS

LIST OF FIGURES

LIST OF TABLES

LIST OF ABBREVIATIONS

7TM.....7-TRANSMEMBRANE

AC .....ADENYLYL CYCLASE

ACMG .....AMERICAN COLLEGE OF MEDICAL GENETICS

ADAM.....A DISINTEGRIN AND METALLOPROTEINASE

AED .....ANTI-EPILEPTIC DRUGS

AP.....ANTERIOR-POSTERIOR

AR-JP.....AUTOSOMAL RECESSIVE JUVENILE PARKINSONISM

ASD.....AUTISM SPECTRUM DISORDER

BBB.....BLOOD-BRAIN BARRIER

BCA.....BICINCHONINIC ACID

CAMP.....CYCLIC ADENOSINE MONOPHOSPHATE

CCA .....COMMON CAROTID ARTERY

CCAO.....COMMON CAROTID ARTERY OCCLUSION

CLR.....CALCITONIN-LIKE RECEPTOR

CMH.....CHILDREN'S MERCY HOSPITAL

CRAP.....COMMON REPOSITORY OF ADVENTITIOUS PROTEINS

CRE.....CAMP RESPONSE ELEMENT

CSF.....CEREBRAL SPINAL FLUID

CT.....C-TERMINUS

D1R.....DOPAMINE D1 RECEPTOR

D2R.....DOPAMINERGIC D2 RECEPTOR

DA.....DOPAMINE

DAG .....DIACYLGLYCEROL

DAT.....DOPAMINE TRANSPORTER

DHH.....DESERT HEDGEHOG

DKO.....DOUBLE KNOCKOUT

DRG.....DORSAL ROOT GANGLION

DTT.....DITHIOTHREITOL

EPAC.....EXCHANGE FACTOR DIRECTLY ACTIVATED BY CAMP

ETB.....ENDOTHELIN B

EV.....EMPTY VECTOR

FDR.....FALSE DISCOVERY RATE

G PROTEINS.....GUANINE-NUCLEOTIDE-BINDING REGULATORY PROTEINS

GA .....G PROTEIN A-SUBUNIT

GABA.....γ-AMINOBUTYRIC ACID

GDH.....GLUTAMATE DEHYDROGENASE

GDP.....GUANOSINE DIPHOSPHATE

GFAP.....GLIAL ACIDIC FIBRILLARY PROTEIN

GLI2.....GLIOMA-ASSOCIATED ONCOGENE FAMILY ZINC FINGER 2

GPCR.....G PROTEIN-COUPLED RECEPTOR

GPS.....GPCR PROTEOLYTIC SITE

GRKS.....G PROTEIN-COUPLED RECEPTOR KINASES

GS .....GLUTAMINE SYNTHETASE

GTCS.....GENERALIZED TONIC-CLONIC SEIZURE

GTP.....GUANOSINE TRIPHOSPHATE

HA.....HEAD ACTIVATOR

HIF1A.....HYPOXIA INDUCIBLE FACTOR 1A

IAA.....IODOACETIMIDE

IBA1.....IONIZED CALCIUM-BINDING ADAPTER MOLECULE 1

ID .....INTERNAL DIAMETER

IP3.....INOSITOL 1,4,5-TRISPHOSPHATE

IRB.....INSTITUTIONAL REVIEW BOARD

KO.....KNOCKOUT

LDH.....LACTATE DEHYDROGENASE

LOF.....LOSS-OF-FUNCTION

MAF.....MINOR ALLELE FREQUENCY

MAG.....MYELIN ASSOCIATED GLYCOPROTEIN

MAPK.....MITOGEN-ACTIVATED PROTEIN KINASE

MCAO.....MIDDLE CEREBRAL ARTERY OCCLUSION

MJ.....MYOCLONIC JERK

ML.....MEDIAL-LATERAL

MMP.....MATRIX METALLOPROTEASE

MUPP1.....MULTI-PDZ DOMAIN PROTEIN 1

NFAT.....NUCLEAR FACTOR OF ACTIVATED T-CELLS

NT.....N-TERMINUS

OGD.....OXYGEN GLUCOSE DEPRIVATION

OGD/R.....OXYGEN GLUCOSE DEPRIVATION/REPERFUSION

OPC.....OLIGODENDROCYTE PRECURSOR CELLS

PAELR.....PARKIN-ASSOCIATED ENDOTHELIN RECEPTOR-LIKE RECEPTOR

PI3K.....PHOSPHOINOSITIDE 3 KINASE

PICK1.....PROTEIN INTERACTING WITH C-KINASE

PIP2 .....PHOSPHATIDYLINOSITOL 4,5-BISPHOSPHATE

PKA.....PROTEIN KINASE A

PLC.....PHOSPHOLIPASE C

PME.....PROGRESSIVE MYOCLONUS EPILEPSY

PSMS.....PEPTIDE SPECTRUM MATCHES

RAMP.....RECEPTOR ACTIVITY-MODIFYING PROTEINS

RGS.....REGULATORS OF PROTEIN SIGNALING

RHOGEFS.....RHOGTPASE NUCLEOTIDE EXCHANGE FACTORS

RS .....RACINE SCORE

RT.....ROOM TEMPERATURE

SC.....SERTOLI CELL

SDS-PAGE.....SODIUM DODECYL SULFATE POLYACRYLAMIDE GEL ELECTROPHORESIS

SH3..... ....SRC HOMOLOGY 3

SHH..... .....SONIC HEDGEHOG

SMO.....SMOOTHENED

SRE.....SERUM RESPONSE ELEMENT

T2R .....TASTE2 RECEPTOR

TAPI.....TUMOR NECROSIS FACTOR–A PROTEASE INHIBITORS

TPA.....TISSUE PLASMINOGEN ACTIVATOR

TTC.....2,3,5-TRIPHENYLTETRAZOLIUM CHLORIDE

WT.....WILD-TYPE

CHAPTER 1:

Introduction to G Protein-Coupled Receptors

1.1 Cell Communication: Role of GPCRs

1.1.1 Discovery of GPCRs

The ability for cells to communicate with one another is essential for all aspects of life. Effective communication requires a means for converting information into a transmissible signal, a method for receiving the signal, and the ability to transfer information into the cell where it can be acted upon. Signaling molecules come in a diverse variety of forms and include neurotransmitters, hormones, lipids, peptides, proteins, and sensory molecules. Receptors for extracellular signals classically reside at the cell surface and upon ligand binding, change conformation, inducing intracellular signaling cascades.

Of the vast array of surface receptors, G protein-coupled receptors (GPCRs) are the largest and most abundant family of receptors, contributing to nearly all physiological processes (Bjarnadottir et al. 2006). Since the purification and cloning of rhodopsin in 1983 (Nathans & Hogness, Cell, 1983) and the β2 adrenergic receptor in 1986 (Dixon et al. 1986), followed by the subsequent homology cloning of additional adrenergic (Kobilka et al. 1987; Lefkowitz and Caron 1990) and serotonin receptors (Fargin et al. 1988), more than 800 GPCRs have been identified (Fredriksson and Schioth 2005; Fredriksson et al. 2003; Munk et al. 2016). All GPCRs share a core structural homology, consisting of seven transmembrane (7TM) helices, an extracellular N-terminus (NT), and intracellular C-terminal domain (CT).

1.1.2 GPCR Classification

Further classification of the GPCR superfamily based on sequence homology and phylogenetic analysis yields five main subfamilies, Glutamate, Rhodopsin, Adhesion, Frizzled/Taste2 and Secretin (Fredriksson et al. 2003). The Rhodopsin family, also commonly referred to as class A (Kolakowski 1994), is named for the first 7TM receptor identified, rhodopsin, the visual receptor for light (Hargrave et al. 1983; Ovchinnikov Iu et al. 1983). Approximately 90% of all GPCRs are members of the Rhodopsin family, more than half of which are olfactory receptors (Munk et al. 2016). While receptors in the Rhodopsin family typically have a short NT, their 7TM configuration and ligand preference are quite heterogeneous (Lagerstrom and Schioth 2008).

The Secretin family of GPCRs contains 15 members, all of which contain an extracellular hormone-binding domain and bind peptide hormones. Secretin family members share relatively high homology, and contain several conserved residues (Lagerstrom and Schioth 2008). Contrary to the Rhodopsin receptors, much of the variation within the Secretin family occurs in the NT domain. The Adhesion family is the second largest family of GPCRs in humans, containing roughly 4% of all GPCRs. Adhesion receptors contain a variety of functional domains and nearly all members have long and diverse N-termini (Bjarnadottir et al. 2004). The most characteristic feature of Adhesion GPCRs is the GPCR proteolytic site (GPS) domain which acts as an intracellular autocatalytic processing resulting in two non-covalently attached fragments of the receptor

(Krasnoperov et al. 1997). The Adhesion and Secretin families are often categorized together into class B type receptors (Kolakowski 1994).

In addition to eight metabotropic glutamate receptors, the Glutamate, or class C, family of GPCRs includes $GABA_B$ receptors, calcium-sensing receptors, taste receptors and seven orphan receptors (Bjarnadottir, Fredriksson, and Schioth 2005). Glutamate family members share two unique features, they possess an unusually large extracellular NT domain containing a Venus flytrap motif, and they form constitutive dimers (Rondard et al. 2011). The last family of receptors, the Frizzled/Taste2 receptors are also referred to as class F and T, respectively (Kolakowski 1994). The Frizzled family consists of 10 Frizzled receptors and Smoothened, originally identified in drosophila (Vinson and Adler 1987; Chang et al. 1994). Frizzled family members are atypical in that their canonical signaling is non-G protein mediated (Schulte 2010). The Taste2 receptor (T2R) subfamily consists of 25 bitter taste receptors. Contrary to the Type 1 taste receptors, which are a part of the Glutamate family, the T2Rs are most closely related to the rhodopsin family.

1.1.3 GPCR Signaling

GPCRs display an extensive variety of structural domains, respond to a diverse assortment of ligands, and induce diverging and complex intracellular signaling cascades, however all GPCRs share a common mechanism for transducing signals across the plasma membrane. As their name implies, G protein-coupled receptors interact with intracellular heterotrimeric guanine-

nucleotide-binding regulatory proteins (G proteins), which serve as mediators of GPCR activation. G protein complexes are composed of three subunits, α, β, and γ. Upon ligand binding, GPCRs shift into a favorable conformation for G protein binding, this conformational change promotes the release of bound guanosine diphosphate (GDP) from the G protein α-subunit (Gα) allowing guanosine triphosphate (GTP) to bind. Exchange of GDP for GTP is driven by a high intracellular concentration of GTP (McKee et al. 1999). GTP binding leads to a conformational change of Gα, causing dissociation of the β/γ subunit which in turn allows both functional subunits to associate with and modulate the activity of downstream effectors (Gilman 1987; Mahoney and Sunahara 2016).

Each G-protein subunit exists in multiple forms. Assembly of different combinations of G protein subunits into heterotrimers can result in distinct intracellular changes. Humans have 15 different types of Gα, which are commonly grouped into four categories, G_s, G_i, G_q and G_{12} (Pierce, Premont, and Lefkowitz 2002; Syrovatkina et al. 2016). The G_s family of receptors contains $G\alpha_s$ and $G\alpha_{olf}$. $G\alpha_s$ is ubiquitously expressed whereas $G\alpha_{olf}$ is mostly restricted to olfactory neurons. Depending on the type of G protein to which the receptor is coupled, a variety of downstream signaling pathways can be activated. Coupling of $G\alpha_s$ family members stimulates adenylyl cyclase, leading to an increase in cAMP which in turn activates protein kinase A (PKA), a serine/threonine kinase with diverse cellular functions, and in some cells can activate cAMP-gated ion channels (Kaupp and Seifert 2002) and exchange factor directly activated by cAMP (EPAC) proteins.

The G_i family is the largest and most diverse family, it includes $G\alpha_{i1\text{-}3}$, $G\alpha_o$, $G\alpha_t$, $G\alpha_g$, and $G\alpha_z$. $G\alpha_i$ proteins are found in most cell types, while $G\alpha_o$ is predominantly expressed in the brain. $G\alpha_t$ and $G\alpha_g$ mediate sensory information and are found in visual and taste receptor cells, respectively. $G\alpha_z$ is expressed in the brain and in platelet cells. Contrary to $G\alpha_s$-mediated signaling, $G\alpha_i$ family members inhibit adenylyl cyclase and the production of cAMP.

The human $G\alpha_q$ family consists of $G\alpha_q$, $G\alpha_{11}$, $G\alpha_{14}$, and $G\alpha_{16}$. $G\alpha_q$ and $G\alpha_{11}$ are ubiquitously expressed, while the remaining family members have restricted expression patterns. $G\alpha_q$ proteins activate phospholipase C (PLC), an enzyme that cleaves phosphatidylinositol 4,5-bisphosphate (PIP2) into diacylglycerol (DAG) and inositol 1,4,5-trisphosphate (IP3). Both DAG and IP3 serve multiple important functions within the cell, including the elevation of intracellular Ca^{2+} and activation of Protein Kinase C.

Both family members of the G_{12} family, $G\alpha_{12}$ and $G\alpha_{13}$, are ubiquitously expressed (Pierce, Premont, and Lefkowitz 2002; Syrovatkina et al. 2016). $G\alpha_{12}$ family proteins are most known for activating RhoGTPase nucleotide exchange factors (RhoGEFs), which are important for regulating intracellular actin dynamics. In addition to the classical signaling pathways described, G proteins are involved in regulating multiple downstream effectors including a variety of metabolic enzymes and ion channels (Neves, Ram, and Iyengar 2002; Pierce, Premont, and Lefkowitz 2002; Syrovatkina et al. 2016).

There is considerable diversity among the β/γ subunit as well. Of the five types of Gβ, Gβ1 -4 are widely expressed, while Gβ5 is mainly restricted to the brain. Similarly, half of the 12 Gγ family members are widely expressed, while the other half have restricted expression in the brain and/or sensory cells (Syrovatkina et al. 2016). Release of the β/γ subunit upon association of GTP with the bound α subunit, can induce distinct downstream signaling. The β/γ subunit can act on multiple second messengers including, inward rectifying potassium channels, Voltage-gated Ca^{2+} channels, AC, PLC, Phosphoinositide 3 Kinases (PI3Ks) and Mitogen-Activated Protein Kinases (MAPKs) (Khan et al. 2013).

Efficient signal transduction requires a mechanism for regulation and termination of signaling. RGS proteins, named for their regulators of protein signaling (RGS) domain, stimulate the intrinsic GTPase activity of Gα subunits, reducing the duration that Gα can interact with effectors (Watson et al. 1996; De Vries et al. 2000). Signal refinement also occurs at the receptor level through desensitization, internalization and down-regulation. Receptor desensitization is primarily achieved via receptor phosphorylation. While activity-independent phosphorylation by second messenger-regulated protein kinases occurs, desensitization is largely mediated by G protein-coupled receptor kinases (GRKs). In addition to facilitating receptor GEF activity, the conformational change induced by ligand binding may expose GRK phosphorylation sites on the receptor (Premont, Inglese, and Lefkowitz 1995). GRK phosphorylation promotes the recruitment of ß-arrestin and the subsequent internalization of the receptor

(Lohse et al. 1990; Goodman et al. 1996). Internalized receptors are either dephosphorylated and recycled to the cell surface where they can begin a new round of signaling or targeted for degradation. Internalization is typically thought to halt receptor signaling, however emerging evidence suggests at least some GPCRs may continue to signal from endosomes (Tsvetanova, Irannejad, and von Zastrow 2015). Sustained receptor activation may lead to a down-regulation or a reduction in receptor number (Tsao and von Zastrow 2000).

GPCRs were originally thought to act as a simple switch, interacting with a specific G protein and shifting into the active confirmation when ligand was present. It is now clear that receptors can adopt multiple active receptor conformations, each with unique G protein coupling and downstream signaling cascades (Wisler et al. 2014). Further signaling complexity is generated by ligand induced signaling via ß-arrestin. In addition to promoting receptor desensitization and internalization, ß-arrestins can stimulate distinct signaling pathways (Luttrell et al. 1999). ß-arrestins signal to many downstream effectors, most notably, MAPK (DeWire et al. 2007; Smith and Rajagopal 2016). Subsequent studies determined that certain ligands are capable of selectively signaling through either ß-arrestin or G proteins without activating the other (Violin and Lefkowitz 2007). The ability of GPCRs to signal through various G proteins and non-G protein mediated pathways creates the remarkable functional diversity of GPCRs that is essential for most biological processes.

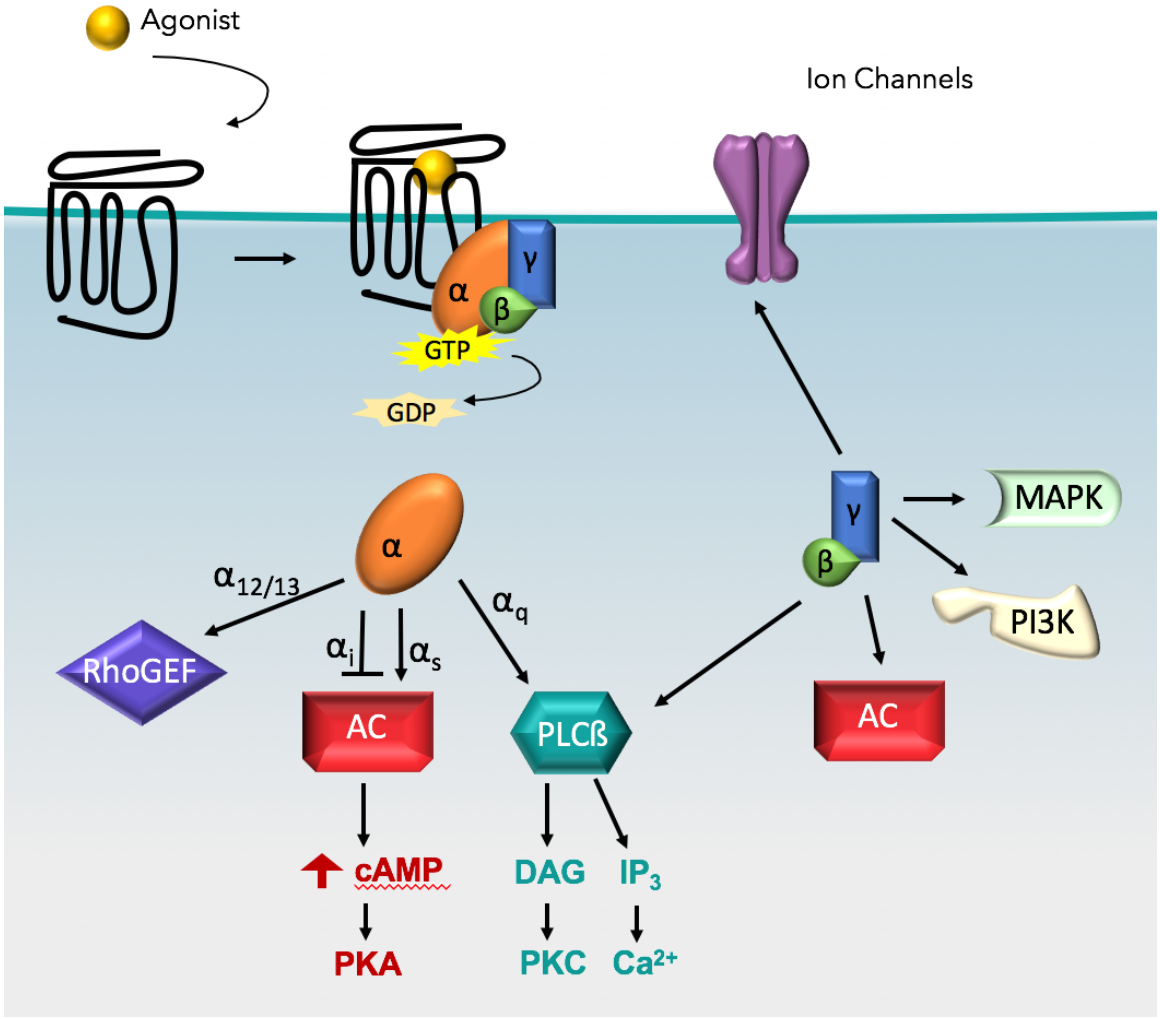
Agonist
Ion Channels
γ
α
β
GTP
GDP
α
γ
β
MAPK
PI3K
$\alpha_{12/13}$
α_q
α_i
α_s
RhoGEF
AC
PLCß
AC
cAMP
DAG
IP_3
PKA
PKC
Ca^{2+}

Figure 1-1. Canonical Signaling Pathways Regulated by Gα and Gβγ Subunits

Schematic representation of classical GPCR signaling via Gα and Gßγ subunits. Upon dissociation of the Gßγ subunits from Gα, individual subunits initiate diverse signaling cascades. $G\alpha_s$ is most known for adenylyl cyclase (AC) stimulation leading to an increase in cytosolic cAMP. Conversely, $G\alpha_i$ inhibits AC reducing cytosolic cAMP. $G\alpha_q$ activates phospholipase C (PLC) which results in increased intracellular Ca^{2+} and activation of PKC, and $G\alpha_{12/13}$ activates RhoGEF. Gßγ subunits are most known for their signaling to various ion channels, PLC, AC, PI3K, and MAPK leading to diverse responses within the cell.

1.1.4 Common GPCR Interacting Partners

GPCR localization, pharmacology, and signal transduction, can be further fine-tuned by a variety of additional interacting partners (Ritter and Hall 2009; Magalhaes, Dunn, and Ferguson 2012). Thus far, GPCR signaling has been discussed in terms of a single GPCR binding a ligand and interacting with intracellular effectors. However considerable evidence indicates GPCRs can form physical associations with other receptors (Bouvier 2001; Ferre et al. 2014; Bulenger, Marullo, and Bouvier 2005). Dimerization of duplicate (homodimerization) or unrelated receptors (heterodimerization) has been shown to affect receptor expression, trafficking, ligand binding, G protein coupling, downstream signaling and regulation (Terrillon and Bouvier 2004). Many examples of functional GPCR oligomers have been described, including the members of the Glutamate family (Kniazeff et al. 2011).

GPCR interactions extend beyond formation of receptor pairs and oligomers. Interactions with PDZ proteins have been shown to affect receptor localization, stability, signaling, and regulation (Magalhaes, Dunn, and Ferguson 2012; Dunn and Ferguson 2015). PDZ proteins contain one or more PDZ domains, named for the first three proteins in which they were discovered: Postsynaptic density protein 95, Discs large, and Zonula occludens protein 1. PDZ domains bind specific PDZ motifs at the extreme CT of interacting partners, including GPCRs. PDZ proteins often act as scaffolds, capable of tethering

multiple proteins into complexes and modulating receptor function (Magalhaes, Dunn, and Ferguson 2012; Dunn and Ferguson 2015).

Receptor activity-modifying proteins (RAMPs) provide another important example of proteins that interact with GPCRs to modify their function. The RAMP family consists of three members, RAMP 1-3, which are single-pass transmembrane proteins with a large extracellular NT domain (McLatchie et al. 1998; Hay and Pioszak 2016). RAMP proteins were discovered because of their integral role in calcitonin like receptor (CLR) biology. RAMPs are essential for CLR trafficking to the cell surface, and RAMP dimerization with CLR is necessary for ligand binding. Indeed, CLR agonist preference is determined by the associated RAMP– dimerization with RAMP1 forms the calcitonin gene-related peptide receptor while association with RAMP2 or 3 forms receptors for adrenomedullin (McLatchie et al. 1998; Poyner et al. 2002). Although the function of RAMPs has been most extensively studied in regard to CLR and the related calcitonin receptor, additional GPCRs have been reported to interact with RAMP proteins. Interaction with RAMPs is emerging as another mechanism for modifying receptor trafficking, signaling and regulation (Hay and Pioszak 2016; Klein, Matson, and Caron 2016).

Another set of important interacting partners for GPCRs are Src homology 3 (SH3) adaptor proteins (Magalhaes, Dunn, and Ferguson 2012). Several GPCRs contain proline-rich, SH3 domain-binding motifs within their third intracellular loops or C-terminal tails. GPCR interactions with SH3-domain containing

proteins can modulate G-protein-coupling, trafficking, and signaling. Src family kinases can associate with GPCRs and ß-arrestins via the SH3 domain to promote receptor signaling to MAPK (McGarrigle and Huang 2007; Magalhaes, Dunn, and Ferguson 2012). Another SH3 domain containing protein, endophilin was recently shown to differentially associate with several GPCRs to mediate a clathrin-independent internalization pathway (Boucrot et al. 2015). Furthermore, association with the SH3 domain of spinophilin can mediate GPCR internalization and regulation. In complex with select GPCRs spinophilin competes with GRK binding, reducing ß-arrestin recruitment, and internalization, while association with other receptors does the opposite. Spinophilin can also affect downstream signaling cascades by recruiting RGS proteins (Magalhaes, Dunn, and Ferguson 2012; Dunn and Ferguson 2015). The interacting proteins described here represent only a small fraction of the known GPCR interacting partners. The dizzying complexity of receptor interacting partners and their effects on G-protein coupling, receptor localization, regulation and the formation of novel signal transduction complexes further contributes to ability of GPCRs to elicit complex cellular responses.

1.2 GPCRs in Health and Disease

1.2.1 GPCRs as Pharmaceutical Targets

GPCRs are essential for most physiological processes and their dysfunction has been shown to contribute to the etiology of many disease states and disorders. GPCRs have been implicated in endocrine and metabolic

disorders, immune dysfunction, cancer and vascular disease, among others (Vassart and Costagliola 2011; Heng, Aubel, and Fussenegger 2013; Rockman, Koch, and Lefkowitz 2002; Smith and Luttrell 2006). In the brain, GPCRs serve as the molecular targets for many neurotransmitters, neuropeptides, and neuromodulators. With over 90% of non-sensory GPCRs expressed in the brain, it is not surprising that GPCRs can contribute to addiction, neurodegeneration, neuropathic pain, and movement disorders, as well as psychiatric and neuroinflammatory diseases (Gainetdinov et al. 2004; Nickols and Conn 2014).

GPCRs make excellent drug targets, with ~30% of drugs on the market targeting GPCRs (Santos et al. 2017). The success of drugs targeting GPCRs is a result of the unique features of GPCRs, they are involved in nearly all physiological processes and disease states, capable of producing diverse effects, have multiple mechanisms for modulation, frequently respond to small molecules, are relatively easy to screen, often have restricted cellular expression, and they are ideally localized to the cell surface. While drugs targeting GPCRs represent a large portion of the market, current drugs only target 10% of human GPCRs, underscoring why they are among the most pursued targets for drug development (Rask-Andersen, Masuram, and Schioth 2014).

1.2.2 Orphan GPCRs

Some of the most attractive receptors for drug development are orphan GPCRs. Orphan receptors are often classified as GPCRs through sequence

homology but their endogenous ligand remains unknown, roughly 140 non-olfactory GPCRs have yet to be linked to an endogenous ligand (Tang et al. 2012). Identifying ligand(s) capable of activating a GPCR is essential for discerning the physiological function of a receptor and defining its signaling and regulatory mechanisms. However, studies examining the phenotype of cells or animals lacking or overexpressing an orphan GPCR provide an alternative method for identifying a receptor's function without a known ligand. Additionally, development of crystallization techniques and technological advances have led to additional approaches for studying these receptors. Identification of new and endogenous ligands for orphan GPCRs is an appealing line of research because orphan receptors hold potential, not only as drug targets, but also a unique avenue for uncovering novel insight into basic biology and disease states.

1.3 GPR37 and GPR37L

1.3.1 Identification and Expression

GPR37 and GPR37L1 were identified by their sequence homology to the endothelin and bombesin receptor families (Zeng et al. 1997; Marazziti et al. 1997; Donohue et al. 1998; Valdenaire et al. 1998; Leng et al. 1999). GPR37L1 shares 68% similarity to GPR37 and both receptors are most highly expressed in the brain. Early transcript data indicated high levels of expression in the corpus callosum and substantia nigra for GPR37 (Marazziti et al. 1997; Zeng et al. 1997; Donohue et al. 1998), and wide expression of GPR37L1 throughout the brain with highest levels in the Bergmann glia of the cerebellum (Valdenaire et al. 1998).

More recently, neuronal and glial cell specific transcriptome databases from mice and humans have revealed both GPR37 and GPR37L1 as enriched in glial cells (Cahoy et al. 2008; Zhang et al. 2014). In humans, GPR37L1 displays very high levels in mature astrocytes (Reddy et al. 2017; Chaboub et al. 2016), some expression in oligodendrocytes, and negligible expression in fetal astrocytes, neurons, microglia, and endothelial cells. In the mouse dataset, GPR37L1 remains highly expressed in astrocytes and is shown to be enriched in oligodendrocyte precursor cells (OPC). Interestingly, GPR37L1 expression is reduced as oligodendrocytes differentiate, showing least expression in myelinating oligodendrocytes in mice.

The expression profile of GPR37 is distinct from the profile of GPR37L1. In humans, GPR37 is highly expressed and enriched in oligodendrocytes with low expression in mature astrocytes and negligible expression in other cell types (Zhang et al. 2014). Interestingly, GPR37 expression in mice is the reverse of GPR37L1, with GPR37 having the highest expression in myelinating oligodendrocytes, with declining expression in newly formed oligodendrocytes, and no expression in OPCs (Cahoy et al. 2008; Oldham et al. 2008). GPR37 also shows very low expression in cortical astrocytes and neurons. However, it has been shown that GPR37 is more highly expressed in some neuronal subtypes (Marazziti et al. 2007; Lopes et al. 2015; Yang et al. 2016).

Cell-specific expression of GPR37 and GPR37L1 has not been extensively defined at the protein level. Early immunohistochemical studies demonstrate

GPR37 colocalization with tyrosine hydroxylase in neurons of the substantia nigra, and CNPase-positive oligodendrocytes (Imai et al. 2001). Additionally, GPR37 expression has been established in hippocampal neurons (Lopes et al. 2015). To work around limited reagents, two groups have used reporter constructs under the GPR37 promoter to assess receptor expression in oligodengroglia and the testes (Yang et al. 2016; La Sala et al. 2015). Immunofluorescence confirms GPR37L1 expression increases in the radial glia of the developing cerebellum and is specifically expressed in Bergmann glia in adulthood (Marazziti et al. 2013).

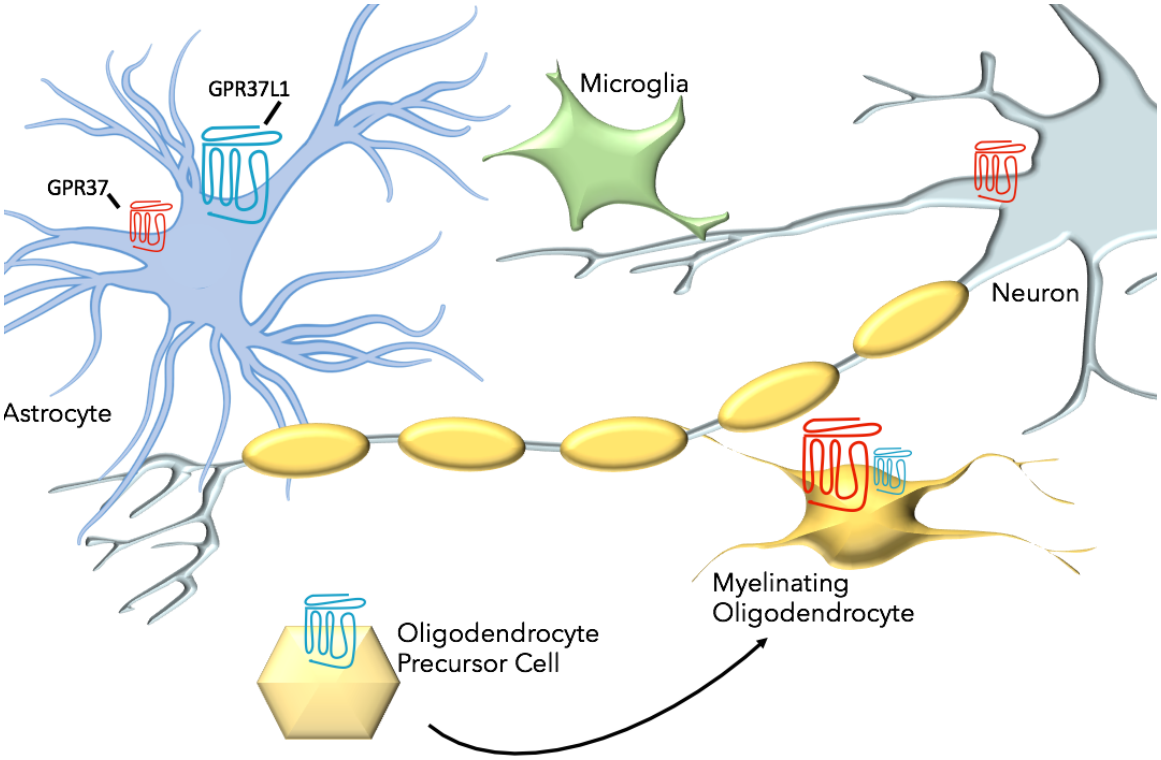

Figure 1-2. Expression of GPR37 and GPR37L1 in Neurons and Glia

Schematic summary of relative expression of GPR37 (red) and GPR37L1 (blue) in neurons and glia. GPR37 is most highly expressed in myelinating oligodendrocytes, with moderate expression in astrocytes and some populations of neurons. GPR37L1 is most highly expressed in astrocytes, with high levels of expression in oligodendrocyte precursor cells and low levels of expression in mature myelinating oligodendrocytes.

1.3.2 Receptor Processing

N-terminal fragments of GPR37L1 have been identified in human cerebral spinal fluid (CSF), suggesting the processing of GPR37L1 may be biologically relevant (Stark et al. 2001; Zhao et al. 2010). Interestingly, while GPR37 and GPR37L1 have predicted molecular weights of 67 and 53kDa respectively, the predominant form of both receptors detected following sodium dodecyl sulfate polyacrylamide gel electrophoresis (SDS-PAGE) is roughly 20kDa below their predicted sizes (Imai et al. 2001; Rezgaoui et al. 2006; Marazziti et al. 2007; Omura et al. 2008; Mattila, Tuusa, and Petaja-Repo 2016; Coleman et al. 2016). Immunodetection with C-terminal antibodies suggests the main form of the receptor is N-terminally cleaved. Endothelin B (ETB), the most closely related neighbor to GPR37 and GPR37L1 is also known to undergo N-terminal cleavage. Studies with N-terminally truncated forms of ETB show reduced surface expression, suggesting receptor processing may regulate surface expression (Grantcharova et al. 2002). Similar studies with an N-terminally truncated form of GPR37 indicate truncated versions of the receptor display increased surface expression (Dunham et al. 2009; Mattila, Tuusa, and Petaja-Repo 2016).

Expression of GPR37 modified to contain dual epitope tags at the N and C termini, clearly demonstrate the existence of several differentially sized versions of the receptor (Mattila, Tuusa, and Petaja-Repo 2016). The most abundantly expressed form was detected at 53kDa and contained only the CT epitope tag, suggesting an N-terminally truncated form of the receptor. Pulse-chase labeling

of HEK cells stably-transfected with GPR37, reveals that cleavage of the receptor occurs after processing of receptor N-glycans in the Golgi (Mattila, Tuusa, and Petaja-Repo 2016). Co-localization with endocytic markers indicate that GPR37 is cleaved only after it leaves the trans-Golgi network. Additionally, broad-range metalloproteinase inhibitors, GM6001, TAPI-1 and marimastat prevent GPR37 cleavage and increase the amount of full-length receptor at the cell surface (Mattila, Tuusa, and Petaja-Repo 2016). The functional role of GPR37 cleavage has yet to be investigated.

Coleman and colleagues (Coleman et al. 2016) set out to determine the functional significance of GPR37L1 N-terminal cleavage. In contrast to GPR37, removal of the N-terminus of GPR37L1 reduces total and surface expression. Furthermore, truncation of the NT completely abolished GPR37L1's constitutive signaling to CRE. High levels of three matrix metalloproteases (MMPs) inhibitors altered the expression pattern of GPR37L1, demonstrating MMPs can cleave the receptor *in vitro*. Both batimastat, a nonspecific MMP and a disintegrin and metalloproteinase (ADAM) inhibitor, and tumor necrosis factor–α protease inhibitors (TAPI) 1 and 2, reduced the truncated form of GPR37L1 detected, while increasing the full-length version of the receptor. To confirm a functional effect in native tissue, the authors probed for GPR37L1 in organotypic slice cultures from the cerebellum. Expression of GPR37L1 in the brain is also detected as two species, with virtually all the detectible receptor existing in the cleaved form, ~30kDa. Treatment of cerebellar slices with batimastat was inconclusive.

1.3.3 Interacting Partners

GPR37 and GPR37L1 contain a consensus PDZ binding motif, G-T-X-C, at their extreme C-termini (Dunham et al. 2009). As previously described, PDZ domain-containing proteins are cytoplasmic scaffolding proteins capable of assembling diverse multiprotein signaling complexes. Interaction of PDZ proteins with GPCRs can impact the signaling, trafficking, and function of targeted receptors (Magalhaes, Dunn, and Ferguson 2012; Dunn and Ferguson 2015). Several studies have described interactions with GPR37 and/or GPR37L1 and PDZ proteins, including syntenin-1 (Dunham et al. 2009; Dutta et al. 2014), multi-PDZ domain protein 1 (MUPP1) (Tanabe et al. 2015), protein interacting with C-kinase (PICK1) and GRIP4/5 (Dutta et al. 2014). Co-expression of GPR37 with syntenin-1 dramatically increases total and surface receptor expression (Dunham et al. 2009). Conversely, interaction with PICK1 reduces GPR37 expression levels (Dutta et al. 2014). However, the physiological relevance of these and other potential PDZ interactions remains to be determined.

In addition to association with PDZ containing proteins, GPR37 and GPR37L1 form heterodimers. Dimerization can occur between two copies of the same monomer, homodimerization, or it can take the form of distinct monomer pairs, as in heterodimerization. GPCR dimerization can modify receptor expression, trafficking, ligand binding, G protein coupling, and downstream signaling. Studies have shown GPR37 and GPR37L1 to physically interact with the dopamine transporter (DAT) and dopaminergic receptors, D1 and D2

(Dunham et al. 2009; Meyer 2014; Marazziti et al. 2007). GPR37 co-immunoprecipitates with DAT in overexpressed HEK293 cells (Marazziti et al. 2007). Although no interaction in native tissues has been reported, both GPR37 and DAT are enriched in the presynaptic fraction of mouse striata, co-expression of GPR37 with the dopaminergic D2 receptor (D2R) increased GPR37 expression and enhanced D2R ligand affinity as measured by [3H]-spiperone competition binding assays (Dunham et al. 2009). Furthermore, D2R ligands had reduced affinity in mice lacking GPR37 (Marazziti et al. 2007).

In contrast to GPR37, physical association between GPR37L1 and D2R has not been reported. However, GPR37L1 does associate with the dopamine D1 receptor (Meyer 2014). This interaction is not only detectable in overexpressed HEK293T cells, but in brain lysates as well, suggesting a physiologically relevant interaction. Interestingly, coexpression of the dopamine D1 receptor (D1R) with GPR37L1, but not GPR37, reduced D1R-mediated cAMP signaling and enhanced D1R-mediated ERK phosphorylation (Meyer 2014).

1.3.4 Ligand Identification

As GPR37 and GPR37L1 share the most homology with endothelin and bombesin receptors, ligands for these receptors were investigated for activity. None of the endothelin or bombesin ligands induced binding or signaling effects at either GPR37 or GPR37L1 (Marazziti et al. 1997; Zeng et al. 1997; Valdenaire et al. 1998; Leng et al. 1999; Donohue et al. 1998). Nearly 10 years after GPR37 was

discovered, head activator (HA), an undecapeptide discovered in *Hydra,* with a disputed human homolog (Bodenmuller and Schaller 1981; Davenport et al. 2013; Smith 2015), was reported to bind and promote internalization of GPR37. This study also described the ability of HA to increase calcium mobilization using a Gα16/aequorin assay (Rezgaoui et al. 2006). HA was also reported to increase signaling to NFAT and inhibit forskolin mediated cAMP via GPR37 (Gandia et al. 2013). This ligand remains in debate however, as two reports show no effect of HA on GPR37 (Dunham et al. 2009; Southern et al. 2013).

GPR37 and GPR37L1 have also been linked to the neurotrophic and neuroprotective protein, prosaposin, and its active peptide fragment, prosaptide (Meyer et al. 2013). Biotinylated prosaptide was shown to specifically pull down GPR37 and GPR37L1, and moreover prosaptide treatment of intact cells induced receptor internalization. Both prosaptide and prosaposin induced a modest increase in ERK phosphorylation in HEK293T cells and primary astrocytes when either GPR37 or GPR37L1 was present. ERK phosphorylation was pertussis toxin sensitive, and cells transfected with GPR37 or GPR37L1 also showed increased [^{35}S]-GTPγS accumulation when coexpressed with $G\alpha_{i1}$. Furthermore, prosaptide treatment of cells transfected with GPR37 or GPR37L1 inhibited forskolin-induced cAMP, indicating both receptors likely couple members of the $G\alpha_{i/o}$ family.

Further studies examining functional interactions between GPR37/GPR37L1 and prosaposin/prosaptide have been mixed. An interaction of

GPR37 with prosaptide was shown by fluorescence correlation spectroscopy, demonstrating that GPR37 is co-localized with prosaptide in lipid rafts of N2a cells expressing a GFP-tagged version of GPR37 (Lundius et al. 2014). However, a subsequent report described no significant effect of prosaptide treatment on GPR37L1 signaling (Coleman et al. 2016). In contrast to previous studies (Meyer et al. 2013; Gandia et al. 2013), the authors reported GPR37L1 as exhibiting constitutive coupling to $G\alpha_s$ to increase cAMP and stimulate the cAMP response element (CRE). Thus, similar to the case for head activator peptide, the literature is currently mixed with regard to potential regulation of GPR37/GPR37L1 signaling by prosaptide.

Recently, the pharmacology of GPR37L1 was the subject of investigation with a novel ligand prediction tool, GPCR–CoINPocket, a measure of GPCR binding-site similarity (Ngo et al. 2016). This tool uses sequence and structural data to determine the relative importance of pocket residues for ligand binding. Thus, while GPR37 and GPR37L1 have the most sequence similarity for the endothelin receptors, the predicted binding pocket of GPR37 and GPR37L1 are most like the bombesin, orexin, and neuropeptide S receptors. The authors screened ten known ligands of its predicted neighbors and found three specifically interacted with GPR37L1 and functioned as partial or full inverse agonists. Further studies will be required to determine their functional relevance, but as it stands currently, GPR37 and GPR37L1 remain orphan receptors with no widely-accepted natural ligand.

1.3.5 Functions of GPR37 & GPR37L1 In Vivo

Without a definite ligand, much of what is known about GPR37 and GPR37L1 has been discovered through studies on mice lacking either receptor. *Gpr37*$^{-/-}$ and *Gpr37L1*$^{-/-}$ mice are viable, have normal gross anatomy and show no overt phenotype (Marazziti et al. 2004; Marazziti et al. 2013). However, *Gpr37*$^{-/-}$ mice do exhibit increased anxiety and depression-like behaviors and have altered motor activity and performance (Mandillo et al. 2013; Marazziti et al. 2004) Mice lacking *Gpr37* also display enhanced surface expression of DAT and increased striatal dopamine (DA) uptake (Marazziti et al. 2007). To assess the functional relevance of altered DAT expression in *Gpr37*$^{-/-}$ mice, the authors assessed behavioral response to cocaine, which blocks DAT and reduces dopamine reuptake. *Gpr37*$^{-/-}$ mice had reduced cocaine-induced locomotor activity, which is surprising considering a previous report showed *Gpr37*$^{-/-}$ mice as more sensitive to amphetamine, which also acts on DAT, albeit through a different mechanism (Marazziti et al. 2004). Moreover, further studies showed *Gpr37*$^{-/-}$ mice failed to respond to either stimulus when used as an incentive in the conditional place preference behavioral test (Marazziti et al. 2011).

GPR37 and GPR37L1 have also been implicated as mediators for hedgehog signaling pathways. In the developing cerebellum, postnatal mice lacking *Gpr37L1* display a reduction of granule cell precursor proliferation, early maturation of Bergmann glia and Purkinje cells, and improved motor performance in adulthood (Marazziti et al. 2013). In general, the expression of a

particular combination of signals, at precisely the right time, is essential for proper development. One such signal involved in cerebellar development is sonic hedgehog (Shh). In mice, postnatal development of the cerebellum begins with the release of Shh by purkinje cells, which stimulates granule cell progenitor proliferation and postnatal maturation of Bergmann glia (Dahmane and Ruiz i Altaba 1999; Wallace 1999; Wechsler-Reya and Scott 1999). Following stimulation by Shh, cerebellar astrocytes and granule cell progenitors express the Shh pathway components, smoothened and patched-1 (Vaillant and Monard 2009; Ruat et al. 2012). Deletion of *Gpr37L1* resulted in a premature elevation of Shh and several important components of the Shh mitognic cascade including smoothened, patched-1 and the downstream transcription factor Gli2. Thus, the altered postnatal development observed in *Gpr37L1*$^{-/-}$ mice is likely a result of premature overexpression of Shh.

While most studies on GPR37 are focused on the role of the receptor in the brain, *Gpr37* is also expressed in the testis. In fact, *Gpr37* is among the most abundant receptor transcripts in Sertoli cells (SCs), a support cell in the testis facilitating spermatogenesis (Sanz et al. 2013; Marazziti et al. 1998). Immature SCs divide until puberty. The appropriate timing of SC maturation is essential, as the exit from the proliferation phase of the cell cycle determines the total number of SCs, which further defines the upper limit of sperm production and fertility (Orth, Gunsalus, and Lamperti 1988). One important factor produced by SC is desert hedgehog (Dhh). Like the effects of *Gpr37L1* deficiency in cerebellar development described above, mice lacking *Gpr37* have a premature maturation

of SCs, resulting in a reduced final number of mature SCs. Furthermore, *Gpr37*$^{-/-}$ mice show altered expression levels of SC maturation markers and premature elevation of Dhh, Patched-1, and Gli2 expression (La Sala et al. 2015).

Most recently, *Gpr37* deficient mice have been shown to have precocious oligodendrocyte differentiation and hypermyelination (Yang et al. 2016). While the authors did not investigate the role of Gpr37 on hedgehog signaling in this study, Shh is essential for proper oligodendrocyte differentiation, proliferation and development (Alberta et al. 2001; Poncet et al. 1996; Nery, Wichterle, and Fishell 2001). Furthermore, Shh signaling is an important player in the timing of neuron-glia fate switching. Thus, it is conceivable, that the precocious oligodendrocyte differentiation seen by Yang and colleagues is mediated by altered expression of Shh and its signaling partners, as previously observed in the testis or cerebellum of *Gpr37* or *Gpr37L1* deficient mice.

1.3.6 Disease Associations

As one of the first identified substrates of parkin (Imai et al. 2001), GPR37, alternatively named the parkin-associated endothelin receptor-like receptor (PaelR), has been extensively studied for its potential role in Parkinson's disease. Parkin is an E3 ubiquitin ligase whose function is to target misfolded proteins for degradation via the proteasome. Mutations in parkin resulting in a loss-of-function (LOF) exacerbate dopaminergic neuron cell death by allowing misfolded protein accumulation and aggregation (Imai, Soda, and Takahashi

2000; Shimura et al. 2000; Zhang et al. 2000). Indeed, LOF mutations in parkin result in the early-onset form of parkonsinism known as autosomal recessive juvenile parkinsonism (AR-JP) (Pickrell and Youle 2015). Misfolded GPR37 is found in the brains of individuals with AR-JP (Imai et al. 2001) and enriched within the Lewy bodies from individuals with Parkinson's disease, implicating GPR37 in parkinsonism pathogenesis (Murakami et al. 2004). While aggregation of misfolded GPR37 probably contributes to dopaminergic cell death, the loss of GPR37 function may also be detrimental.

In addition to Parkinson's disease, GPR37 has been associated with several other disorders. For instance, GPR37 was identified as a differentially expressed gene in human samples from subjects with either bipolar disorder or major depressive disorder, as GPR37 mRNA was found to be upregulated in bipolar disorder and downregulated in major depressive disorder (Tomita et al. 2013). Likewise, the gene for GPR37 was found within the first autism spectrum disorder (ASD) locus identified, AUT1. Several mutations in GPR37 have been associated with autism (Fujita-Jimbo et al. 2012; Tanabe et al. 2015), but a definitive role for GPR37 in ASD has not been identified. GPR37 has also been implicated as contributing to peritoneal metastasis of gastric cancer (Wang et al. 2016) and is associated with several other forms of cancer (Toyota et al. 2001; Junaid et al. 2011; Liu, Zhu, et al. 2014).

1.3.7 Protective Mechanisms

Although overexpression and misfolding of GPR37 is associated with cytotoxicity, endogenous GPR37 and GPR37L1 presumably serve a functional purpose. The loss of these receptors in mouse models, as described above, establish a role for GPR37 and GPR37L1 in proper development and normal dopaminergic signaling. Furthermore, increased surface expression of GPR37 protects N2a cells, a catecholaminergic neuronal-like cell line, against three toxins known to recapitulate certain cellular aspects of Parkinson's disease (Lundius et al. 2013). Additionally, expression of GPR37 and/or GPR37L1 in astrocytes was shown to be protective in a model of oxidative stress-induced toxicity (Meyer et al. 2013). While these studies shed light on the functional effects of GPR37 and GPR37L1, the exact role of these receptors and the extent of their protective effects, remains unknown.

1.4 Dissertation Goals

The purpose of the studies described in this dissertation were to identify functional roles for GPR37 and GPR37L1 in models of disease. Chapter 2 of the dissertation establishes an association between a variant in GPR37L1 (c.1047G>T [Lys349Asp]) with a novel progressive myoclonic epilepsy. Although no striking differences were observed between GPR37L1 and the K349N variant in transfected cells, loss of *Gpr37L1 in vivo* resulted in increased seizures susceptibility in two seizure induction paradigms. Additionally, mice lacking the closely related receptor, GPR37 also resulted in increased seizure susceptibility in

a seizure induction paradigm and elicited spontaneous seizures. Finally, mice lacking both Gpr37 and Gpr37L1 are much more susceptible to seizures than single knockout mice and elicit significantly longer spontaneous seizures than mice lacking only GPR37.

Chapter 3 discusses the role of GPR37 in models of ischemic stroke. It was found that loss of GPR37 results in a larger infarct volume after induction of focal cerebral ischemia. Interestingly, Gpr37 expression increases dramatically in the penumbra region following the middle cerebral artery occlusion (MCAO) model of ischemic stroke. However, GPR37L1 expression is significantly reduced in the penumbra following MCAO in WT, but not *Gpr37*$^{-/-}$ mice. Loss of *Gpr37* also resulted in attenuated expression of the hypoxia inducible factor 1α (HIF1α) and the astrocytic marker glial acidic fibrillary protein (GFAP), but not the microglial marker, ionized calcium-binding adapter molecule 1 (Iba1). Furthermore, primary astrocytes cultured from *Gpr37*$^{-/-}$ mice were more susceptible oxygen glucose deprivation, an *in vitro* model of stroke, than wild type (WT) astrocytes. The final chapter of this dissertation discusses the larger implications of the data presented in Chapters 2 and 3.

CHAPTER 2:

GPR37L1 Modulates Seizure Susceptibility: Evidence from Mouse Studies and Analyses of a Human *GPR37L1* Variant

This chapter is adapted in part from:

Giddens, M.M., Wong, J.C., Schroeder, J.P., Farrow, E.G., Smith, B.M., Owino, S., Soden, S.E., Meyer, R.C., Saunders, C., LePichon, J.B., Weinshenker, D., Escayg, A., and Hall, R.A. GPR37L1 Modulates Seizure Susceptibility: Evidence from Mouse Studies and Analyses of a Human GPR37L1 Variant. Submitted.

Author contributions: All trafficking, signaling and protein-protein interaction studies described in this chapter were designed by M.M. Giddens and R.A. Hall and performed by M.M Giddens. B.M. Smith conducted GloSensor cAMP experiments. S. Owino conducted CRE luciferase experiments. B. Meyer contributed to generation of knockout mice. The 6 Hz seizures and spontaneous seizure studies were designed by J. Wong, M. Giddens, R.A. Hall and A. Escayg, and performed by J. Wong. Flurothyl seizure studies were designed by J. Schroeder, M. Giddens, R.A. Hall and D. Weinshenker, and performed by J. Schroeder. Patient data was collected and organized by E.G. Farrow, S.E. Soden, C. Saunders, J.B. LePichon. The pedigree was prepared by M. Giddens with input from E. Farrow.

o

2.1 Rationale

Deletion studies of *Gpr37* and *Gpr37L1 in vivo* suggest that these receptors contribute to proper development (Marazziti et al. 2013; La Sala et al. 2015; Yang et al. 2016) and normal dopaminergic signaling (Imai et al. 2007; Marazziti et al. 2007; Marazziti et al. 2004). Furthermore, *in vitro* studies indicate expression of GPR37 and/or GPR37L1 as protective in primary astrocytes (Meyer et al. 2013) and a catecholaminergic neuronal-like cell line (Lundius et al. 2013). While these studies shed light on the functional effects of GPR37 and GPR37L1, the exact roles of these receptors and the extent of their protective effects remain unknown. To further characterize the function of GPR37L1 we examined a novel homozygous variant, c.1047G>T [Lys349Asp], of unknown significance from a large, consanguineous family presenting with a novel progressive myoclonus epilepsy (PME). PMEs are disorders characterized by myoclonic and generalized seizures with progressive neurological deterioration. Individuals homozygous for the *GPR37L1* variant (K349N) developed symptoms in adolescence which resulted in death by early adulthood.

To identify the impact of the K349N mutation on GPR37L1 function, we compared K349N to GPR37L1 wild-type (WT). Both versions of the receptor were assessed for ability to express, traffic and signal in both HEK293T cells and a more neuronal-like cell line. Regulation and degradation of the receptor were also investigated. Although no striking differences were observed in the fundamental trafficking and constitutive signaling properties of GPR37L1 WT vs. the K349N variant *in vitro*, it is possible that the K349N variant results in a

significant change in ligand-induced signaling, resulting in a reduction or loss of receptor function. Without a functional ligand, it is not feasible to address this possibility *in vitro*. Thus, to shed light on whether loss of GPR37L1 function can affect seizure susceptibility *in vivo*, mice lacking a single copy or both copies of *Gpr37L1* were evaluated in two seizure-induction paradigms. As *GPR37L1* shares 68% similarity with GPR37, it is likely that these two receptors share the same ligand and perhaps also share a number of redundant functions *in vivo*. Thus, in parallel experiments, mice lacking a single copy or both copies of *Gpr37*, and double-knockout mice lacking both receptors (DKO), were also assessed in the same paradigms. Together these approaches were used to investigate the potential role of GPR37L1 in epilepsy.

2.2 Experimental Methods

2.2.1 Clinical Reports

The proband, VI:9 was the sixth child born to a consanguineous couple of Iraqi descent (Figure 1). She presented to clinic at approximately 11 years of age with complaints of recurrent headaches. Subsequently, she developed visual hallucinations, in the form of colors and lines and myoclonic seizures. Prior to the development of recurrent headaches, she had normal growth and development. All of her symptoms were progressive in nature, becoming more frequent and severe. The first EEG performed at 10 years was abnormal and supported a diagnosis of generalized epilepsy. In addition to epileptic seizures, the proband developed psychogenic non-epileptic seizures. By 13 years of age, she began to

demonstrate signs of dementia with cognitive decline and mood disturbances. The most recent EEG at 18 years of age showed intermittent superimposed posterior 5-6 Hz background activity, recurrent generalized high voltage 4-6 Hz spike, polyspike and slow wave discharges with occasional abortive generalized high voltage spike and slow wave discharges. MRI and MRS of the brain at 18 years of age detected only a mild prominence of the subarachnoid spaces and were otherwise unremarkable. The patient's symptoms continued to worsen with generalized and diffuse myoclonic jerks and fasciculations over much of her body, including her face and limbs. Her epilepsy and dementia also gradually worsened and she required multiple hospitalizations in the last year of her life. The patient's seizures became intractable and she died at 20 years of age from aspiration pneumonia'.

Four older sisters, VI:4, VI:5, VI:6, and VI:7, were described as having a similar clinical presentation. They first presented around the age of puberty with headaches, followed by visual hallucinations and eventually developed progressive myoclonic epilepsy. All four sisters died from complications of their disease. Two sisters, VI:8 and VI:10, have reported headaches but no documented seizure activity. They are currently 24 and 18 years old, respectively, and in good health. A younger brother, VI:11, developed headaches and visual hallucinations in the form of black spots at 11 years of age. An EEG showed generalized spike and wave complexes in addition to occipital sharp waves, but no seizure activity was recorded. He was initially treated with anticonvulsants, but medications were subsequently stopped, and he has remained seizure free for

10 months. The youngest child, VI:12, currently 11 years of age, also recently presented with headaches but has had no documented seizure activity. The extended family history was positive for a maternal first cousin, VI:1, who also died prematurely after being diagnosed with headaches and seizures. Additional clinical details are not available.

2.2.2 Human Exome Sequencing

The study was approved by the Institutional Review Board (IRB) at Children's Mercy Hospital (CMH). Informed written assent/consent to participate in this study was obtained from all available family members. DNA was extracted from peripheral blood from the five living siblings and their parents. Exome sequencing was completed for V:14, VI:8, VI:9., and VI:11. DNA was not available from the four affected siblings who had died prior to moving to the United States. Library preparation was performed utilizing the KAPA Biosystems kit (KAPA Biosystems, Woburn, MA.) Enrichment using Illumina TruSeq Exome enrichment (Illumina, San Diego, CA) was performed according to manufacturers' instructions. Samples were sequenced on an Illlumina HiSeq 2500 instrument with TruSeq v3 reagents, paired ~100 nucleotide reads. Alignment and variant calling was performed as previously reported(Soden et al. 2014; Willig et al. 2015). Exome-enriched DNA was sequenced to a depth of 10.6Gb resulting in median target coverage of 67x. Variants were filtered to 1% minor allele frequency (MAF) in an internal database of 3974 samples, then

prioritized by the American College of Medical Genetics (ACMG) categorization (Richards et al. 2015).

2.2.3 Sanger Confirmation

Sanger sequencing was completed for all available family members. Sequencing confirmed that both parents are heterozygous for the *GPR37L1* variant, and the unaffected sisters (VI:8 and VI:10) are heterozygous and wild-type, respectively. Like the proband (VI:9), the two younger brothers (VI:11 and VI:12) were found to be homozygous for the K349N *GPR37L1* variant.

2.2.4 Cell culture

HEK-293T/17, N2a, and NIH-3T3 cells were acquired from ATCC (Manassas, VA) and maintained in DMEM (Life Technologies) supplemented with 10% fetal bovine serum and 1% penicillin/streptomycin in a humid, 5% CO2, 37°C incubator. HEK293T and NIH-3T3 cells were transfected using Mirus TransITLT1 (Madison, WI) per the manufacturer's protocol. N2a cells were transfected using Lipofectamine LTX (Thermo Fisher Scientific) per the manufacturer's protocol.

2.2.5 Western Blotting

Protein samples were reduced and denatured in Laemmli buffer, loaded into 4-20% Tris-Glycine gels (Bio-Rad) for SDS-PAGE, and then transferred to nitrocellulose membranes (Bio-Rad). Blots were blocked with 5% milk (in 50mM

NaCl, 10mM HEPES, pH 7.3 with 0.1% Tween-20 (Sigma)) and incubated with primary antibodies overnight at 4°C. Flag-tagged GPR37L1 and K349N were detected with mouse HRP-conjugated anti-Flag (Sigma). Protein quantification was done using densitometry, performed with ImageJ software.

2.2.6 Cell Surface Biotinylation

HEK-293T/17 cells were transfected with 2µg of DNA (empty vector or receptor). At 24 h post-transfection, cells were placed on ice and washed with ice-cold PBS+Ca^{2+}. Cells were then incubated with 10 mM Sulfo-NHS-Biotin (Thermo Scientific) in PBS+Ca^{2+} on ice for 1 h and then washed three more times with PBS+Ca^{2+} + 100 mM glycine to quench. Cells were harvested in 500 µl of lysis buffer (1% Triton X- 100, 10 mM Hepes, 50 mM NaCl, 5 mM EDTA, and protease inhibitor cocktail (Roche Diagnostics)) and lysed by end-over-end rotation for 30 min at 4°C. Cell debris was cleared by centrifugation, and soluble cell lysates were incubated with 50µl of streptavidin agarose beads (Thermo Scientific) for 1 h at 4°C. Beads were washed 3 times with lysis buffer and resuspended in 100 µl of Laemmli buffer. Biotinylated proteins were detected via Western blot, as described above.

2.2.7 Confocal Microscopy

NIH-3T3 cells transiently transfected with GFP-tagged constructs were grown on collagen I-coated culture slides (BD Biosciences), and 48 h after transfection cells were fixed with 4% PFA at room temperature (RT) for 10

minutes. Following one wash with PBS+Ca^{2+}, cells were blocked in blocking buffer (PBS+Ca^{2+} + 1% goat serum (Invitrogen) and 0.1% Triton-X-100) for 30 minutes at RT. Cilia were labeled with rabbit anti-Arl13b antibody (1:500; ProteinTech) overnight in blocking buffer. Following primary antibody incubation, cells were washed three times in blocking buffer and incubated with Alexa 546 fluorophore (red) conjugated anti-rabbit secondary antibody (Invitrogen) in blocking buffer for 1h at RT. After a single rinse, cell nuclei were stained with DAPI (USB Affymetrix) for 10 min. Following two additional rinses, cells were mounted onto slides using Vectashield mounting medium (Vector Laboratories) and sealed. Images were captured using an Olympus FV1000 confocal microscope (Olympus).

2.2.8 Phosphorylation assays

HEK-293T/17 cells were plated in 6-well plates (Corning) 20-24 h prior to transfection. Each well was transfected with 0.33µg of receptor plasmid or empty vector. After 36-48h, cells were serum-starved for 2h before drug treatment by replacing complete growth medium with DMEM. To initiate stimulation, half (1ml) of the DMEM was removed and slowly replaced with 1mL fresh DMEM, containing a 2X concentration of vehicle, prosaptide, or head activator (HA) peptide. Plates were carefully returned to a 37°C incubator for 10 min. Following stimulation, cells were rapidly harvested in Laemmli buffer. Samples were sonicated and loaded into 4-20% Tris-Glycine gels (Bio-Rad) for SDS-PAGE, and then transferred to nitrocellulose membranes (Bio-Rad). Membranes were

blocked via shaking at RT for 30 min in Odyssey blocking buffer and incubated overnight with shaking at 4 °C with mouse anti-phospho ERK (Santa Cruz) and rabbit anti-total ERK (Cell Signaling Technologies) or rabbit anti-phospho AKT (Cell Signaling Technologies and mouse anti-total AKT (Cell Signaling Technologies) in antibody buffer (equal parts blocking buffer and PBS + 0.1% Tween-20). Membranes were then washed three times in a wash buffer (PBS with 0.1% Tween-20) and incubated with Alexa-fluor anti-mouse 700-nm conjugated secondary antibody (1:20,000; Invitrogen) and anti-rabbit 800-nm conjugated secondary antibody (1:20,000; Li-Cor) for 30 min in antibody buffer. Blots were washed three times and rinsed in PBS until they were visualized on an Odyssey Imaging System (Li-Cor). Protein quantification was done using densitometry, performed with ImageJ software

2.2.9 Luciferase reporter assays

HEK-293T/17 cells were seeded in 96-well plates 20-24 h prior to transfection. Each well was transfected with 50ng of firefly reporter, 1ng of Renilla luciferase, and 10ng of either receptor plasmid or empty vector (EV). Reporter constructs (CRE: pGL4.29, SRE: pGL4.33, NFAT: pGL4.30, Gli: pGL4, Renilla pRLSV40) were acquired from Promega (Madison, WI). After 24-48hrs, DualGlo luciferase assays (Promega) were performed according to the manufacturer's protocol and plates were read on a BMG Omega plate reader. Two hours prior to reading CRE luciferase, the media was removed from all wells and 100uL of DMEM or DMEM with 1μM forskolin was added. Results were

calculated for each assay by determining the luminescence ratio of firefly:Renilla luciferase counts, normalized to EV transfected wells. Error bars for all EV-transfected conditions were represented as the standard errors of the normalized raw value means.

2.2.10 cAMP Assay

HEK293T/17 cells were stably transfected by transfecting 2µg of the pGloSensor™-22F cAMP plasmid (Promega) in complete medium of DMEM supplemented with 10% FBS and 1% Penicillin/Streptomycin. After 48 hours, cell culture media was changed to selection media, which included complete media supplemented with 200µg/ml hygromycin B. Media was changed every 72 hours until cells reached confluency and were passaged. To plate for the assay, cells were detached from the culture dish using 0.05% trypsin-EDTA (Invitrogen) and reseeded on a clear-bottomed white 96-well assay plate. After 24 hours, cells were transiently transfected with 10 ng/well EV, GPR37L1, or GPR37L1 K349N plasmid DNA. Cells were transfected at 50% confluency. Cells were incubated for 18-24 hours, then complete medium was removed and replaced with 90 µl assay medium (complete medium with 2% GloSensor™ cAMP reagent stock solution). Cells were returned to the incubator for 2 hours, and then removed and equilibrated to room temperature by sitting on benchtop for 10 minutes. A baseline luminescence measurement was read on a BMG Omega plate reader. Cells were then treated with 10µl of drugs or vehicle at 10X concentration in HBSS. Cells were returned to the plate reader and luminescence readings were

taken every 2 minutes for 1 hour. The baseline readings were subtracted from each measurement to account for well-to-well variability.

2.2.11 Co-immunoprecipitation Assays

HEK-293T/17 cells were plated and transfected as described above with 2µg of receptor and 1 µg of empty vector, HA-ubiquitin or HA-ß-arrestin2. For ubiquitination experiments, after 24 h post-transfection, cells were treated overnight with 100nM MG-132 (Tocris) to inhibit the proteasome. Cells were washed, harvested, and solubilized as described above 48 h post-transfection. Cleared lysates were incubated with anti-HA agarose beads (Sigma) for 1h, washed, and eluted in Laemmli buffer. Tagged constructs were detected via Western blotting with mouse HRP-conjugated anti-Flag (Sigma) rabbit HRP-conjugated anti-HA (Abcam).

2.2.12 Degradation Experiments

HEK-293T/17 cells were plated and transfected as described above with 2µg of receptor and 1 µg of empty vector, HA-ubiquitin or HA-ß-arrestin2. For ubiquitination experiments, after 24 h post-transfection, cells were treated overnight with 100nM MG-132 (Tocris) to inhibit the proteasome. Cells were washed, harvested, and solubilized as described above 48 h post-transfection. Cleared lysates were incubated with anti-HA agarose beads (Sigma) for 1h, washed, and eluted in Laemmli buffer. Tagged constructs were detected via

Western blotting with mouse HRP-conjugated anti-Flag (Sigma) rabbit HRP-conjugated anti-HA (Abcam).

2.2.13 Generation of Knockout Mice (KO) and Maintenance of Mouse Colony

Gpr37 knockout mice (*Gpr37*$^{-/-}$) were obtained from Jackson Laboratory (strain Gpr37^{tm1Dgen}, stock number 005806) and GPR37L1 knockout mice (*Gpr37L1*$^{-/-}$) were obtained from the NIH Mutant Mouse Regional Resource Centers (strain Gpr37l1^{tm1Lex}, stock number 011709-UCD). These mouse lines were backcrossed with wild-type C57BL/6J mice (Jackson Laboratory) for 10 generations each to ensure uniformity of genetic background. Following this backcrossing, *Gpr37*$^{-/-}$ and homozygous *Gpr37L1*$^{-/-}$ mice were crossed to generate the Double-KO (DKO) line of mice. Genetic deletion of *Gpr37* and/or *Gpr37L1* was confirmed by DNA sequencing, and loss of GPR37 and/or GPR37L1 protein expression was confirmed by Western blotting of brain tissue samples with specific anti-GPR37 and anti-GPR37L1 antibodies (MAb Technologies).

All mice were maintained on a C57BL/6J background and housed on a 12-h light/dark cycle, with food and water available *ad libitum*. All experiments were conducted during the light cycle prior to 4:00 p.m. and were performed in accordance with the guidelines of the Institutional Animal Care and Use Committee of Emory University. Wild-type (WT) littermates were used as controls for all single mutant experiments, and age-matched WT littermates from each single mutant line were combined and used as controls for experiments

involving DKO mice. Male mice were used in all seizure induction paradigms. In all experiments, the experimenter was blinded to the genotypes of the animals.

2.2.14 6 Hz Seizure Induction

Seizures were induced using the 6 Hz paradigm, as previously described(Barton et al. 2001; Gilchrist et al. 2014; Wong et al. 2016). Briefly, 30 minutes prior to seizure induction, a topical anesthetic (0.5% tetracaine hydrochloride) was applied to the cornea. Each mouse was manually restrained during corneal stimulation (6 Hz, 0.2-ms pulse, 3 s) using a constant current device (ECT Unit 57800; Ugo Basile, Comerio, Italy). Behavioral seizures were scored based on a modified Racine Scale (RS): RS0 = no abnormal behavior; RS1 = immobile for ≥3 s, then resumption of normal behavior; RS2 = forelimb clonus, paw waving; RS3 = generalized tonic-clonic seizure with rearing and falling(Gilchrist et al. 2014). Mice were tested at three current intensities: 18 mA (N = 11-16/group), 22 mA (N = 16-22/group), and 27 mA (N = 16-22/group) with a one-week recovery between each test session.

2.2.15 Flurothyl Seizure Induction

Seizures were induced using the chemiconvulsant flurothyl (2,2,2-trifluroethylether; Sigma-Aldrich). Each mouse was placed in a clear, Plexiglas chamber contained within a chemical fume hood, and flurothyl was introduced into the chamber (20 μl/min) such that it vaporized and filled the chamber. Latencies to the first myoclonic jerk and generalized tonic-clonic seizure (GTCS)

were recorded(Szot et al. 1999; Cubells et al. 2016). Mice were removed from the chamber immediately after the GTCS.

2.2.16 EEG Analyses

Gpr37L1$^{-/-}$, *Gpr37*$^{-/-}$, and DKO mice (*N* = 5/group) were implanted with four cortical EEG recording electrodes at the following coordinates, relative to bregma: anterior-posterior (AP) 0.5mm, medial-lateral (ML) -2.2mm; AP -3.5mm, ML -2.2mm; AP 2.0mm, ML 1.2mm; AP -1.5mm, ML 1.2mm. Two wires were also implanted into the neck muscle to obtain EMG recordings. Mice were allowed to recover for one-week prior to EEG analyses.

Continuous video and EEG analyses (24 hours/day) were performed over a two-week period. Using Harmonie software for rodent studies (Stellate), EEG/EMG signals were analyzed utilizing a notch filter (60 Hz) and a low- and high-pass filter of 5 and 35 Hz, respectively. Seizures were manually identified and characterized as high-frequency electrographic signals with an amplitude at least twice the background. Synchronous video recordings were used to observe behavior during electrographic activity.

2.3 Results

2.3.1 A homozygous variant in GPR37L1 (K349N) implicates GPR37L1 in seizure susceptibility

In a highly consanguineous family (Figure 2-1) with multiple siblings affected by intractable, progressive myoclonus epilepsy (PME), exome

sequencing revealed a homozygous variant (c.1047G>T [Lys349Asn] [Genebank NM_004767.3]) in *GPR37L1*. Unaffected parents were carriers, and healthy siblings, of sufficient age to be symptomatic, were found to lack the variant or have a single copy. All affected individuals presented with recurrent headaches and visual hallucinations in the form of colors and lines in early adolescence (Table 2-1), followed by onset of myoclonic seizures. Symptoms progressively worsened and were accompanied by gradual and continuous cognitive decline culminating in death in late adolescence. The variant was not found in 3970 in-house (*Center for Pediatric Genomic Medicine)* control exomes but was identified in a heterozygous state in 3 European (Non-Finnish) individuals from a total of 121,328 alleles (minor allele frequency = 0.002%), per the ExAC Browser. The variant was predicted to be pathogenic by three web-based prediction tools, SIFT (Ng and Henikoff 2001), Polyphen (Sunyaev et al. 2001), and MutationTaster (Schwarz et al. 2014).

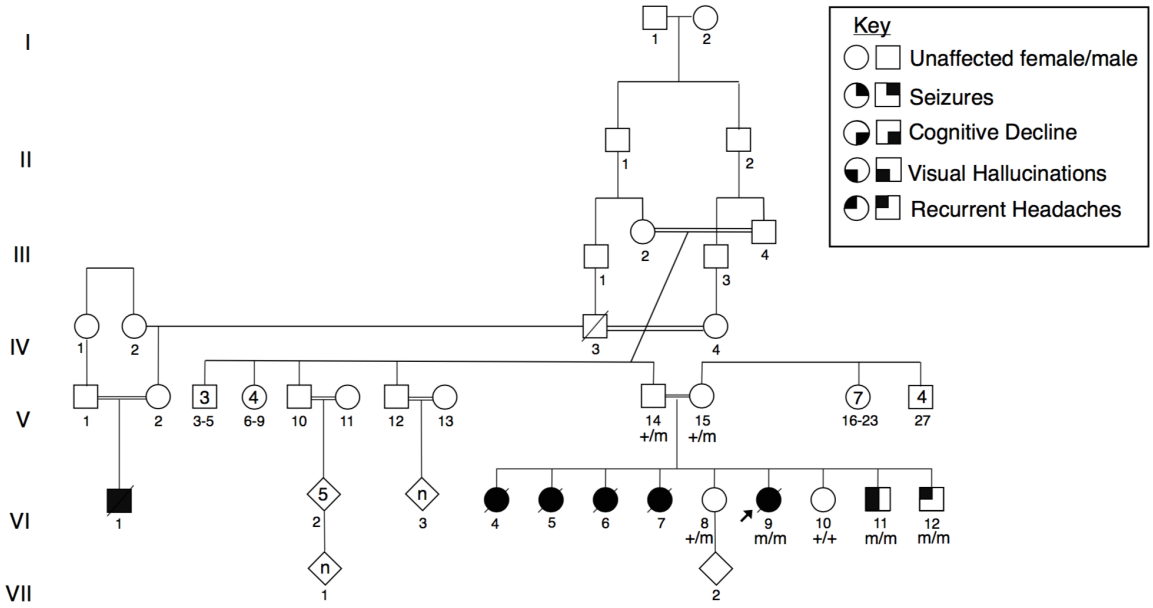
I
II
III
IV
V
VI
VII
Key
Unaffected female/male
Seizures
Cognitive Decline
Visual Hallucinations
Recurrent Headaches
3-5
6-9
10
11
12
13
14 +/m
15 +/m
16-23
27
n
+/m
m/m
+/+

Figure 2-1. Consanguineous family with multiple affected children presenting with a progressive myoclonus epilepsy associated with *GPR37L1* variant (K349N)

The proband (VI:9) was the sixth child born to a consanguineous couple of Iraqi descent, four older sisters, VI:4, VI:5, VI:6, and VI:7, were described as having a very similar clinical presentation. Affected children presented around the age of puberty with recurrent headaches, followed by visual hallucinations and seizures. Individuals eventually presented with cognitive decline and developed a progressive myoclonic epilepsy. Exome sequencing was completed for V:14, VI:8, VI:9., and VI:11. The proband was found to have a homozygous missense variant of unknown significance, *GPR37L1*: c.1047G>T (p.K349N). Sanger sequencing was completed for all available family members and confirmed that both parents are heterozygous for the variant, and the unaffected sisters are either heterozygous or wild type. The two younger brothers were found to be homozygous for the K349N variant. Each copy of the K349N mutant is labeled with an “m” in the pedigree shown here, as opposed to a “+” for the wild-type variant, in all individuals available for genetic testing.

Table 2-1. Comparison of Family Members with GPR37L1-K349N Variant

	VI:1*	VI:4*	VI:5*	VI:6	VI:7	VI:8	VI:9	VI:10	VI:11	VI:12
Age of Clinical Presentation (Years)	14	14	13	12	10	n/a	13	n/a	11	12
Age of Death (Years)	19	19	18	18	16	n/a	20	n/a	n/a	n/a
Current Age (Years)	n/a	n/a	n/a	n/a	n/a	24	n/a	18	15	12
Sex	male	female	female	female	female	female	female	female	male	male
K349N mutation	Not tested	Not tested	Not tested	Not tested	Not tested	Hetero-zygous	c.1047G>T (Lys349Asp)	WT	c.1047G>T (Lys349Asp)	c.1047G>T (Lys349Asp)
Recurrent Headaches	+	+	+	+	+	-	+	-	+	+
Visual Hallucinations	+	+	+	+	+	-	+	-	+	-
Seizures	+	+	+	+	+	-	+	-	-	-
Cognitive Decline	+	+	+	+	+	-	+	-	-	-
Progressive Myoclonic Epilepsy	+	+	+	+	+	-	+	-	-	-
Brain Imaging							mild prominence of the subarachnoid spaces; otherwise unremarkable			
EEG							intermittent superimposed posterior 5-6 Hz background activity, recurrent generalized high voltage 4-6 Hz spike, polyspike and slow wave discharges with occasional abortive generalized high voltage spike and slow wave discharges		generalized spike and wave complexes; occipital sharp waves	

* Denotes individuals for whom clinical information was relayed by family members

2.3.2 The K349N substitution does not alter receptor expression or trafficking

To assess the effect of the K349N variant on the ability of GPR37L1 to express and traffic to the cell surface, we expressed GPR37L1 WT or the K349N variant receptor in HEK293T cells (Figure 2-2). Total expression of K349N was equal to GPR37L1 WT (upper panels). The predicted molecular weight for GPR37L1 WT and the K349N mutant is ~53kDa. Both versions of the receptor have several predicted glycosylation sites, and thus the full-length receptor likely runs at ~70-75kDa (arrowhead) with higher order bands representing oligomeric forms of the receptor and the ~37kDa band representing a cleaved form of the receptor. To determine whether the K349N substitution might alter trafficking to the plasma membrane, surface proteins were labeled with a membrane-impermeant biotinylation reagent and pulled down with streptavidin beads. The K349N mutant receptor trafficked to the cell surface to a similar extent as GPR37L1 WT (Figure 2-2, lower panels).

To further examine the expression and trafficking of the receptors, we also expressed GPR37L1 WT and the K349N mutant receptor into the neuronal-like cell line, N2a (Figure 2-3). Again, The K349N mutation did not impact total or surface expression of the receptor. However, contrary to HEK293T cells, the primary form of GPR37L1 and K349N at the surface of N2a cells is the full-length version of the receptor.

As Marazziti and colleagues (Marazziti et al. 2013) reported Gpr37L1 to be localized to cilia in cerebellar Bergmann glial cells, we assessed receptor localization in NIH-3T3 cells (Figure 2C), a cell type commonly used for studying cilia (Alieva et al. 1999). Both versions of the receptor were found predominantly on the cell surface and exhibited generally similar patterns of subcellular localization in confocal microscopy analyses. However, in the NIH-3T3 cells, no co-localization of GPR37L1 WT or the K349N mutant with the cilia marker Arl13b was observed (Figure 2-4).

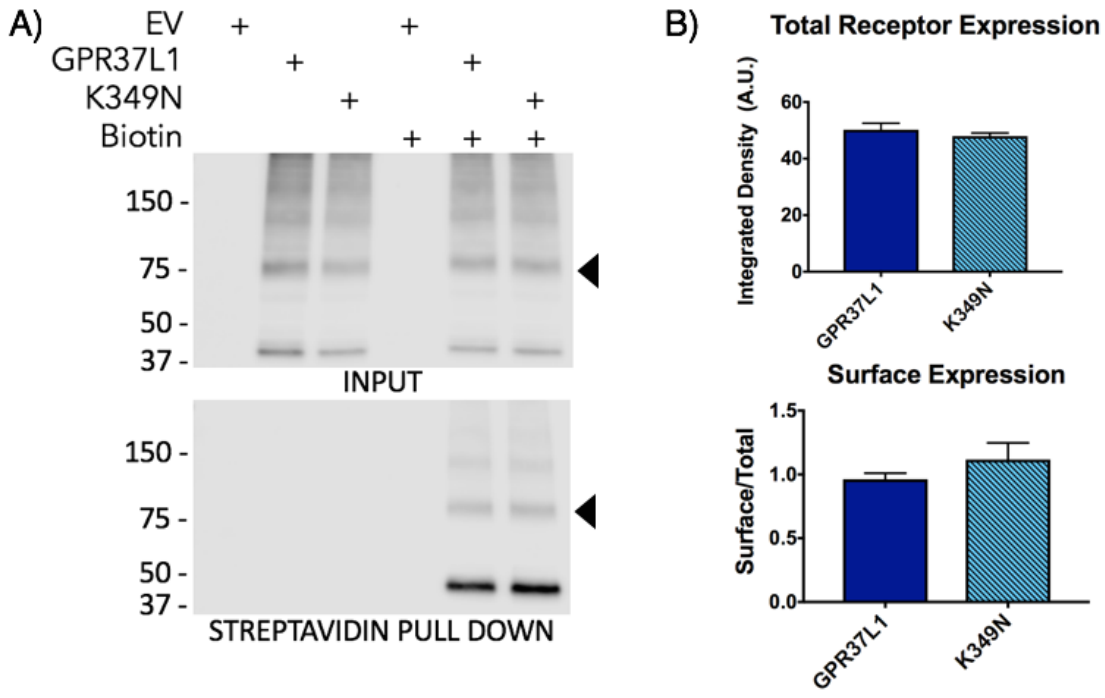

Figure 2-2. Expression and trafficking of GPR37L1 WT and K349N mutant are equivalent in HEK293T cells

(A & B) Transient transfection of Flag-tagged versions of GPR37L1 wild-type or K349N mutant in HEK293T cells yielded comparable levels of receptor expression (upper panels). Surface proteins were labeled with a membrane-impermeant biotinylation reagent and pulled down with streptavidin beads. Both versions of the receptor trafficked equally well to the surface (bottom panels). Full-length GPR37L1 runs on SDS-PAGE gels at ~70-75kDa (arrow head) with higher order bands representing oligomeric forms of the receptor and the ~37kDa band representing a cleaved form of the receptor. Results are from three independent experiments (± SEM shown).

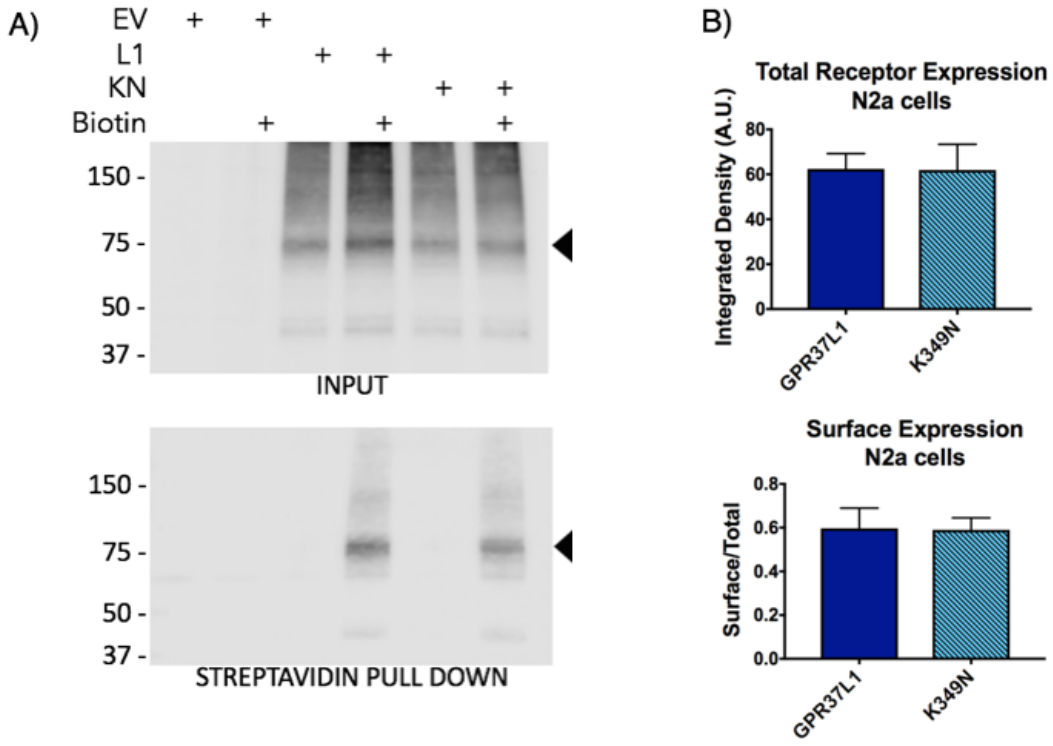

Figure 2-3. Expression and trafficking of GPR37L1 WT and K349N mutant are equivalent in a neuronal-like cell line

(A & B) Transient transfection of Flag-tagged versions of GPR37L1 wild-type or K349N mutant in N2a cells yielded comparable levels of receptor expression (upper panels). Surface proteins were labeled with a membrane-impermeant biotinylation reagent and pulled down with streptavidin beads. Both versions of the receptor trafficked equally well to the surface (bottom panels). Full-length GPR37L1 runs on SDS-PAGE gels at ~70-75kDa (arrow head) with higher order bands representing oligomeric forms of the receptor and the ~37kDa band representing a cleaved form of the receptor. Results are from three independent experiments (± SEM shown).

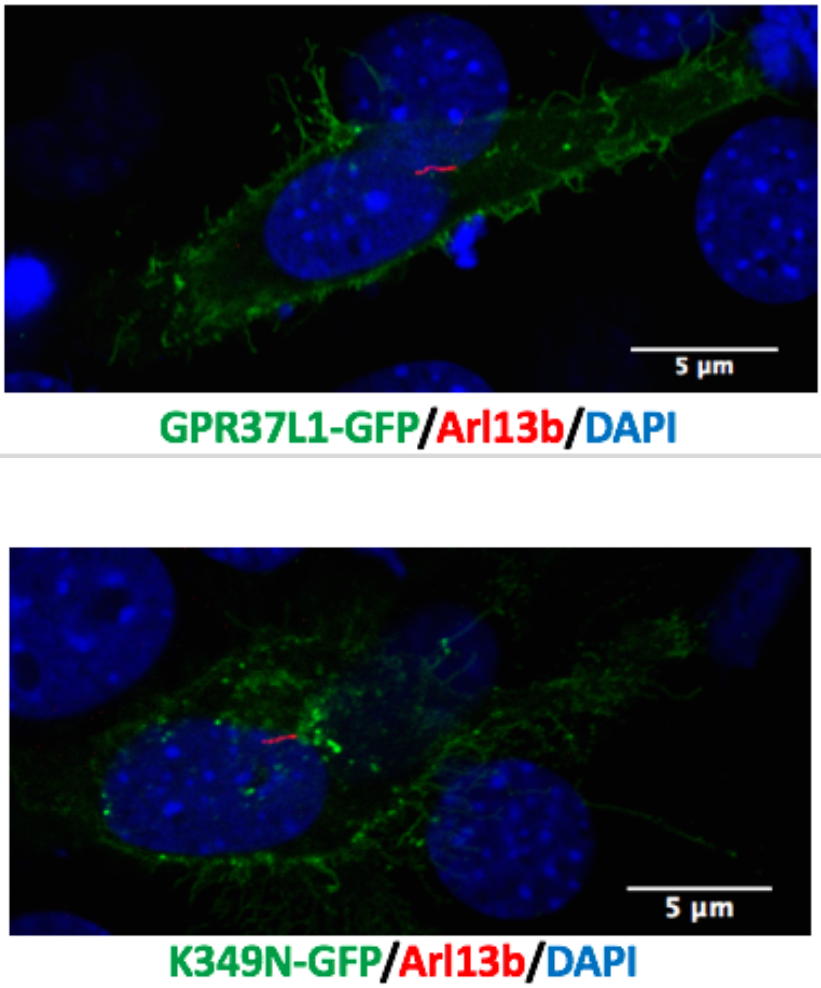

Figure 2-4. GPR37L1 WT and K349N mutant do not localize to cilia in NIH3T3 cells

Confocal microscopy analysis of GFP-tagged versions of GPR37L1 wild-type (left panel) and K349N mutant (right panel) revealed a similar pattern of subcellular localization in NIH-3T3 cells, with both receptor variants being predominantly localized to the plasma membrane and neither version of the receptor exhibiting ciliary localization. Cilia were labeled using an anti-Arl13b antibody, indicated in red.

2.3.3 Constitutive signaling by GPR37L1 is not affected by the K349N mutation

To assess the signaling activity of GPR37L1 WT vs. the K349N mutant, induction of ERK phosphorylation was measured, as signaling from both GPR37 and GPR37L1 has been shown to stimulate ERK phosphorylation (Meyer et al. 2013). Transient transfection of HEK-293T cells with either GPR37L1 WT or the K349N mutant raised basal ERK phosphorylation to a similar extent (Fig. 2-5A & B). However, neither prosaptide nor HA stimulation significantly increased ERK phosphorylation further. As prosaptide has also been shown to induce phosphorylation of AKT (Campana, Darin, and O'Brien 1999; Lee et al. 2004; Ochiai et al. 2008; Meyer et al. 2014), we investigated the ability of prosaptide or HA to induce signaling to AKT. Again, neither ligand affected AKT phosphorylation.

GPR37 and GPR3L1 also to signal to cAMP, however recent reports have had diverging results as to the effect of the receptor on cAMP production. Meyer and colleagues (Meyer et al. 2013) described GPR37 and GPR37L1 as inhibiting cAMP in response to prosaptide, and Gandia and colleagues (Gandia et al. 2015) reported that GPR37 inhibits the cAMP response element (CRE), a transcription factor downstream of cAMP, in response to HA. However, a more recent finding (Coleman et al. 2016) indicated that expression of GPR37L1 constitutively increased basal CRE activity. Here, we observed that expression of either GPR37L1 WT or K349N resulted in comparable increases in constitutive

signaling to CRE luciferase in the absence (Figure 2-6A), and presence of forskolin (Figure 2-6B). However, no effect of either prosaptide or HA was observed. To assess the ability of prosaptide and HA to affect transient cAMP production, we also utilized the GloSensor bioreagent to measure cAMP levels at 30 minutes after addition of either vehicle, prosaptide or HA. No significant effect of either drug was observed (Fig. 2-6C).

To fully assess the potential impact of the K349N variant on GPR37L1 function, it is necessary to study receptor signaling to different pathways downstream of the receptor. As neither reported ligand modulated receptor signaling to ERK, AKT or cAMP, we assessed all other reported signaling outputs of either GPR37 or GPR37L1. Activation of the serum response element (SRE), downstream of ERK phosphorylation, has been measured as an output for GPR37L1 (Coleman et al. 2016). Similarly, activation of nuclear factor of activated T-cells (NFAT), a transcription factor regulated by calcium signaling, is reported in cells expressing GPR37 (Gandia et al. 2013). Lastly, in vivo deletion of GPR37L1 resulted in altered levels of the intracellular effectors of the sonic hedgehog (shh)-Smoothened (Smo) cascade, including the increased transcription factor glioma-associated oncogene family zinc finger 2 (Gli2) (Marazziti et al. 2013).

Expression of both GPR37L1 and the K349N variant significantly increased basal SRE (Figure 2-7A), NFAT (Figure 2-7B), and Gli (Figure 2-7C), but there was no difference between the WT and variant versions of the receptor.

Moreover, treatment with prosaptide or head activator did not further modulate signaling to any of these readouts. These experiments were also replicated in the neuronal-like cell line, N2a. Contrary to the constitutive signaling observed in HEK293T cells, transfection with GPR37L1 WT and K349N into N2a cells did not result in any evidence of constitutively signaling to SRE or NFAT (Figure 2-8A & B). Interestingly, expression of either version of the receptor yielded a reduction in Gli signaling in N2a cells (Figure 2-8C), a result that is in alignment with the elevated Gli2 expression in mice lacking *Gpr37L1* (Marazziti et al. 2013). Similar to the HEK293T cell results, neither ligand induced signaling. Furthermore, in all *in vitro* signaling experiments, the K349N variant receptor was not significantly different from GPR37L1 WT.

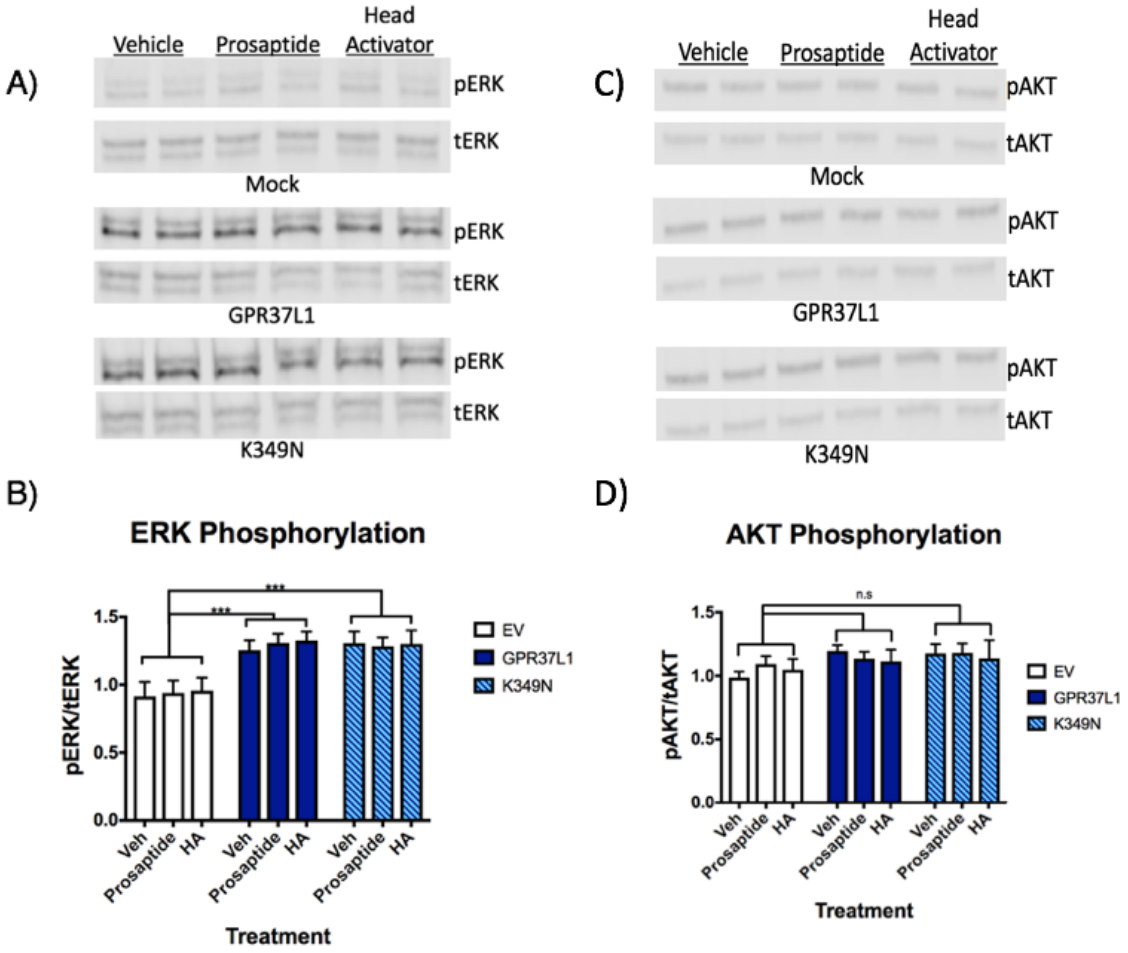
A)
Vehicle
Prosaptide
Head Activator
pERK
tERK
Mock
pERK
tERK
GPR37L1
pERK
tERK
K349N
C)
Vehicle
Prosaptide
Head Activator
pAKT
tAKT
Mock
pAKT
tAKT
GPR37L1
pAKT
tAKT
K349N
B)
ERK Phosphorylation
pERK/tERK
1.5
1.0
0.5
0.0
***
***
EV
GPR37L1
K349N
Veh
Prosaptide
HA
Treatment
D)
AKT Phosphorylation
pAKT/tAKT
n.s
EV
GPR37L1
K349N
Veh
Prosaptide
HA
Treatment

Figure 2-5. GPR37L1 WT and K349N variant increase basal ERK phosphorylation, but show no response to previously reported ligands, prosaptide and head activator

HEK-293T cells transiently transfected with GPR37L1 or K349N variant exhibited increased levels of ERK phosphorylation (A & B) compared to cells transfected with empty vector (EV). In contrast, receptor transfection did not affect phosphorylation of AKT (C & D). At 48h post transfection, cells were treated with 100nM prosaptide, 100nM head activator peptide (HA) or vehicle for 10 minutes at 37˚C. Neither treatment significantly increased ERK or AKT phosphorylation. Results shown are from 3-5 independent experiments (± SEM shown. Two-way ANOVA followed by Tukey's post-hoc analyses, ***p<.001).

A)

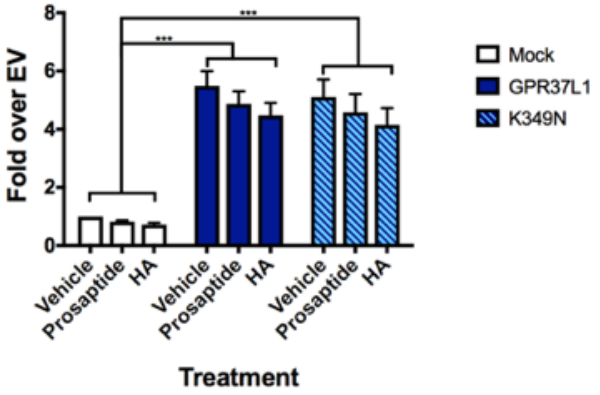
CRE Luciferase
Fold over EV
8
6
4
2
0
***
***
Vehicle
Prosaptide
HA
Vehicle
Prosaptide
HA
Vehicle
Prosaptide
HA
Treatment
Mock
GPR37L1
K349N

B)

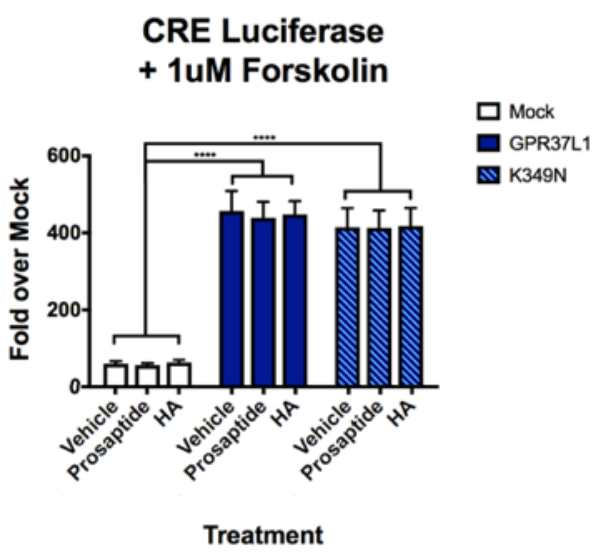
CRE Luciferase
+ 1uM Forskolin
Fold over Mock
600
400
200
0
****
****
Vehicle
Prosaptide
HA
Vehicle
Prosaptide
HA
Vehicle
Prosaptide
HA
Treatment
Mock
GPR37L1
K349N

C)

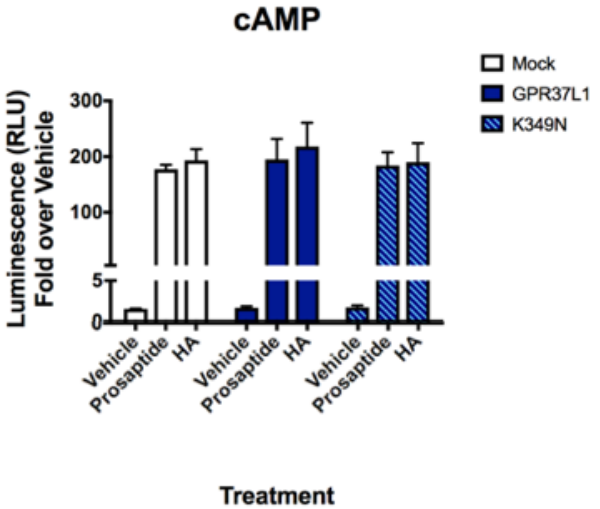
cAMP
Luminescence (RLU)
Fold over Vehicle
300
200
100
5
0
Vehicle
Prosaptide
HA
Vehicle
Prosaptide
HA
Vehicle
Prosaptide
HA
Treatment
Mock
GPR37L1
K349N

Figure 2-6. No difference in signaling to cAMP or the cAMP response element (CRE) between GPR37L1 WT and K349N variant

HEK-293T cells transiently transfected with GPR37L1 or K349N mutant exhibited significant constitutive signaling activity to CRE luciferase in the absence (A) or presence (B) of 1nM forskolin treatment for 2 hours. Neither prosaptide or HA modulated this signaling. (C) HEK cells stably transfected with the GloSensor plasmid and transiently transfected with empty vector, GPR37L1 or K349N exhibited no transient cAMP response when treated with vehicle or prosaptide for 15 minutes. Experimental values were divided by a pre-read measurement taken prior to compound delivery to determine transient fold response. Results shown are from 3-5 independent experiments (± SEM shown. Two-way ANOVA followed by Tukey's post-hoc analyses, ***p<.001).

A)

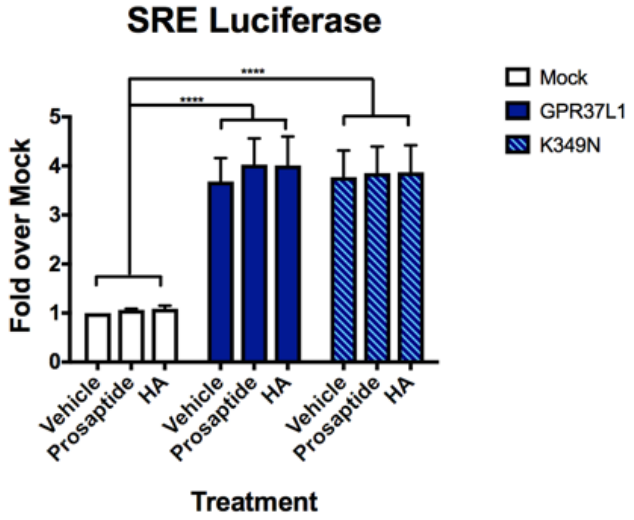
SRE Luciferase
Mock
GPR37L1
K349N
****
****
Fold over Mock
0
1
2
3
4
5
Vehicle
Prosaptide
HA
Vehicle
Prosaptide
HA
Vehicle
Prosaptide
HA
Treatment

B)

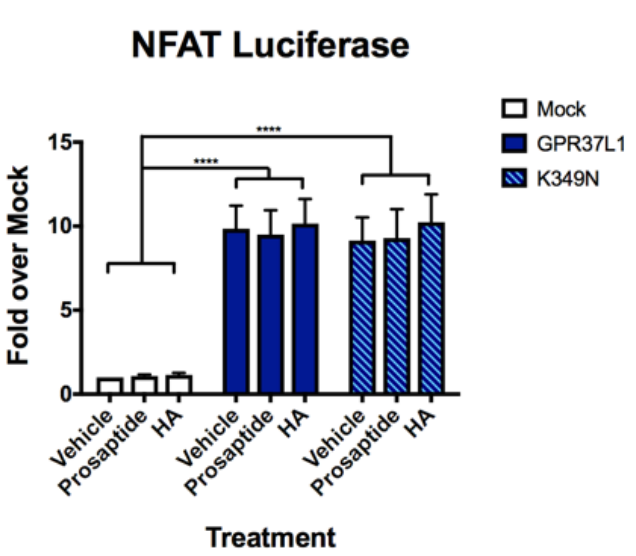
NFAT Luciferase
Mock
GPR37L1
K349N
****
****
Fold over Mock
0
5
10
15
Vehicle
Prosaptide
HA
Vehicle
Prosaptide
HA
Vehicle
Prosaptide
HA
Treatment

C)

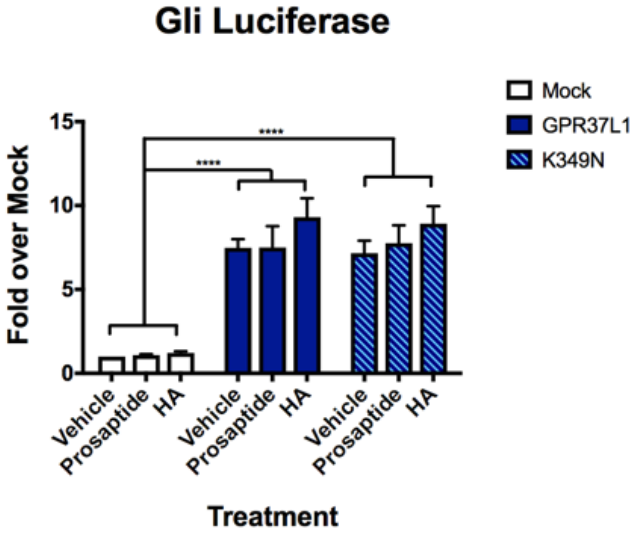
Gli Luciferase
Mock
GPR37L1
K349N
****
****
Fold over Mock
0
5
10
15
Vehicle
Prosaptide
HA
Vehicle
Prosaptide
HA
Vehicle
Prosaptide
HA
Treatment

Figure 2-7. No difference in constitutive signaling between GPR37L1 WT and K349N mutant in HEK293T cells

HEK-293T cells transiently transfected with GPR37L1 or K349N mutant exhibited increased levels of constitutive signaling to SRE (A), NFAT (B), and Gli (C) compared to cells transfected with empty vector (EV). At 48h post transfection, cells were treated with 100nM prosaptide, 100nM head activator peptide (HA) or vehicle for 10 minutes at 37˚C. Neither treatment significantly affected signaling. Results shown are from 3-5 independent experiments (± SEM shown. Two-way ANOVA followed by Tukey's post-hoc analyses, ****p<.0001).

A)

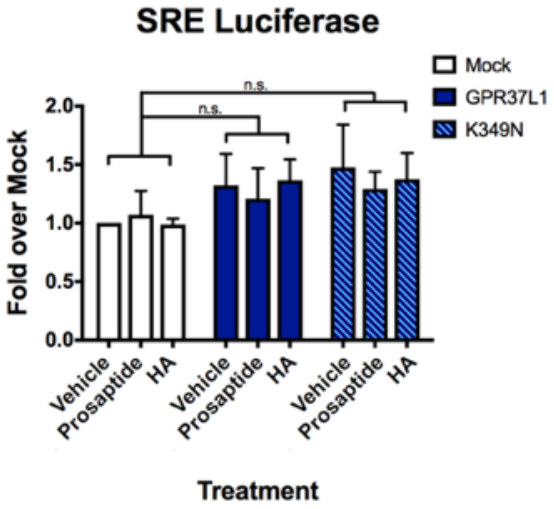
SRE Luciferase
Mock
GPR37L1
K349N
n.s.
n.s.
Fold over Mock
2.0
1.5
1.0
0.5
0.0
Vehicle
Prosaptide
HA
Vehicle
Prosaptide
HA
Vehicle
Prosaptide
HA
Treatment

B)

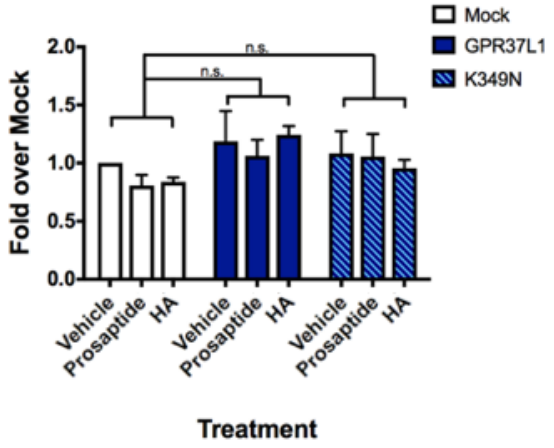
NFAT Luciferase
Mock
GPR37L1
K349N
n.s.
n.s.
Fold over Mock
2.0
1.5
1.0
0.5
0.0
Vehicle
Prosaptide
HA
Vehicle
Prosaptide
HA
Vehicle
Prosaptide
HA
Treatment

C)

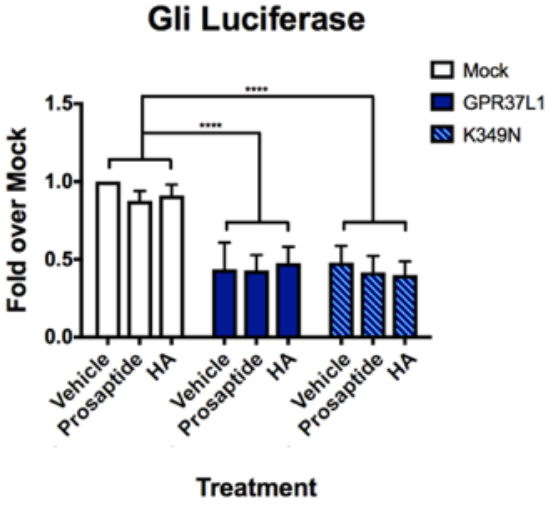
Gli Luciferase
Mock
GPR37L1
K349N
****
****
Fold over Mock
1.5
1.0
0.5
0.0
Vehicle
Prosaptide
HA
Vehicle
Prosaptide
HA
Vehicle
Prosaptide
HA
Treatment

Figure 2-8. No difference in constitutive signaling between GPR37L1 WT and K349N mutant in a neuronal-like cell line

N2a cells transiently transfected with wild-type GPR37L1 or K349N mutant did not exhibit significantly different levels of constitutive signaling to SRE (A) or NFAT (B) compared to cells transfected with empty vector (EV). Conversely, expression of GPR37L1 or K349N significantly reduced constitutive Gli signaling (C) compared to cells transfected with empty vector (EV). At 48h post transfection, cells were treated with 100nM prosaptide, 100nM head activator peptide (HA) or vehicle for 10 minutes at 37˚C. Neither treatment significantly affected signaling. Results shown are from 3-5 independent experiments (± SEM shown. Two-way ANOVA followed by Tukey's post-hoc analyses, ***p<0.001****p<.0001).

2.3.4 GPR37L1 is ubiquitinated in HEK293T cells, and the K349N substitution does not alter ubiquitination

We next assessed the regulation of GPR37L1 WT and K349N mutant by ubiquitination and interaction with other proteins. As GPR37L1 is known to be ubiquitinated (Imai et al. 2001) and ubiquitination occurs on lysine residues, we investigated whether mutation of lysine 349 might alter ubiquitination of GPR37L1. However, GPR37L1 WT and the K349N mutant were found to be ubiquitinated to a similar extent (Figure 2-9).

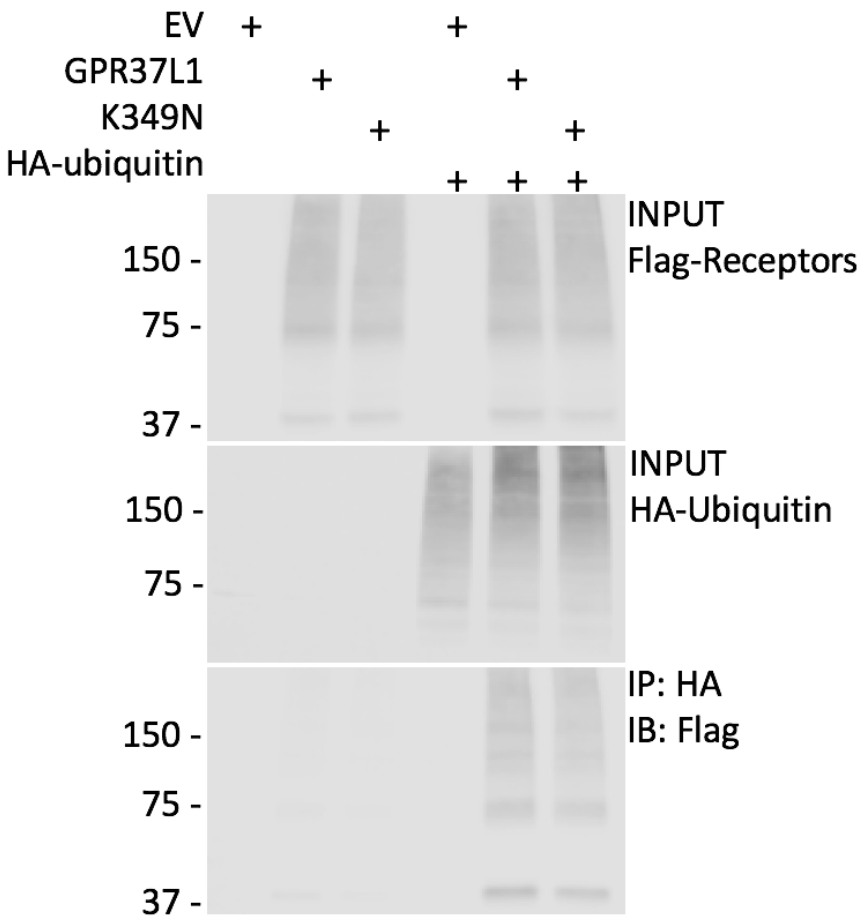

Figure 2-9. No difference in ubiquitination between GPR37L1 WT and K349N mutant

Loss of the lysine residue in the K349N mutant did not affect ubiquitination of the receptor in HEK293T cells. Trasiently transfected Flag-GPR37L1 wild-type and Flag-K349N mutant are ubiquitinated in HEK293T cells as measured by coimmunoprecipitation. Results shown are representative of three independent experiments.

2.3.6 *The K349N substitution does not disrupt association of GPR37L1 with ß-arrestin2 in HEK293T cells*

Although we did not observe ligand induced signaling, both GPR37L1 and the K349N variant increased signaling in many of our assays, suggesting constitutive activity or the presence of an unknown ligand in the media. It is well-known that sustained receptor activation can lead to receptor desensitization (Sterne-Marr and Benovic 1995; Hausdorff, Caron, and Lefkowitz 1990; Ferguson et al. 1998; Lefkowitz 1998; Claing et al. 2002; Perry and Lefkowitz 2002; Gainetdinov et al. 2004). Desensitization is primarily achieved via receptor phosphorylation, which promotes the recruitment of ß-arrestins and subsequent internalization of the receptor (Lohse et al. 1990; Goodman et al. 1996). Thus, we expected that the GPR37L1 might constitutively associate with ß-arrestin.

In addition to promoting receptor desensitization and internalization, ß-arrestins are capable of inducing G-protein-independent signaling (Luttrell et al. 1999; DeWire et al. 2007; Smith and Rajagopal 2016). Therefore, alterations in binding of K349N to ß-arrestin might suggest a mechanism by which the mutation could disrupt GPR37L1 function. However, while both GPR37L1 WT and the K349N mutant were found to bind ß-arrestin2, there was no difference in binding between the two versions of the receptor (Figure 2-9).

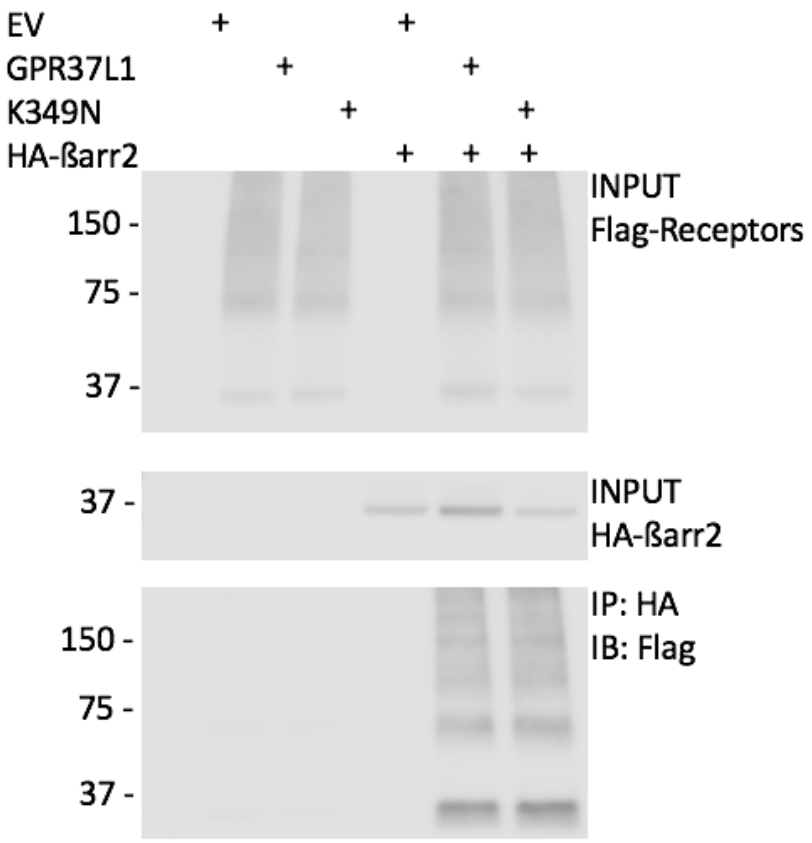

Figure 2-10. GPR37L1 WT and the K349N mutant bind robustly to ß-arrestin2

Traniently transfected GPR37L1 or K349N mutant robustly bind ß-arrestin2 in HEK293T cells as measured by coimmunoprecipitation of Flag-tagged receptors with HA-ß-arrestin2. Results shown are representative of 3-5 independent experiments.

2.3.5 GPR37L1 and K349N are preferentially degraded by the autophagy-lysosome pathway

Following ß-arrestin binding and subsequent internalization, GPCRs can be recycled back to the cell surface or directed to the lysosomal for degradation (Marchese et al. 2008). Disruption of the recycling/degradation pathway can lead to alterations in cell signaling. In mammalian cells, there are two main pathways for degradation of proteins: the autophagy-lysosome pathway and the ubiquitin-proteasome system (Yorimitsu and Klionsky 2005; Ciechanover 2006). To identify the pathway through which GPR37L1 is preferentially degraded, and to assess the effect of the K349N mutation on receptor degradation, we utilized four proteasomal or autophagy-lysosome inhibitors and measured the change in receptor expression. Inhibition of the proteasome with MG132 or Lactacystin had no significant effects on GPR37L1 or the K349N variant. However, treatment with Bafilomycin, an inhibitor of the acidification of lysosomes that blocks the autophagy-lysosome pathway, significantly increased GPR37L1 and K349N expression to a comparable extent (Figure 2-11). Treatment with another inhibitor of the autophagy-lysosome pathway, thapsigargin, which does not affect autophagosome formation but blocks autophagosome fusion with lysosomes (Ganley et al. 2011), also exhibited a trend toward increased receptor expression, although these results were not statistically significant.

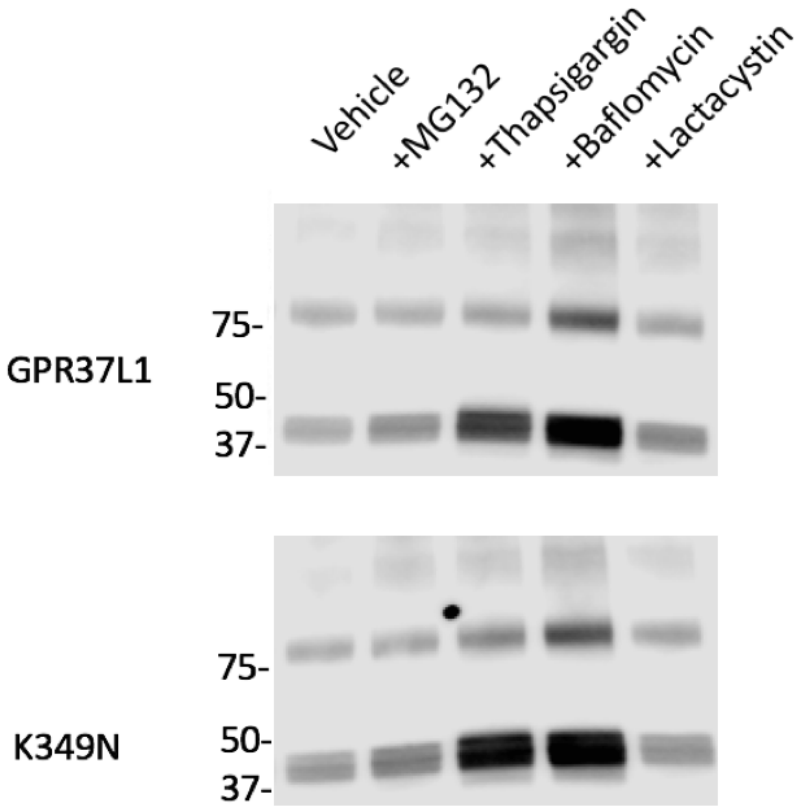
Vehicle
+MG132
+Thapsigargin
+Baflomycin
+Lactacystin
GPR37L1
75-
50-
37-
K349N
75-
50-
37-

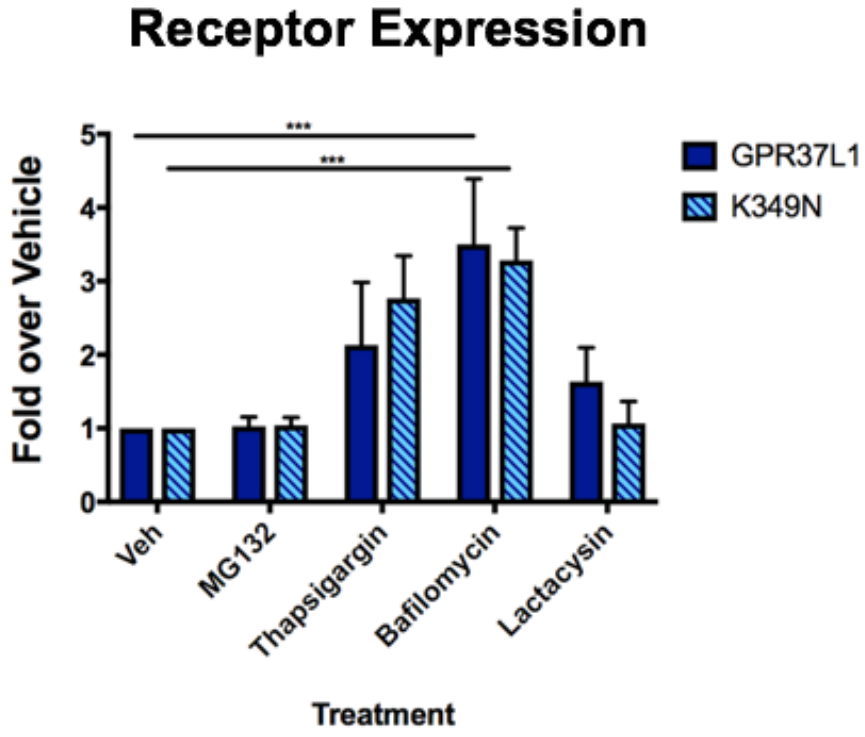
Receptor Expression
Fold over Vehicle
0
1
2
3
4
5
***
***
GPR37L1
K349N
Veh
MG132
Thapsigargin
Bafilomycin
Lactacysin
Treatment

Figure 2-11. Expression of GPR37L1 WT and the K349N variant is regulated by lysosomal degradation

(A & B) Expression of GPR37L1 WT and the K349N variant in stably transfected HEK293T cells is comparably enhanced following treatment with the lysosomal inhibitor bafilomycin (10 nM). Conversely, overnight treatment of stably-transfected HEK293T cells with proteosomal inhibitors 100nM MG132 or 500nM Lactacystin, and Thapsigargin (100μM), which blocks autophagosome–lysosome fusion, did not significantly increase receptor expression. Two-way ANOVA followed by Tukey's multiple comparisons post-hoc analyses, ***$p<0.001$

2.3.6 Mice lacking Gpr37L1, Gpr37 or both receptors, are susceptible to 6 Hz induced seizure

While no significant differences were observed between GPR37L1 WT and the K349N variant *in vitro*, it is possible that the K349N variant results in alterations in ligand-induced signaling, resulting in a reduction or loss of receptor function. Without a functional ligand, it is not feasible to address this possibility *in vitro*. Therefore, to shed light on whether loss of GPR37L1 function can affect seizure susceptibility *in vivo*, mice lacking a single copy (*Gpr37L1*$^{+/-}$) or both copies of *Gpr37L1* (*Gpr37L1*$^{-/-}$) were evaluated in seizure-induction paradigms. As *GPR37L1* shares 68% similarity with *GPR37*, it is likely that these two receptors share the same ligand and perhaps also share redundant functions *in vivo*. Thus, in parallel experiments, mice lacking a single copy (*Gpr37*$^{+/-}$) or both copies of GPR37 (*Gpr37*$^{-/-}$), and double-knockout mice lacking both receptors (DKO), were also assessed in the same paradigms.

The effects of *Gpr37* and/or *Gpr37L1* deletions were first examined using the 6 Hz psychomotor seizure induction model. Interestingly, a greater number of *Gpr37L1*$^{-/-}$ mice exhibited more severe seizures compared to WT and *Gpr37L1*$^{+/-}$ littermates at 27 mA (Figure 2-12 A). Of the *Gpr37L1*$^{-/-}$ mice tested at 27mA, 5 did not seize (RS0), and among the other mice, 2 RS1, 11 RS2 and 3 RS3 seizures were observed. In contrast, for the WT littermates, the Racine scores were 9 RS0, 7 RS1, 5 RS2 and 1 RS3. Similarly, for the *Gpr37L1*$^{+/-}$ mice, the

Racine scores were 10 RS0, 5 RS1, 6 RS2, and 1 RS3. All 3 genotypes had similar seizure responses at 18 and 22mA, although 3 *Gpr37L1*$^{-/-}$ exhibited RS3 seizures at 22mA.

Gpr37$^{-/-}$ mice were significantly more susceptible to 6 Hz-induced seizures compared to WT and *Gpr37*$^{+/-}$ littermates at 22 and 27mA (Figure 2-12B). At 22mA, 13/18 *Gpr37*$^{-/-}$ mice exhibited RS2 seizures while 5 did not seize (RS0). In contrast, 13/18 WT littermates did not have a seizure. While not statistically significant, a greater number of *Gpr37*$^{+/-}$ exhibited more severe RS2 seizures compared to WT littermates at 18 and 22mA. Both *Gpr37*$^{+/-}$ and *Gpr37*$^{-/-}$ mice exhibited increased seizure susceptibility ($p < 0.05$) compared to WT littermates at the highest test current (27mA) although susceptibility was comparable between the two groups of mutants. At 27mA, 16/18 *Gpr37*$^{+/-}$ and 14/18 *Gpr37*$^{-/-}$ exhibited a seizure whereas only 8/16 WT littermates exhibited a seizure, 3 of which were mild (RS1). Strikingly, at all three test currents, mice lacking both Gpr37L1 and Gpr37 (DKO) exhibited either RS2 or RS3 seizures and were therefore significantly more susceptible compared to age-matched WT mice (Figure 2-12C). Furthermore, compared to *Gpr37L1*$^{-/-}$ and *Gpr37*$^{-/-}$ animals, DKO mice also demonstrated higher average Racine scores at each test current (Figure 2-12D).

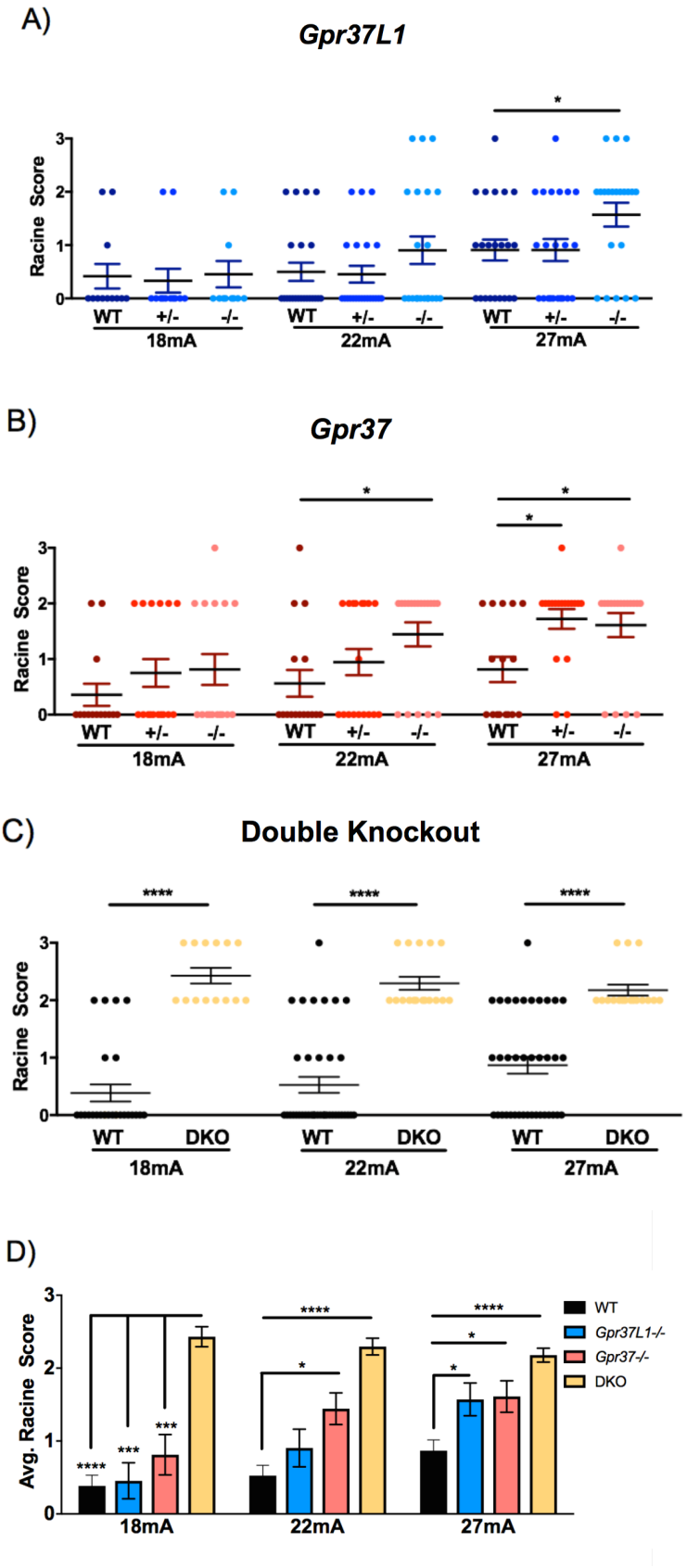
A)
Gpr37L1
Racine Score
WT
+/-
-/-
18mA
22mA
27mA
B)
Gpr37
C)
Double Knockout
DKO
D)
Avg. Racine Score
WT
Gpr37L1-/-
Gpr37-/-
DKO

Figure 2-12. Loss of *Gpr37L1* and/or *Gpr37* in vivo increases susceptibility to 6 Hz-induced seizures

(A) *Gpr37L1*$^{-/-}$ mice exhibited increased susceptibility to 6-Hz-induced seizures compared to wild-type (WT) and *Gpr37*$^{+/-}$ littermates at 27mA (*N* = 11–22/genotype/current). (B) *Gpr37*$^{-/-}$ mice exhibited significantly increased seizure susceptibility compared to their WT and *Gpr37*$^{+/-}$ littermate controls at 22 mA, whereas both *Gpr37*$^{+/-}$ and Gpr37$^{-/-}$ mice had significantly higher susceptibility to 6 Hz-induced seizures at 27mA (*N* = 16–18/genotype/current). (C) Mice lacking both receptors (DKO) exhibited increased seizure susceptibility compared to age-matched WT mice at all currents tested (*N* = 14–38/genotype/current) (D) DKO mice exhibited increased susceptibility to 6 Hz-induced seizures compared to WT controls and homozygous mutants at 18mA. *Gpr37*$^{-/-}$ and DKO mice displayed higher susceptibility compared to WT controls at 22mA. All homozygous mutants and DKO mice exhibited increased seizure susceptibility compared to WT at 27mA. One-way ANOVA followed by Dunn's multiple comparisons post-hoc analyses. *p < 0.05, **p < 0.01, ***p < 0.001, ****p < .0001.

2.3.7 Mice lacking GPR37L1, but not GPR37, are more susceptible to Flurothyl induced seizure

Given that the most dramatic differences in the 6 Hz paradigm were observed with the homozygous knockout mice, we next compared susceptibility to flurothyl-induced seizures in homozygous knockout mice and WT littermates. *Gpr37L1*$^{-/-}$ and DKO mice exhibited significantly decreased latencies to both the first myoclonic jerk (MJ) (Figure 2-13A) and generalized tonic-clonic seizure (GTCS) (Figure 2-13B). In contrast, *Gpr37*$^{-/-}$ mice exhibited latencies comparable to WT littermates at each seizure event.

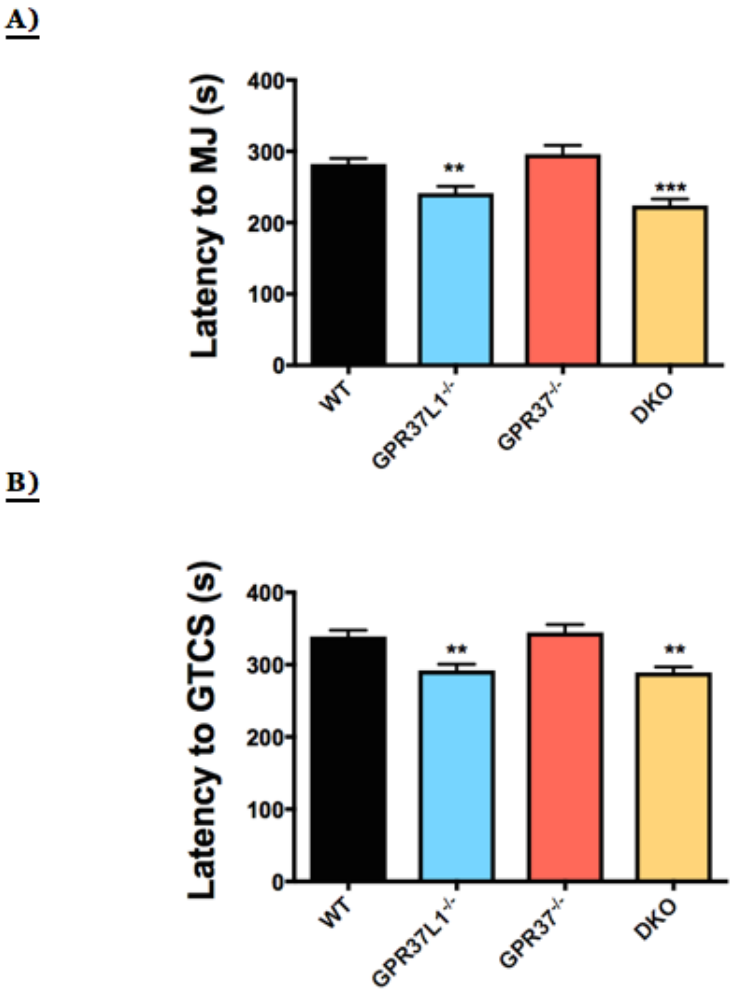

Figure 2-13. Loss of Gpr37L1 but not Gpr37 in vivo decreases susceptibility to flurothyl-induced seizures

(A & B) *Gpr37L1*$^{-/-}$ mice exhibited decreased latency to first myoclonic jerk (MJ) and generalized tonic-clonic seizure (GTCS) compared to WT littermates. Latency to the MJ and GTCS were comparable between *Gpr37L1*$^{-/-}$ and DKO mice. *Gpr37*$^{-/-}$ mice were not significantly different from WT littermates. One-way ANOVA, Dunnett's post hoc, *$p < 0.001$, 10–42 animals/genotype.

2.3.8 Mice lacking both GPR37L1 and GPR37 have spontaneous seizures

Finally, to assess whether the knockout mice exhibit spontaneous seizures, we obtained two weeks of continuous video/EEG recordings for *Gpr37L1*$^{-/-}$, *Gpr37*$^{-/-}$, and DKO mice. Spontaneous seizures were not observed in the five *Gpr37L1*$^{-/-}$ mice examined. However, seizures were detected in 2/5 Gpr37$^{-/-}$ and 4/5 DKO mice (Figure 2-14A). Furthermore, the average duration of the seizures was significantly longer in mice lacking both receptors (Figure 2-14B). Examination of video recordings revealed that spontaneous seizures were accompanied by abnormal behaviors, which began with rearing, paw waving, and head bobbing at seizure onset with subsequent progression to generalized tonic-clonic seizure and loss of posture. Motor activity during the seizure is indicated by increased EMG activity (Figure 2-14C).

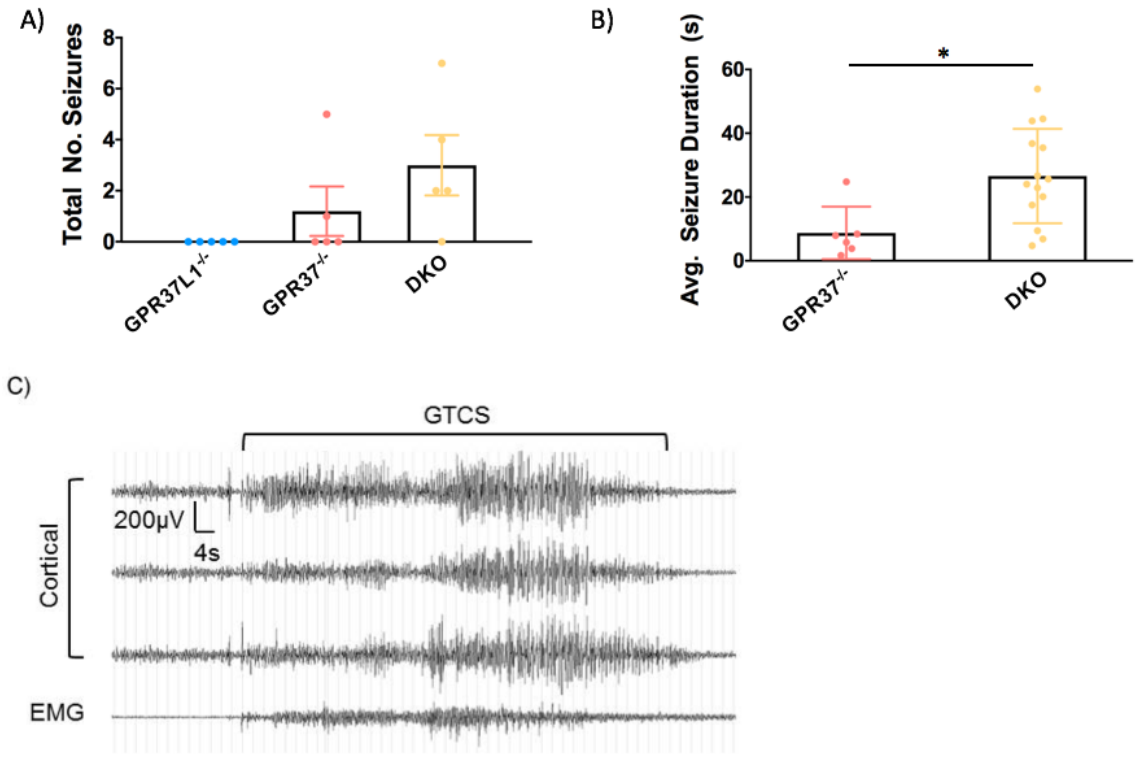

Figure 2-14. *Gpr37-/-* and DKO mice exhibit spontaneous seizures

(A) Spontaneous seizures were observed in *Gpr37*$^{-/-}$ and DKO mice (N = 5/genotype). (B) Mice lacking both receptors exhibited significantly longer spontaneous seizure duration compared to *Gpr37*$^{-/-}$ mice. (C) Representative EEG trace of a spontaneous seizure. One-way ANOVA, Dunnett's post hoc, *p < .05.

2.4 Summary and Discussion

Through the experiments discussed in this chapter, we describe the evaluation of a *GPR37L1* variant identified in a family with a novel progressive myoclonus epilepsy (PME). The homozygous autosomal recessive variant (c.1047G>T, [Genebank NM_004767.3]) identified in the proband (VI:9), and results in a K349N substitution in the third intracellular loop of the receptor. Individuals VI:8 and VI:10, found to be heterozygous and wild type, respectively, are well beyond the age of presentation of all their siblings and are considered clinically unaffected. The youngest members, and the only males in the sibship (VI:11 and VI:12), were also found to be homozygous for the *GPR37L1* variant. To date, these youngest individuals have not had a clinical presentation of PME but have exhibited abnormal neurological symptoms: VI:11 has had daily recurrent headaches, two abnormal EEGs, and visual disturbances, while VI:12 has reported daily recurrent headaches (no EEG performed). Interestingly, VI:11, who at the time of the present study is 16 years of age, is beyond the average age of seizure onset of his sisters and cousin. While there are well-known neurodevelopmental differences between males and females (Giatti et al. 2012), and previous studies have identified *GPR37L1* as differentially expressed between the sexes (Shi, Zhang, and Su 2016), further observation of the youngest siblings will be required to determine if any sex differences exist in this case.

We and others have shown that expression of GPR37L1 and/or GPR37 can mediate cytoprotective effects *in vitro* (Lundius et al. 2013; Meyer et al. 2013).

Therefore, it is possible that these receptors play important roles in mediating protective effects following insult or injury *in vivo*. No differences were observed between GPR37L1 WT and the K349N mutant in terms of receptor expression, localization, constitutive signaling, or regulation in HEK293T, N2a cells or NIH-3T3 cell lines *in vitro*. The natural ligand for GPR37L1 remains uncertain, and in the studies described here, we assessed two peptides that have been proposed as ligands for GPR37L1 and/or GPR37: prosaptide (Meyer et al. 2013; Meyer et al. 2014; Lundius et al. 2014) and head activator (Rezgaoui et al. 2006; Gandia et al. 2013). However, no significant increases in receptor signaling activity were observed with either peptide, and therefore, the previously-reported agonistic actions of these two peptides could not be confirmed here. It is possible that the regulation of GPR37/GPR37L1 signaling activity by these peptides is dependent on cellular context and/or other variables, although another recent study also reported a lack of activation of GPR37L1 signaling by prosaptide (Coleman et al. 2016). Thus, while the *in vitro* data described here cannot confirm the pathogenicity of the K349N variant, it is plausible that functional differences between GPR37L1 WT and the K349N mutant may be observed only with agonist-induced signaling. More generally, it is possible that the K349N variant may perturb GPR37L1 function in ways that are not easily testable at present using *in vitro* models of receptor trafficking and signaling activity. Therefore, even though no striking effects of the K349N mutation on receptor function were observed in the *in vitro* studies, we assessed the importance of GPR37L1 for seizure susceptibility *in vivo*.

Until the present work, seizure susceptibility had not been evaluated in mice lacking *Gpr37L1* and/or *Gpr37*. Indeed, mice lacking both receptors had not previously been described at all. In the 6 Hz seizure induction paradigm, *Gpr37L1*$^{-/-}$ mice displayed increased seizure susceptibility at the highest test current (27mA). However, *Gpr37L1*$^{+/-}$ and WT littermates had comparable seizure responses at each test current, which indicates that having a single copy of *GPR37L1* is sufficient to maintain normal susceptibility to 6 Hz-induced seizures. In contrast, *Gpr37*$^{+/-}$ and *Gpr37*$^{-/-}$ exhibited significantly increased seizure susceptibility at 27mA; therefore, reduced GPR37 expression results in altered seizure susceptibility. Given this finding, it is interesting to note that *GPR37* is one of six genes located within a heterozygous deletion that has been reported in an epilepsy patient (Heinzen et al. 2010). Another point of interest in the present study is that mice lacking both receptors exhibited markedly increased seizure susceptibility compared to WT controls at each test current. These results suggest that loss of both Gpr37L1 and Gpr37 has an additive effect in the DKO mice. This is particularly clear at 18mA, where DKO mice exhibit increased susceptibility to 6 Hz-induced seizures compared to WT controls, but both single homozygous mutants have normal seizure susceptibility.

In the flurothyl seizure induction paradigm, *Gpr37L1*$^{-/-}$ and DKO mice exhibited decreased latencies to both the MJ and GTCS, whereas *Gpr37*$^{-/-}$ mice were not significantly different from WT littermates. This result suggests that loss of GPR37L1 drives the decreased susceptibility to flurothyl-induced seizures in the mice lacking both receptors. Considered together with the 6 Hz data, these

findings from the flurothyl studies suggest that GPR37L1 and GPR37 alter seizure susceptibility via different mechanisms. The 6 Hz paradigm is a model of limbic seizures, whereas flurothyl-induced seizures are generalized. Finally, spontaneous seizures were observed in both *Gpr37*$^{-/-}$ and DKO mice, which is consistent with the 6 Hz results in which GPR37 appeared to be the major contributor to the dramatic increase in seizure susceptibility in the mice deficient for both receptors.

Taken together, the data presented here represent the first evidence linking *GPR37L1* and *GPR37* to seizure etiology. Future work will focus on elucidating the cellular mechanism(s) underlying the observed increases in seizure susceptibility and assessing cell-specific effects of the GPR37L1 K349N mutation in native cell types. The findings presented here set the stage for future studies that will shed light on the functional roles of these receptors in the brain and provide new insights into the pathogenesis and potential treatment of progressive myoclonus epilepsies.

CHAPTER 3:

Loss of GPR37 Results in Increased Infarct Volume and Altered Astrocytic Response in Models of Stroke

Author contributions: All protein studies and *in vitro* experiments described in this chapter were designed by M.M. Giddens and R.A. Hall and performed by M.M Giddens. The middle cerebral occlusion MCAO studies and TTC staining were designed by S.P. Yu, L.Wei, X Gu, M. Giddens and R.A. Hall, and performed by X. Gu. Penumbra tissue was harvested by M.Q. Jiang.

3.1 Rationale

Stroke is a leading cause of death worldwide (Donnan et al. 2008) and ischemic stroke, caused by occlusion of blood vessels in the brain, underlies more than 80% of all stroke cases (Roger et al. 2012). Within minutes of insufficient blood flow, ionic homeostasis within the brain is disrupted. Continued interruption of blood flow leads to energy failure, neuronal depolarization, elevation in intracellular calcium concentrations, release of glutamate and subsequent excitotoxicity (Ceulemans et al. 2010; Dirnagl, Iadecola, and Moskowitz 1999; Barone and Feuerstein 1999). These effects are accompanied by cellular edema and the generation of reactive oxygen species, which can promote further cell damage and death via oxidative cell stress (Dirnagl, Iadecola, and Moskowitz 1999; Ceulemans et al. 2010). In the hours and days after an ischemic insult, the acute consequences result in apoptotic cell death, increased proteolytic activity, and the initiation of neuroinflammatory responses (Dirnagl, Iadecola, and Moskowitz 1999; Barone and Feuerstein 1999; Hossmann 2006; Ceulemans et al. 2010).

Following ischemic stroke, two distinct regions of damage develop: *i)* the ischemic core, the area most severely affected, which is the result of a complete or near-complete loss of blood flow, and *ii)* the peri-infarct region, or penumbra, where blood flow is diminished but not absent. Cell death is effectively irreversible within the core. The penumbra region is the primary target for therapeutic interventions, as cells within the penumbra have the capacity for

recovery (Hossmann 1994; Dirnagl, Iadecola, and Moskowitz 1999; De Keyser et al. 2005; Hossmann 2006). Oxidative stress and excitotoxicity are major contributors to cell death following an ischemic insult (Wong and Crack 2008; Hossmann 1996; Dirnagl, Iadecola, and Moskowitz 1999). As expression of GPR37 is protective against oxidative stress (Meyer et al. 2013), and may contribute to resistance against excitotoxicity, we sought to assess the role of GPR37 in models of stroke.

To assess the effect of GPR37 in ischemic stroke, we compared WT and *Gpr37*$^{-/-}$ littermates in a focal cerebral ischemia model. Cortical ischemia was achieved by permanent occlusion of the distal branches of the right middle cerebral artery supplying the sensorimotor cortex. This model results in a consistent cortical infarction, comparable to damage imposed by most human ischemic strokes (Llovera et al. 2014). As loss of *Gpr37* resulted in a larger infarct volume compared with WT littermate controls, we explored the mechanisms involved by assessing expression of GPR37, the closely related receptor Gpr37L1, hypoxia inducible factor 1α (HIF1α) and markers of microglia and astrocytes in the penumbra of WT and *Gpr37*$^{-/-}$ following MCAO. To further assess the role of GPR37 in astrocytes in a model of stroke, we compared cultured astrocytes from WT and *Gpr37*$^{-/-}$ following oxygen glucose deprivation/reperfusion (OGD/R). Together, these experiments have begun to suggest a role for GPR37 in the astrocytic response in models of stroke.

3.2 Experimental Methods

3.2.1 Generation of Knockout Mice and Maintenance of Mouse Colony

Gpr37 knockout mice (*Gpr37*$^{-/-}$) were obtained from Jackson Laboratory (strain Gpr37^{tm1Dgen}, stock number 005806). The mouse line was backcrossed with wild-type C57BL/6J mice (Jackson Laboratory) for 10 generations to ensure uniformity of genetic background. Genetic deletion of *Gpr37* was confirmed by DNA sequencing, and loss of GPR37 protein expression was confirmed by Western blotting of brain tissue samples with specific anti-GPR37 antibodies (MAb Technologies).

All mice were maintained on a C57BL/6J background and housed on a 12-h light/dark cycle, with food and water available *ad libitum*. All experiments were performed in accordance with the guidelines of the Institutional Animal Care and Use Committee of Emory University. Wild-type (WT) littermates were used as controls for experiments. In all experiments, the experimenter was blinded to the genotypes of the animals.

3.2.2 Induction of a Focal Cortical Ischemic Stroke

A focal cerebral ischemic stroke targeting the right sensorimotor cortex was induced as previously described (Jiang et al. 2016). Before and after surgery, the animals were housed at 4-5 animals per cage, with ad libitum access to food and water.

3.2.3 Infarct Volume Measurement

Mice were sacrificed 72 hours after the onset of MCAO, for quantification of brain infarct volume by 2,3,5-triphenyltetrazolium chloride (TTC; Sigma-Aldrich) staining. Brains were removed and placed in a brain matrix and sliced into 1-mm coronal sections. Slices were incubated in 2% TTC solution at 37˚C for 5 minutes, then stored in 10% buffered formalin for 24 h. Digital images of the caudal aspect of each slice were obtained by a flatbed scanner. Infarct, ipsilateral hemisphere, and contralateral hemisphere areas at different levels were measured using ImageJ software (NIH, Bethesda, MD, USA). The indirect method (subtraction of residual right hemisphere cortical volume from cortical volume of the intact left hemisphere) was used for total infarct volume calculation. Infarct measurements were performed under double-blind conditions

3.2.4 Western Blotting

The peri-infarct/penumbra region was defined as a 500-μm boundary extending from the edge of the infarct core, medial, and lateral to the infarct. Tissue samples were taken from the peri-infarct/penumbra region of the cortex, and proteins were extracted by homogenization in protein lysis buffer (1% Triton X- 100, 10 mM Hepes, 50 mM NaCl, 5 mM EDTA, and protease inhibitor cocktail (Roche Diagnostics)). Protein samples were reduced and denatured in Laemmli buffer, loaded into 4-20% Tris-Glycine gels (Bio-Rad) for SDS-PAGE, and then transferred to nitrocellulose membranes (Bio-Rad). Blots were blocked with 5%

milk (in 50mM NaCl, 10mM HEPES, pH 7.3 with 0.1% Tween-20 (Sigma)). Primary antibodies GPR37 and GPR37L1 (MAb Technologies); HIF1α (Novus Biologicals); Iba1 (Wako); GFAP (Invitrogen); and GAPDH antibody (Millipore) were applied overnight at 4°C. Protein quantification was done using densitometry, performed with ImageJ software.

3.2.5 Cell Culture

Cortical astrocytes cultures were generated from C57BL/6 mice between postnatal day 1-5. Cortices were isolated, separated from the meninges, minced and dissociated with 0.25% trypsin + EDTA at 37 degrees Celsius and 5% CO_2. After 5 minutes, 600 U DNase was added, immediately followed by DMEM supplemented with 10% (vol/vol) FBS and 100µg/ml penicillin-streptomycin to inhibit trypsin activity. Tissue was triturated with a glass pipette approximately ten times and then centrifuged for 10 minutes at 100 × g. The resulting tissue pellet was resuspended in 15 mL of DMEM with FBS and penicillin-streptomycin and triturated approximately 20 times to fully homogenize the tissue and passed through a 100µm tissue strainer. Cells were plated in a poly-D-lysine-coated T75 flask and grown for 7-10 days at 37 degrees Celsius with 5% CO_2 to reach confluency. Once astrocytes formed a confluent monolayer they were split into two 6-well plates for experiments.

3.2.6 Oxygen Glucose Deprivation/Reperfusion

Astrocytes were rinsed 2X with DMEM without glucose (GIBCO) and then immersed in 1mL deoxygenated DMEM without glucose (GIBCO). Cells were placed inside a hypoxia chamber (Billups-Rothenberg Inc.) and flushed with a premixed gas (95 % N_2, 5 % CO_2). The hypoxia chamber was placed in a 37 °C incubator for 6 h. Control cultures were rinsed 2X with DMEM containing 5.5-mM D-glucose (GIBCO) and immersed in 1mL DMEM with glucose (GIBCO) and placed in 5 % CO_2 in air at 37 °C for 6 h. Following treatment both groups were rinsed 2X with DMEM wth glucose and immersed in 1mL DMEM with glucose and transferred to a CO_2 incubator (95 % air and 5 % CO_2) for 24 h reperfusion. Following reperfusion, the media was collected for cytotoxicity assays.

3.2.7 Cytotoxicity

To measure cytotoxicity, media from astrocyte cultures treated with OGD or controls was analyzed using the CytoTox 96 nonradioactive cytotoxicity assay per the manufacturer's instructions. Briefly, media samples were added to equal parts lactate dehydrogenase substrate in clear 96-well plates and incubated at 37 degrees Celsius in the dark for 30 minutes. Following incubation, the reaction was stopped and the plate was read at 490 nm to assess the colormetric change. Cell death was calculated using the following formula:

$$\frac{(Treatment\ LDH - Spontaneous\ Release\ LDH)}{(Total\ Kill\ LDH - Spontaneous\ Release\ LDH)}$$

3.3 Results

3.3.1 Loss of Gpr37 leads to increased infarct size in a cortical ischemic stroke model

To determine the contribution of GPR37 to stroke, we assessed the severity of a cortical ischemic stroke model in mice lacking *Gpr37*$^{-/-}$ compared to wild-type (WT) littermates. Permanent middle cerebral artery occlusion (MCAO) combined with seven minutes of common carotid artery (CCA) occlusion was used to induce a cortical ischemic stroke (Figure 3-1). Animals were sacrificed 72h after MCAO and the size of the infarct was assessed via 2,3,5-triphenyltetrazolium chloride (TTC), a measure of cell death. *Gpr37*$^{-/-}$ mice had a significantly larger infarct size than their WT littermates at 72h post MCAO (Figure 3-2A & B).

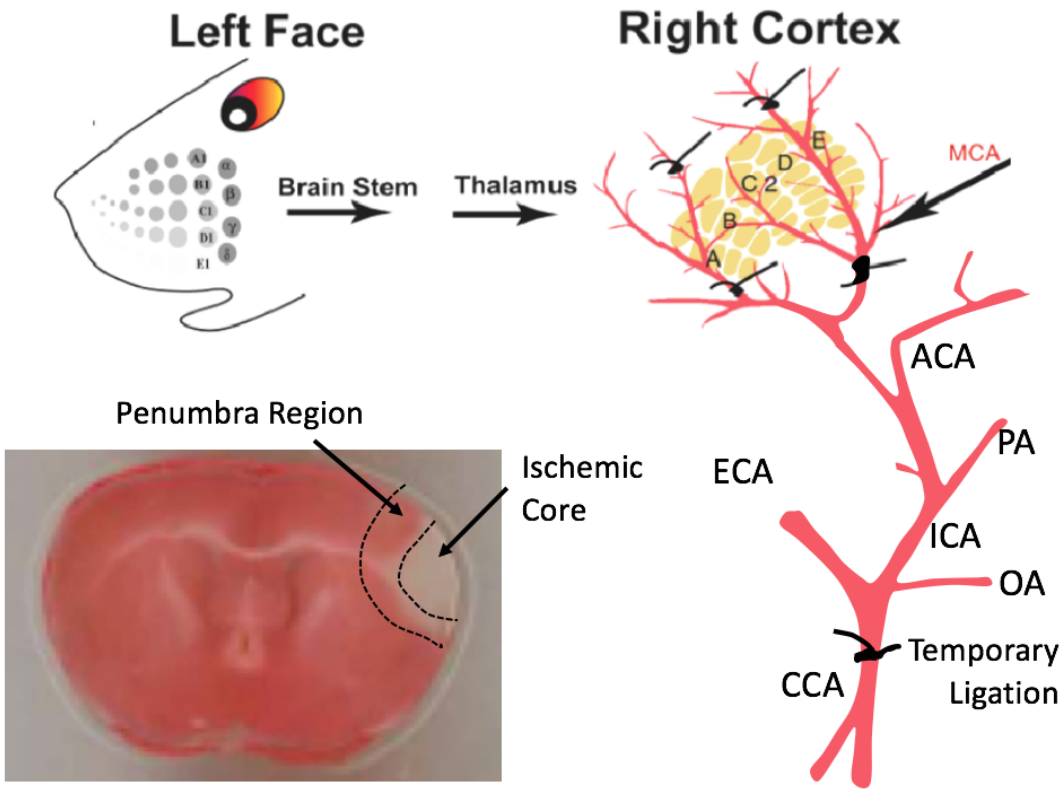

Figure 3-1. Schematic of induction of focal cerebral stroke in mice

Focal ischemic cerebral stroke was induced with permanent distal middle cerebral artery occlusion (MCAO) in combination with seven minutes of common carotid artery occlusion (CCAO). This paradigm results in an ischemic insult restricted to the right sensorimotor cortex, comparable in size to typical human ischemic stroke damage. The infarct consists of a region of permanent damage and cell death (core), and a region of hypoperfusion resulting in vulnerable tissue with partial or total loss of function and the potential for recovery (penumbra).

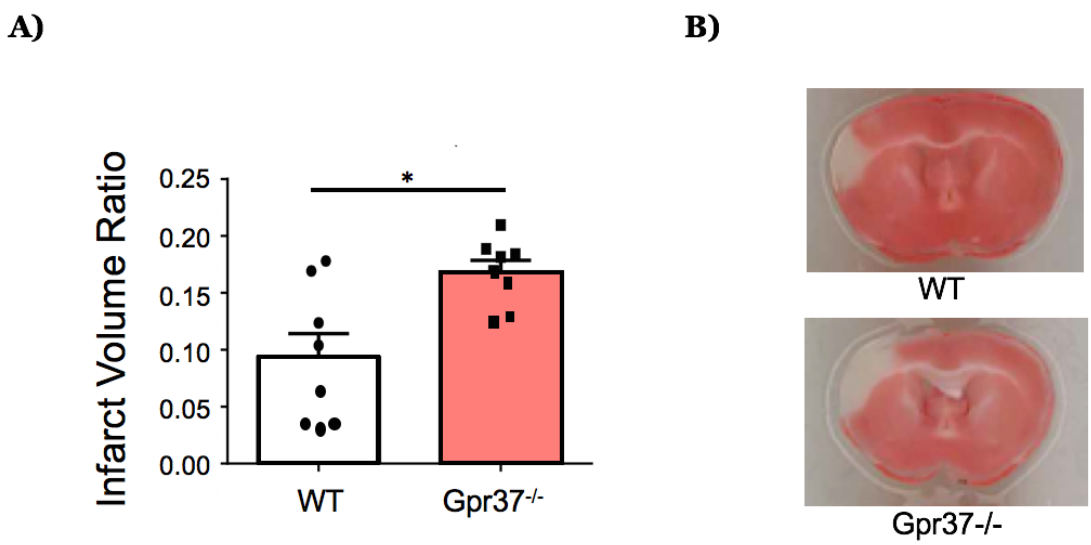

Figure 3-2. Mice lacking Gpr37 have a larger infarct volume than WT mice in the MCAO model

Cerebral infarct volume was assessed via 2,3,5-triphenyltetrazolium chloride (TTC) staining 72h after middle cerebral artery occlusion (MCAO) combined with seven minutes of common carotid artery (CCA) occlusion. Quantification of infarct volume (A). Representative image of TTC-stained brain slice in coronal section of WT and Gpr37$^{-/-}$ littermates (B). Infarct volume was calculated as ratio of contralateral volume and expressed as mean ± SEM (n = 8/group). *$p < 0.05$.

3.3.2 Expression of GPR37 is dramatically increased in the penumbra following MCAO while GPR37L1 expression is significantly reduced

To begin to characterize the mechanism underlying the increased infarct size observed in *Gpr37*$^{-/-}$ mice, we assessed Gpr37 expression in the penumbra region of WT and *Gpr37*$^{-/-}$ mice. In sham animals, tissue samples were obtained from a comparable cortical region. As expected, Gpr37 was not detected in the knockout mice (Figure 3-3A & B). However, while we could not detect significant levels of Gpr37 in WT sham samples, consistent with the low GPR37 mRNA expression levels in cerebral cortex that have previously been reported (Marazziti et al. 1997; Zeng et al. 1997; Valdenaire et al. 1998; Regard, Sato, and Coughlin 2008), Gpr37 expression was massively elevated in the penumbra of WT mice at 72h after MCAO.

GPR37L1 shares 68% similarity with *GPR37*, and has been shown to be protective in models of oxidative stress (Meyer et al. 2014). As it is possible that these receptors share a number of redundant functions and potentially compensate for one another *in vivo*, we also assessed the expression levels of GPR37L1 following MCAO. Gpr37L1 expression was unchanged in penumbra regions from sham WT mice as compared to *Gpr37*$^{-/-}$ sham littermates. However, in WT, but not *Gpr37*$^{-/-}$ mice, Gpr37L1 expression was significantly reduced in the penumbra region 72h after MCAO (Figure 3-4A & B).

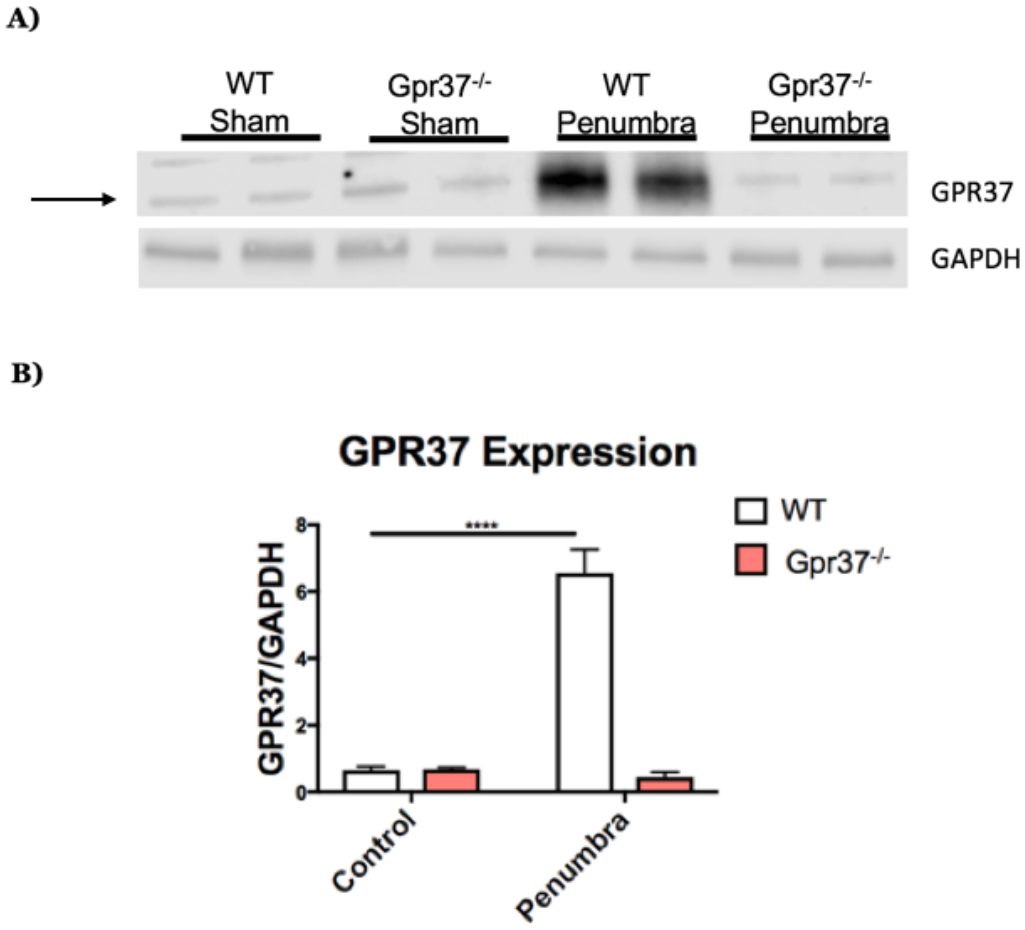

Figure 3-3. GPR37 expression is dramatically increased in the penumbra region 72h post MCAO

Quantification of GPR37 expression in the penumbra region of WT and Gpr37$^{-/-}$ 72h after MCAO and in an analogous region of sham controls (A) Representative Western blot. GAPDH expression is shown in the lower panel for comparison. (B) Arrow indicates location of a non-specific band. Data expressed as mean ± SEM (n = 4/group). Two-way ANOVA followed by Sidak's multiple comparisons post-hoc analyses, ****$p < 0.0001$.

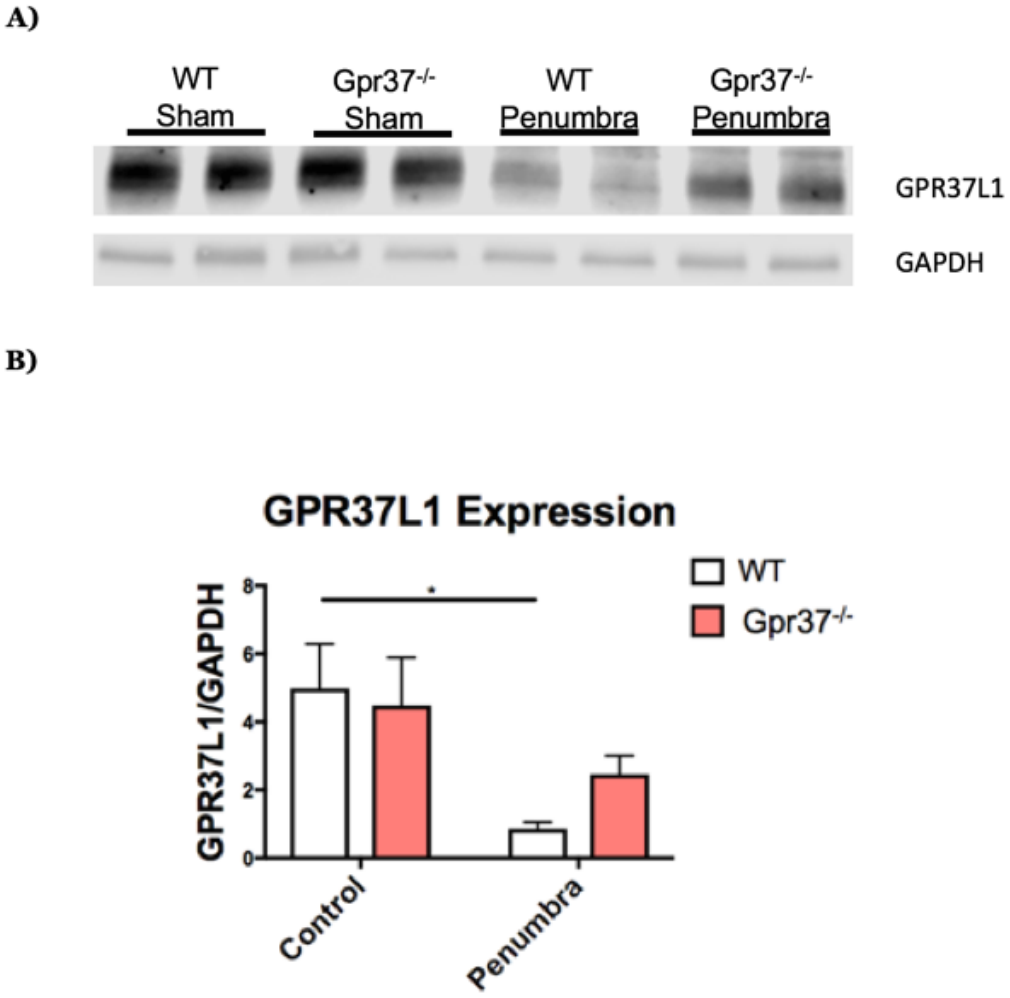

Figure 3-4. GPR37L1 expression is reduced in the penumbra region 72h post MCAO

Quantification of GPR37L1 expression in the penumbra region of WT and Gpr37$^{-/-}$ 72h after MCAO and in an analogous region of sham controls (A) Representative Western blot of GPR37L1 expression in the penumbra region of Gpr37$^{-/-}$ mice compared to WT mice. GAPDH levels are shown in the lower panel. (B) Data expressed as mean ± SEM (n = 4/group). Two-way ANOVA followed by Sidak's multiple comparisons post-hoc analyses, *$p < 0.05$.

3.3.3 HIF1α expression fails to upregulate in the penumbra of Gpr37$^{-/-}$ mice following MCAO

Hypoxia inducible factors (HIFs) are transcription factors that respond to low oxygen levels and upregulate the transcription of genes involved in promoting adaptation to hypoxic and ischemic stress 1 (Kaelin and Ratcliffe 2008; Semenza 1999, 2000). HIF1α expression is regulated by oxygen availability and expression is elevated during periods of hypoxia (Ivan et al. 2001; Jaakkola et al. 2001; Lando, Peet, Gorman, et al. 2002; Lando, Peet, Whelan, et al. 2002). As expected, 72h following MCAO, HIF1α expression was dramatically increased in the penumbra of WT mice compared to sham littermates (Figure 3-5A & B). Surprisingly, though, in mice lacking *Gpr37*, HIF1α expression was unchanged.

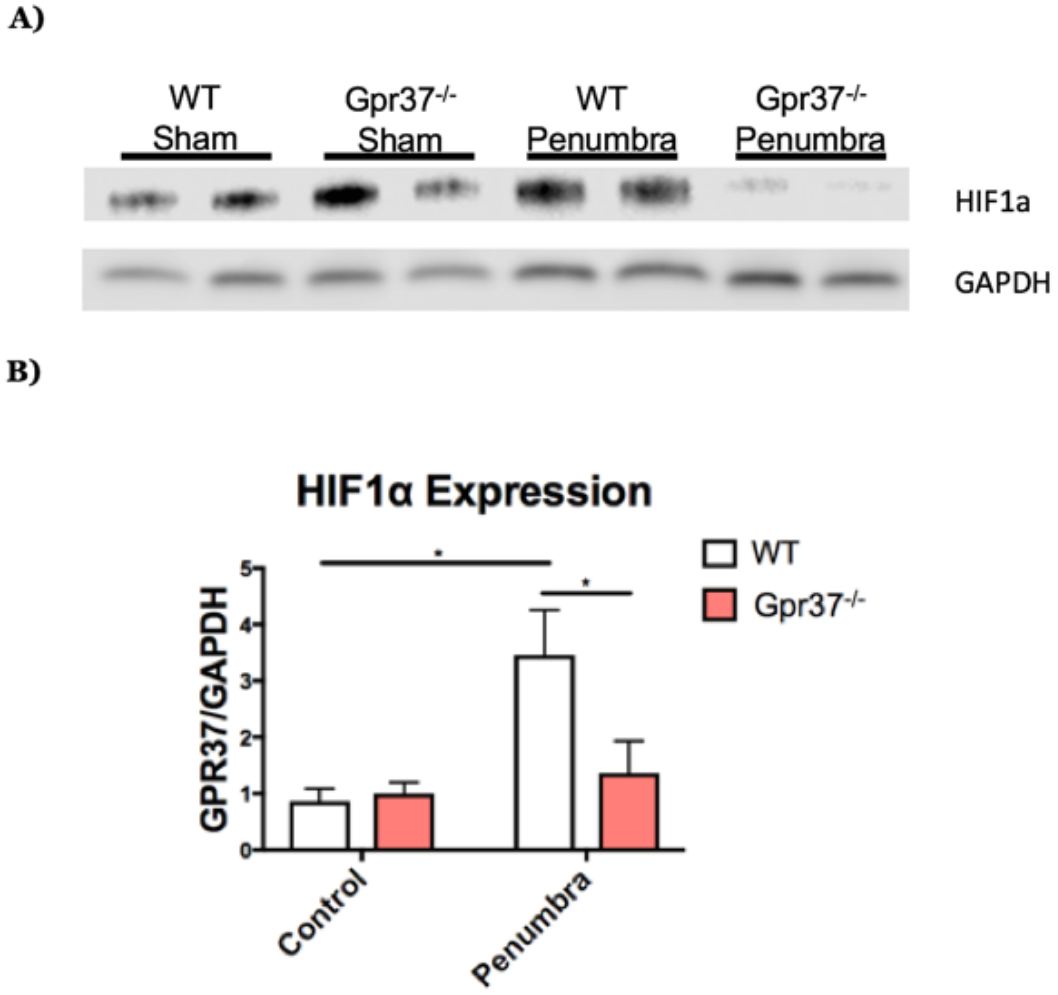

Figure 3-5. HIF1a expression is elevated in the penumbra region of WT but not Gpr37$^{-/-}$ mice 72h post MCAO

(B) Representative Western blot of HIF1a expression in the penumbra region of WT and Gpr37$^{-/-}$ mice 72h after MCAO and in an analogous region of sham controls. (B) Quantification of the data shown in panel A. Data are expressed as mean ± SEM (n = 4/group). Two-way ANOVA followed by Sidak's multiple comparisons post-hoc analyses, *$p < 0.05$.

3.3.4 Altered inflammatory marker expression of GFAP in the penumbra of WT, but not Gpr37$^{-/-}$ mice following MCAO

Inflammation is a characteristic response following ischemia (Jin, Yang, and Li 2010; Kriz 2006; Amantea et al. 2009; Sofroniew 2009). To begin assessing the inflammatory response in the penumbra of WT and *GPR37*$^{-/-}$ mice following focal cerebral ischemia, we assessed common markers for microglial and astrocyte activation 72h after MCAO. Expression of Iba1, a marker for microglia and microglial activation, was significantly elevated in the penumbra region from both WT and *GPR37*$^{-/-}$ mice following induction of focal cerebral ischemia by MCAO (Figure 3-6A & B).

Conversely, expression of GFAP, a marker of astrocytes that is upregulated with astrocytic gliosis (Sofroniew 2009), was also robustly elevated in the penumbra of WT mice 72h after MCAO (Figure 3-7A & B). However, there was no significant increase in GFAP expression in *GPR37*$^{-/-}$ mice, and GFAP expression overall was significantly lower in the penumbra of *GPR37*$^{-/-}$ mice compared to WT littermates following MCAO.

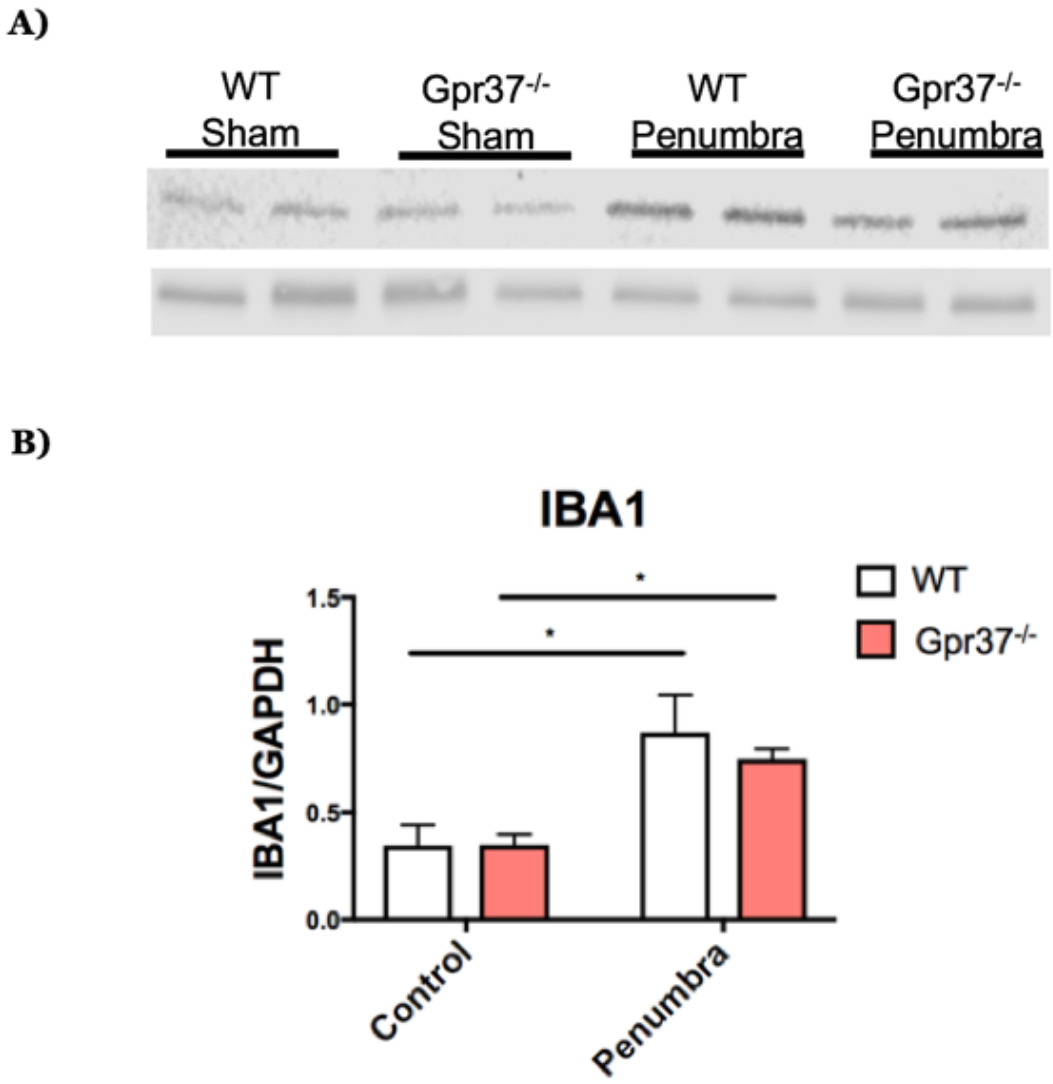

Figure 3-6. IBA1 expression was significantly increased in the penumbra region of both WT and Gpr37$^{-/-}$ mice 72h post MCAO

(A) Representative Western blot of Iba1 expression in the penumbra region of WT and Gpr37$^{-/-}$ 72h after MCAO and in an analogous region of sham controls. (B). Quantification of the data shown in panel A. Data are expressed as mean ± SEM (n = 4/group). Two-way ANOVA followed by Sidak's multiple comparisons post-hoc analyses, *$p<0.05$.

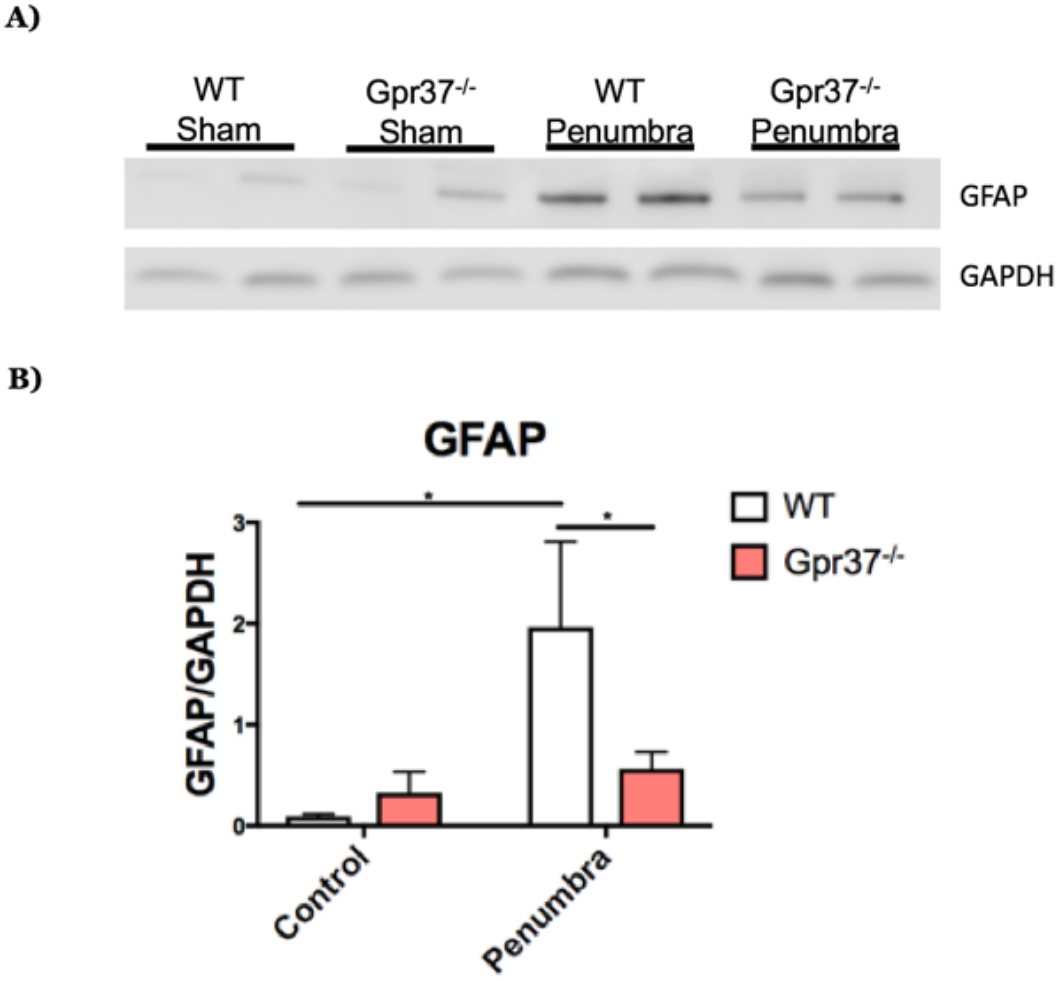

Figure 3-7. GFAP expression is elevated in the penumbra region of WT but not Gpr37$^{-/-}$ mice 72h post MCAO

(A) Representative Western blot of GFAP expression in the penumbra region of WT and Gpr37$^{-/-}$ 72h after MCAO and in an analogous region of sham controls. (B) Quantification of the data shown in panel A. Data are expressed as mean ± SEM (n = 4/group). Two-way ANOVA followed by Sidak's multiple comparisons post-hoc analyses, *$p < 0.05$.

3.3.5 Primary cultured astrocytes from Gpr37$^{-/-}$ mice are more susceptible to oxygen and glucose deprivation.

As GPR37 is expressed in astrocytes (Meyer et al. 2013; Galey et al. 2003) and mice deficient for the receptor show reduced GFAP expression following MCAO, we assessed the role of GPR37 in astrocytes in the oxygen glucose deprivation/reperfusion model of stroke. *GPR37$^{-/-}$* astrocytes were significantly more susceptible than WT astrocytes to death induced by a 6h of oxygen and glucose deprivation treatment followed by 24h of reperfusion, as measured by lactate dehydrogenase release into the media.

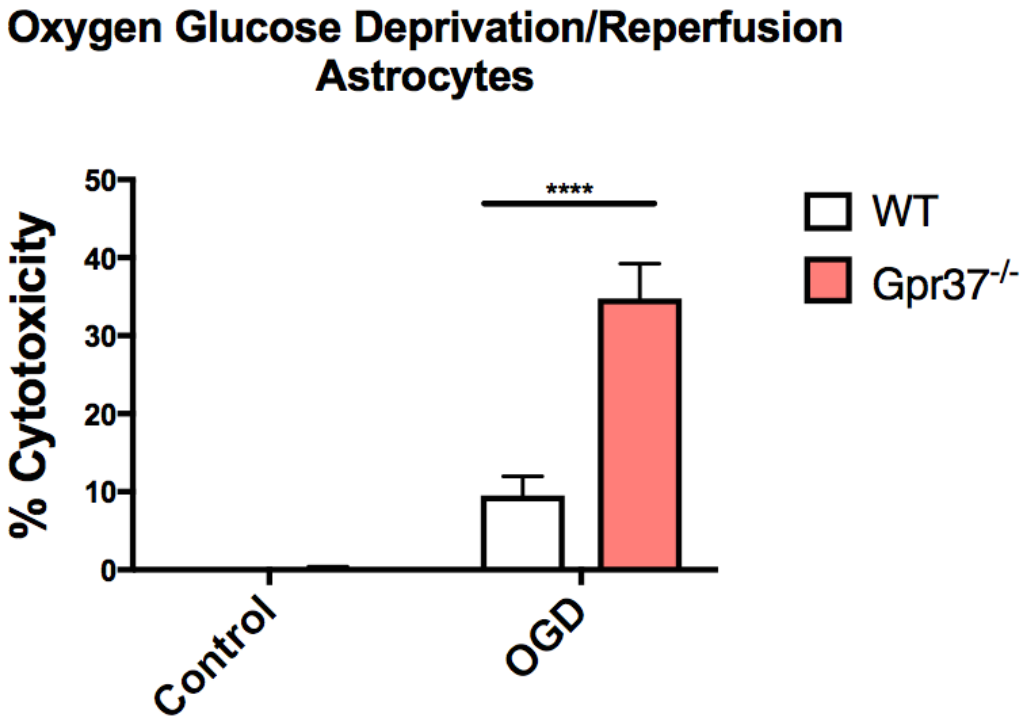

Figure 3-8. Loss of GPR37 in cultured astrocytes increases susceptibility to oxygen and glucose deprivation

Primary cortical astrocytes were deprived of oxygen and glucose for 6h followed by 24h of reperfusion (replenished oxygen and glucose). Cytotoxicity was assessed by measuring the release of lactate dehydrogenase (LDH) in the media. Data are expressed as mean ± SEM (n = 4/group). Two-way ANOVA followed by Sidak's multiple comparisons post-hoc analyses, ****$p < 0.0001$.

3.4 Summary and Discussion

As expression of GPR37 is protective against insults for cultured cells (Meyer et al. 2013; Lundius et al. 2013; Lundius et al. 2014) and loss of the receptor is detrimental in models of seizure (Chapter 2), we sought to determine if expression of Gpr37 might be protective in ischemic stroke. Consistent with our hypothesis, the work presented in this chapter reveals that loss of *Gpr37* leads to increased infarct volume in a model of focal cerebral ischemia. Furthermore, we found that GPR37 expression is massively upregulated in the penumbra of WT animals following MCAO, suggesting an important role for GPR37 following infarct. Surprisingly, Gpr37L1 expression was found to be significantly reduced in the penumbra of WT mice 72h after ischemia, but not in *Gpr37*$^{-/-}$ mice, suggesting the possibility that GPR37L1 may play a compensatory role in mice lacking *Gpr37*.

In the penumbra tissue following MCAO, we also assessed the expression of hypoxia inducible factor 1α (HIF1α). HIF1 has been widely studied under hypoxic and ischemic conditions because it regulates several hypoxia-responsive genes that facilitate adaptation to low oxygen conditions (Kaelin and Ratcliffe 2008; Semenza 1999, 2000). We found a significant increase in HIF1α in the penumbra of WT, but not *Gpr37*$^{-/-}$ at 72h post MCAO. As HIF1α activation can be protective following an ischemic insult (Siddiq, Aminova, and Ratan 2008; Shi

2009), dysregulation of HIF1a may contribute to the increased infarct volume observed in *Gpr37*$^{-/-}$ mice.

Following an ischemic insult, an inflammatory response is initiated within a few hours and can persists for several weeks (Jin, Yang, and Li 2010; Kriz 2006; Amantea et al. 2009; Sofroniew 2009). This response is primarily spearheaded by glia. As with other neurological conditions, the effect of microglia in the ischemic brain is multifaceted. Microglia can exacerbate ischemic damage via the production of inflammatory cytokines and reactive oxygen species, while conversely, microglia can also contribute to tissue repair and remodeling through phagocytosis of dead cells and debris, as well as the production of anti-inflammatory cytokines and growth factors (Kriz 2006; Amantea et al. 2009; Jin, Yang, and Li 2010; Barone and Feuerstein 1999; Lucas, Rothwell, and Gibson 2006; Lakhan, Kirchgessner, and Hofer 2009). Following an ischemic insult, the number of microglia is increased within and around the ischemic core. As expected, we detected increased expression of the microglial marker, ionized calcium-binding adapter molecule 1 (Iba1) in the penumbra of WT and *Gpr37*$^{-/-}$ mice 72h after MCAO. These data suggest the loss of *Gpr37* did not lead to a gross alteration in microglial response. However, additional studies assessing cytokine and growth factor release will be necessary to fully characterize the microglial response following MCAO in *Gpr37*$^{-/-}$ mice.

Astrocytes also contribute to inflammation following an ischemic insult. Astrocytes can provide trophic support, inhibit apoptosis, scavenge oxygen

radicals and take up excess glutamate. Astrocytes also form the glial scar, and like microglia, can release inflammatory and cytotoxic mediators which may exacerbate neuronal death. (Jin et al. 2013; Kriz 2006; Barone and Feuerstein 1999; Lakhan, Kirchgessner, and Hofer 2009; Amantea et al. 2009; Jin, Yang, and Li 2010; Wang, Tang, and Yenari 2007; Sofroniew 2009). GFAP, a marker of astrocytes that is upregulated during astrocytic gliosis, was elevated in the penumbra of WT mice 72h after MCAO. However, increased GFAP expression did not occur in *GPR37*$^{-/-}$ mice, and in general GFAP expression was significantly lower in the penumbra of *GPR37*$^{-/-}$ mice compared to WT littermates following MCAO. Interestingly, mice lacking GFAP have a significantly larger infarct volume following ischemic insult compared to control mice (Nawashiro et al. 2000; Li et al. 2008). This suggests the attenuation of GFAP expression may also contribute to increased infarct volume in *Gpr37*$^{-/-}$ mice. Thus, to further assess the role of GPR37 in astrocytes in stroke, we compared cultured astrocytes from WT and *Gpr37*$^{-/-}$ mice in an *in vitro* model of ischemia. Astrocytes cultured from *Gpr37*$^{-/-}$ mice were significantly more susceptible to 6h of oxygen glucose deprivation followed by 24 h of reperfusion compared to WT astrocytes. Interestingly, astrocytes cultured from mice lacking GFAP and vimentin, another immediate filament protein, are more susceptible to OGD/R (de Pablo et al. 2013). Furthermore, these astrocytes also conferred less protection to co-cultured neurons following OGD/R (de Pablo et al. 2013). Thus, it is possible that reduced GFAP expression contributes to increased cell death observed in astrocytes cultured from *Gpr37*$^{-/-}$ mice. Taken together, these data suggest that astrocytes may be more susceptible to ischemic insult in mice lacking *Gpr37*.

The mechanism by which loss of Gpr37 leads to increased infarct volume is not clear. However, the data presented in this chapter suggest three potential mechanisms: *i)* attenuation of the normal elevation of HIF1a, *ii)* attenuation of the normal elevation of GFAP, and/or *iii)* increased susceptibility of astrocytes to oxygen and glucose deprivation. It is conceivable that these results are interconnected. One possible interpretation is that GPR37 upregulation stimulates an increase in HIF1a, which has been shown to promote the elevation of GFAP expression (Na et al. 2015; DeNiro, Al-Mohanna, and Al-Mohanna 2011). Loss of the normal stress-induced elevations of both GFAP and/or HIF1α could contribute to reduced astrocyte survival. An increased loss of astrocytes during and after ischemic insult would in turn negatively impact neuronal survival (Liu, Li, et al. 2014; Na et al. 2015), thus resulting in increased astrocytic and neuronal cell death. Future studies will be necessary to characterize the precise mechanism(s) by which loss of Gpr37 leads to increased infarct volume in the MCAO model of stroke, but the data presented here suggest that alterations in astrocytic response and/or survival are likely to play a role.

CHAPTER 4:

Conclusions and Future Directions

4.1 Summation of Dissertation Work

GPR37 and GPR37L1 are a pair of closely-related orphan receptors, highly expressed in glia (Valdenaire et al. 1998; Cahoy et al. 2008; Zhang et al. 2014). Most published work on this pair of receptors has focused on GPR37 and its role in Parkinson's disease (Imai et al. 2001; Takahashi and Imai 2003; Yang et al. 2003; Murakami et al. 2004; Marazziti et al. 2004; Kitao et al. 2007; Wang et al. 2008; Dusonchet et al. 2009; Marazziti et al. 2009; Zou et al. 2012; Lundius et al. 2013; Zou et al. 2014) and dopaminergic signaling (Marazziti et al. 2007; Marazziti et al. 2004; Marazziti et al. 2011; Imai et al. 2007) as GPR37 was discovered to be a substrate of parkin over 15 years ago (Imai et al. 2001). More recent work has begun to establish a role for GPR37 and GPR37L1 in development (Marazziti et al. 2013; La Sala et al. 2015; Yang et al. 2016), and *in vitro* studies have suggested that these receptors confer protection in response to cellular insults (Lundius et al. 2013; Meyer et al. 2013). Thus, we sought to examine the role of GPR37 and GPR37L1 in two models of disease: seizure and ischemic stroke.

In the data shown in Chapter 2, we analyzed a variant in *GPR37L1* identified in affected individuals with a novel progressive myoclonus epilepsy (PME) from a large family. To assess the pathogenicity of the *GPR37L1* variant (K349N), we examined expression and signaling of a K349N variant construct in transfected cells. While no striking differences were observed between the wild-

type (WT) version of GPR37L1 and the K349N variant, we were unable to assess agonist-induced signaling, as two previously-reported ligands were ineffective in the various signaling outputs tested. Thus, hypothesizing that the K349N variant may have a loss of function in native cell types *in vivo* that is not evident in cultured cells *in vitro*, we proceeded to study *Gpr37L1*$^{-/-}$ mice as a potential *in vivo* model for human patients harboring GPR37L1 mutations.

We evaluated seizure susceptibility of the *Gpr37*$^{-/-}$ mice in two seizure-induction paradigms. In parallel experiments, we also assessed seizure susceptibility of *Gpr37* deficient mice as well as double-knockout mice lacking both receptors. Mice lacking Gpr37L1 had increased susceptibility to seizures in both induction paradigms, whereas *Gpr37*$^{-/-}$ mice were susceptible only in the 6Hz model of seizure induction, suggesting distinct effects of Gpr37 vs. Gpr37L1 deficiency. Additionally, we found that mice lacking both Gpr37 and Gpr37L1 were much more dramatically susceptible to seizures than either single knockout alone.

We also examined the role of GPR37 in models of ischemic stroke. The studies described in Chapter 3 demonstrate that a loss of *Gpr37* results in increased infarct volume in a model of focal cerebral ischemia. We also found that Gpr37 expression is massively upregulated in the penumbra of WT animals following middle cerebral artery occlusion (MCAO), a model of focal cerebral ischemia, suggesting an important role for GPR37 following ischemic damage. Surprisingly, Gpr37L1 expression was significantly reduced in the penumbra of

WT mice after ischemia, but not in *Gpr37*$^{-/-}$ mice. Furthermore, loss of Gpr37 attenuated the increases in HIF1α and GFAP expression that are normally observed in the penumbra following ischemic insult. Additionally, cultured astrocytes lacking Gpr37 were significantly more susceptible to oxygen and glucose deprivation, suggesting GPR37 expression is beneficial in astrocytes following ischemia. Taken together with the seizure data, these studies have demonstrated novel roles for Gpr37 and Gpr37L1 in models of disease.

4.2 GPR37 and GPR37L1: Ligand Identification

A major limitation in the studies described in this dissertation, and indeed in all studies of GPR37 and GPR37L1 to date, is the lack of efficacious ligands to activate the receptors in a temporally-controlled manner. Animal models deficient for the receptors are extremely useful and provide insights into the functional roles of Gpr37 and Gpr37L1. However, as the ultimate goal of studies of the type described here is to elucidate the therapeutic potential of GPR37 and/or GPR37L1, the ability to agonize and antagonize the receptors would be a major benefit.

Shortly after their cloning, GPR37 and GPR37L1 were initially assessed for potential activation by ligands for their closest relatives, the endothelin and bombesin receptors, but none of the endothelin or bombesin peptides induced signaling downstream of either receptor (Marazziti et al. 1997; Zeng et al. 1997; Valdenaire et al. 1998; Leng et al. 1999; Donohue et al. 1998). As described in

Chapter 2, GPR37 and GPR37L1 have been linked to two potential peptide ligands: head activator (HA), an undecapeptide discovered in *Hydra* (Davenport et al. 2013; Smith 2015; Rezgaoui et al. 2006; Gandia et al. 2013), and prosaposin, a neurotrophic and neuroprotective protein, and its active peptide fragment, prosaptide (Meyer et al. 2013; Lundius et al. 2014). Several reports have failed to find any effect of HA on GPR37 signaling (Dunham et al. 2009; Southern et al. 2013). Furthermore, HA is an unlikely endogenous ligand as the existence of a human homolog remains unproven (Davenport et al. 2013).

Prosaposin is a multifunctional protein. In addition to serving as a precursor protein for four lysosomal proteins called saposins (Kishimoto, Hiraiwa, and O'Brien 1992), full-length prosaposin is released as a secreted factor into many secretory fluids including cerebrospinal fluid, semen, milk, pancreatic juice, and bile (Hineno et al. 1991). Secreted full-length prosaposin serves a discrete function beyond its role as the saposin precursor protein, as a neurotrophic factor capable of promoting cell survival, neurite outgrowth and differentiation (O'Brien et al. 1994; O'Brien et al. 1995; Meyer et al. 2014). Following identification of the neurotrophic region of prosaposin, prosaptides, or small peptide fragments containing the neurotrophic sequence, were shown to recapitulate the neurotrophic actions of prosaposin (O'Brien et al. 1995; Hiraiwa et al. 1997; Campana et al. 1998; Campana, Hiraiwa, and O'Brien 1998; Hiraiwa et al. 2001; Meyer et al. 2014). Prosaptide was shown to specifically bind GPR37 and GPR37L1, promote receptor internalization, and enhance receptor-mediated regulation of cAMP and ERK phosphorylation levels (Meyer et al. 2013).

Furthermore, an interaction with prosaptide was demonstrated by fluorescence correlation spectroscopy showing GPR37 is co-localized with prosaptide and lipid rafts of N2a cells expressing a GFP-tagged version of GPR37 (Lundius et al. 2014). Interestingly, depletion of endogenous prosaposin from the media of transfected N2a cells resulted in a reduction of GPR37 surface expression. A perplexing result, as the removal of ligand is typically expected to upregulate receptor expression, and the addition of exogenous prosaptide was previously shown to provoke internalization. One interpretation put forth by the authors was that like the δ-opioid receptor, which internalizes upon agonist binding but also facilitates its own insertion into the plasma membrane (Bao et al. 2003), prosaposin might be capable of stabilizing GPR37 surface expression while also inducing internalization. It is also possible that GPR37 trafficking is regulated differently in N2a cells and HEK293T cells.

The effectiveness of prosaptide has also been assessed in native cell types *in vitro*. Prosaposin and prosaptides can promote the production of myelin components and cell survival in myelinating cells (Hiraiwa et al. 1999; Hiraiwa et al. 2001; Hiraiwa et al. 1997; Campana, Hiraiwa, and O'Brien 1998). To assess GPR37 as a potential mediator for this process, co-cultures were made of OPCs and dorsal root ganglion (DRG) neurons from wild type (WT) and GPR37KO mice. Cells were treated for three days with either 50nM or 1μM prosaptide. In WT cultures, the percent of myelinating oligodendroglia rose from 10% to ~80% when treated with 1μM prosaptide. In comparison, GPR37KO cultures rose from

30% myelinating cells at baseline to ~80% with 1μM prosaptide. No change was observed with 50nM treatment. The authors concluded that there was a significant effect of prosaptide on the myelinating cells, but that this effect was not mediated by GPR37. However, as previously described, GPR37L1 is most highly expressed in OPC cells with GPR37 having little expression in mouse OPC cells (Cahoy et al. 2008; Zhang et al. 2014). Also, as GPR37KO cultures begin from a different baseline, it is possible that the reduced delta in GPR37KO mice compared to WT could be indicative of a functional effect of GPR37 in mediating oligodendrocyte differentiation.

Despite the multiple reports concerning the ability of prosaposin and prosaptide to bind to GPR37 and GPR37L1 (Meyer, 2013; Lundius, 2013), the actions of prosaposin and prosaptide as agonists for receptor signaling is uncertain. Meyer et al. (2013) reported relatively modest enhancements in receptor signaling induced by prosaposin or prosaptide, and another study (Coleman et al. 2016) reported no significant effects of prosaptide on GPR37L1 signaling in any output tested. Indeed, in the studies shown in this dissertation, no significant effects of prosaposin or prosaptide were observed on signaling downstream of GPR37 or GPR37L1. However, we did see a significant increase in ERK phosphorylation upon expression of GRP37 and GPR37L1. Thus, it is possible that prosaposin and prosaptide may serve as modulators for GPR37 and/or GPR37L1 function, as opposed to authentic agonists, with this modulatory action being dependent on experimental conditions and/or cellular context. Future studies may shed light on the structural determinants of the interaction

between prosaptide and GPR37 and GPR37L1 as well as the physiological significance of this interaction.

4.3 Discussion and Future Directions

4.3.1 K349N Pathogenicity

In the studies described in Chapter 2, a point mutation in the third intracellular loop of GPR37L1 resulting in the substitution of lysine for asparagine at the 349th residue (K349N) was assessed. This variant was discovered in individuals from a large family with several individuals affected by a novel progressive myoclonus epilepsy (PME). Individuals homozygous for the *GPR37L1* variant presented with recurrent headaches and visual hallucinations in the form of colors and lines in early adolescence (Table 2-1), followed by onset of myoclonic seizures. Symptoms progressively worsened and were accompanied by gradual and continuous cognitive decline culminating in death in late adolescence.

We set out to assess the pathogenicity of the K349N mutation through evaluation of the ability of the variant to express, traffic and signal in cultured HEK cells relative to the WT receptor. However, our initial experiments yielded no observable differences between the WT and K349N variant. To address the possibility that cell context might be crucial for observing differences between the WT and variant forms of the receptor, we repeated many of the experiments in N2a cells, a more neuronal-like cell line that has been used successfully for the

study of GPR37 (Lundius et al. 2013; Lundius et al. 2014). However, these studies in the N2a cells again resulted in no significant functional differences between GPR37L1 WT and the K349N variant in terms of receptor localization, regulation, degradation, and constitutive signaling to a variety of signaling outputs.

While we did not detect any clear functional effects of the K349N substitution in our studies, there are several types of future studies that might still reveal the K349N substitution as a pathogenic mutation. Firstly, if efficacious agonists of GPR37L1 are found in the near future (either synthetic agonists from compound screens or a more efficacious putative endogenous agonist), then assessment of agonist-induced signaling between GPR37L1 and the K349N variant would be very interesting. If this mutation confers an effect on receptor signaling, it is plausible that this effect is only observable for agonist-induced signaling but not for constitutive signaling. It is also plausible that the K349N substitution might impact association of GPR37L1 with an unknown interacting partner. We have begun to pursue this avenue through identification of novel GPR37L1 interacting partners in brain via mass spectrometry (Appendix I). It is also possible that the K349N substitution affects GPR37L1 function in a way that is not observable in heterologous cell lines. Thus, future analyses of the K349N variant could be done in *i)* primary astrocytes, the cell type with highest GPR37L1 expression (Cahoy et al. 2008; Zhang et al. 2014), *ii)* patient derived induced pluripotent stem cells, and/or *iii) in vivo* mouse models. Additionally, further genetic characterization of affected individuals and healthy siblings to

conclusively eliminate the possibility of an alternative causal mutation could further support the pathogenicity of the K349N variant.

4.3.2 Loss of GPR37 and/or GPR37L1 Elevates Seizure Susceptibility

If indeed the K349N variant and/or other GPR37L1 variants exhibit decreases in receptor functionality, then *Gpr37L1*$^{-/-}$ mice can be a useful model system for assessing what physiological consequences might result from a loss of GPR37L1 function. Thus, we made use of *Gpr37L1*$^{-/-}$ mice to evaluate whether loss of GPR37L1 function can affect seizure susceptibility *in vivo*. We compared mice lacking a single copy or both copies of *Gpr37L1* in two seizure induction paradigms. As *Gpr37L1* shares 68% similarity with GPR37 and it is possible these two receptors share redundant functions *in vivo*, we also assessed mice lacking a single copy or both copies of *Gpr37*, as well as double-knockout mice lacking both receptors (DKO), in parallel experiments.

Gpr37L1$^{-/-}$ mice displayed increased seizure susceptibility at the highest test current (27mA) in the 6 Hz seizure induction model. However, *Gpr37L1*$^{+/-}$ and WT littermates had comparable seizure responses at each test current, which indicates that having a single copy of GPR37L1 is sufficient to maintain normal susceptibility to 6 Hz-induced seizures. This result aligns with the observed phenotype of family members with the K349N variant. Individuals with a single copy of the variant are normal, whereas individuals homozygous for the K349N variant display the phenotype. In contrast, *Gpr37*$^{+/-}$ and *Gpr37*$^{-/-}$ mice both

exhibited significantly increased seizure susceptibility at 27mA. *Gpr37*$^{-/-}$ mice also displayed significantly increased susceptibility at 22mA. These data provide evidence that reduced Gpr37 expression also results in increased seizure susceptibility. We also assessed double knockout (DKO) mice, lacking both GPR37 and GPR37L1, and found that they were dramatically more susceptible to seizures than either single knockout alone. These results suggest that loss of both Gpr37L1 and Gpr37 can have additive effects in the DKO mice. This was particularly clear in our experiments at 18mA, where DKO mice exhibited increased susceptibility to 6 Hz-induced seizures compared to WT controls, but both single homozygous mutants exhibited normal seizure susceptibility.

In the flurothyl seizure induction paradigm, *Gpr37L1*$^{-/-}$ but not *Gpr37*$^{-/-}$ exhibited decreased latencies to both the myoclonic jerk (MJ) and generalized tonic-clonic seizure (GTCS). Considered together with the 6 Hz data, these findings from the flurothyl studies suggest that Gpr37L1 and Gpr37 alter seizure susceptibility via different mechanisms. The 6 Hz paradigm is a model of limbic seizures, with the highest expression of c-Fos, an indicator of seizure-induced neuronal activation, appearing in the amygdala and piriform cortex (Barton et al. 2001). In contrast, induction of seizures with flurothyl, a GABA-A receptor antagonist, results in seizures that are fairly generalized throughout the brain. Thus, differential receptor expression patterns may underlie the divergent results. Gpr37L1 is most highly expressed in the cerebellum, whereas Gpr37 is most enriched in the corpus callosum, brain stem and substantia nigra, although overall both receptors are fairly widely expressed throughout the brain (Marazziti

et al. 1997; Zeng et al. 1997; Valdenaire et al. 1998; Marazziti et al. 2013; Regard, Sato, and Coughlin 2008). One interesting distinction is that GPR37 is highly expressed in the eye, particularly in Muller glia, which are astrocyte-like cells in the eye (Regard, Sato, and Coughlin 2008; Roesch et al. 2008). Therefore, it is possible that a loss of GPR37 within the eye could increase propagation of currents, leading to an increased susceptibility of *Gpr37*$^{+/-}$ and *Gpr37*$^{-/-}$ mice to 6 Hz, but not flurothyl, induced seizures.

Loss of Gpr37 alters dopaminergic signaling and tone (Marazziti et al. 2004; Marazziti et al. 2007; Imai et al. 2007; Marazziti et al. 2011). Indeed, GPR37 has been shown to physically associate with the dopamine D2 receptor (D2) and co-expression of GPR37 significantly increases D2 ligand affinity (Dunham et al. 2009). Given that D2 activity is typically considered anti-epileptogenic (Starr 1996; Bozzi and Borrelli 2013), a loss of GPR37 may reduce D2 activity and thereby increase seizure susceptibility. As dopaminergic signaling most affects limbic seizures (Starr 1996; Bozzi and Borrelli 2013), another possible explanation for the discrepancy observed between seizure induction paradigms is that loss of Gpr37 may lead to alterations in dopaminergic signaling that exacerbate 6 Hz induced seizure but not the more general seizure induction by flurothyl. Thus, future studies will need to address the mechanism by which GPR37 leads to seizure susceptibility.

We also assessed Gpr37, Gpr37L1 and double knockout mice for spontaneous seizures. Two of five *Gpr37*$^{-/-}$ mice displayed spontaneous seizures

as measured by two weeks of continuous video/EEG recordings, whereas spontaneous seizures were not observed in the five *Gpr37L1*$^{-/-}$ mice examined. Four of the five DKO mice displayed spontaneous seizures, and DKO mice had a significantly longer seizure duration than *Gpr37*$^{-/-}$ mice. These data suggest that while a loss of Gpr37L1 alone does not lead to spontaneous seizures, lack of Gpr37L1 in the DKO mice exacerbates the phenotype of *Gpr37*$^{-/-}$ mice.

One major difference between GPR37 and GPR37L1 expression is in cells of oligodendroglial lineage (Figure 1-2). GPR37L1 is most highly expressed in oligodendrocyte progenitors and exhibits decreasing expression as oligodendrocytes mature, whereas GPR37 expression is low in OPCs and highest in myelinating oligodendrocytes (Cahoy et al. 2008; Zhang et al. 2014). While the effect of myelin deficits on seizure susceptibility is poorly understood, loss of myelin has been observed in individuals with epilepsy (Concha et al. 2009; Nilsson et al. 2008; Scanlon et al. 2013; Schoene-Bake et al. 2009). A recent exome analysis of focal cortical dysplasias, local brain malformations with strong epileptogenic potential, found reduced expression of myelin-associated transcripts, and follow-up imaging analysis revealed disrupted myelin sheath formation and maintenance (Donkels et al. 2016). Furthermore, we found that mice lacking GPR37 have reduced expression of myelin associated glycoprotein (MAG; Appendix I), an important component of myelin. MAG is known to contribute to myelin stability (Fruttiger et al. 1995; Pan et al. 2005; Montag et al. 1994), and MAG deficient mice are more susceptible to seizures (Lopez et al. 2011). Thus, it is possible that lack of Gpr37 expression results in changes in

myelination that contribute to increased seizure susceptibility and spontaneous seizures.

Relative to GPR37, less is known about the fundamental biology of GPR37L1, However, it is known that GPR37L1 is one of the most highly expressed genes in astrocytes (Cahoy et al. 2008; Zhang et al. 2014). Astrocytes are involved in many important physiological functions and may contribute to seizure susceptibility through potassium buffering, transmitter uptake, release, degradation blood-brain barrier (BBB) stability, osmotic balance, and inflammation (Steinhauser and Seifert 2002; Kofuji and Newman 2004; Binder et al. 2006; Djukic et al. 2007; Campbell and Hablitz 2008; Chever et al. 2010; de Lanerolle, Lee, and Spencer 2010; Haj-Yasein et al. 2011; Das et al. 2012; Eid et al. 2004; Verkhratsky et al. 2016; Hubbard and Binder 2016). It is possible that loss of GPR37L1 disrupts astrocyte function leading to increased seizure susceptibility. One method for identifying relevant functions of GPR37L1 is to assess changes in protein expression in mice deficient for the receptor. As mice lacking both receptors were most susceptible to seizure, we assessed overall protein expression in mice lacking GPR37 and GPR37L1 using mass spectrometry (Appendix I). Most proteins assessed in this analysis did not show significant differences in expression levels between WT and DKO brain tissue, but there were a handful of proteins (like the aforementioned MAG) that exhibited large differences in expression between WT and DKO. Additional studies will be necessary to evaluate whether any of these differences of protein expression

levels observed in DKO mice are related to the dramatic seizure phenotype exhibited by these mice.

Lastly, it will be important to consider gender in future studies. As noted in Chapter 2, the oldest surviving child with the K349N variant is a male who is now several years beyond the average age of seizure onset of his sisters, but his symptoms to this point have been fairly mild. As there are well-known neurodevelopmental differences between males and females (Giatti et al. 2012), and previous studies have identified *GPR37L1* and *GPR37* as differentially expressed between the sexes (Shi, Zhang, and Su 2016), further observation of the youngest siblings may shed light on novel gender effects of GPR37L1. Additionally, as we used exclusively male mice in the described studies, an important future direction will be to assess the role of Gpr37L1 and Gpr37 in female mice, particularly in regard to seizure susceptibility.

4.3.3 Loss of Gpr37 Increases Infarct Volume

In the studies described in Chapter 3, we compared WT and *Gpr37*$^{-/-}$ mice in a model of focal cerebral ischemia. Ischemia was achieved by permanent occlusion of the distal branches of the right middle cerebral artery supplying the sensorimotor cortex. This model results in a consistent cortical infarction of a comparable size to damage imposed by most human ischemic strokes (Llovera et al. 2014). Our results demonstrated that mice lacking *Gpr37* exhibit a significantly increased infarct volume compared to wild-type (WT) littermates.

Following an ischemic insult, cell death occurs within minutes for neurons deprived of adequate blood flow. Lack of oxygen and glucose result in disruption of ionic homeostasis, energy failure, neuronal depolarization, elevation in intracellular calcium concentration and ultimately the release of glutamate and subsequent excitotoxicity and oxidative stress (Ceulemans et al. 2010; Dirnagl, Iadecola, and Moskowitz 1999; Barone and Feuerstein 1999). In the hours and days after ischemic further cell damage and death occur as a result of apoptosis, increased proteolytic activity, and the initiation of a neuroinflammatory response (Dirnagl, Iadecola, and Moskowitz 1999; Barone and Feuerstein 1999; Hossmann 2006; Ceulemans et al. 2010). Surrounding this core region of cell death is the penumbra, a region of vulnerable tissue located between the core and healthy tissue, resulting from severely diminished blood flow. Cells within the penumbra can survive up to a few days, depending on the level of collateral blood flowing to the area (Dirnagl, Iadecola, and Moskowitz 1999; De Keyser et al. 2005; Hossmann 2006). Thus, the penumbra is a major target for therapeutic potential.

To better understand the role of GPR37 within the penumbra following an ischemic insult, we measured Gpr37 expression within the penumbra after induction of ischemia with the middle cerebral artery occlusion (MCAO) model. We observed a massive upregulation of Gpr37 following ischemic insult. We also measured expression of GPR37L1. Interestingly, we found GPR37L1 expression was significantly reduced after MCAO in WT, but not *Gpr37*$^{-/-}$ mice. These data

suggest that Gpr37 serves an important function after ischemic insult and that GPR37L1 may compensate for loss of GPR37. However, the mechanism underlying GPR37 and GPR37L1 receptor regulation following ischemia remains unknown. Future studies should examine which cell type(s) upregulate GPR37 expression and down regulate GPR37L1. GPR37 is most highly expressed in myelinating oligodendrocytes, with moderate expression in astrocytes and some populations of neurons, while GPR37L1 is most highly expressed in astrocytes and oligodendrocyte precursor cells (Cahoy et al. 2008; Zhang et al. 2014). However, it is certainly possible that this pattern of expression changes following ischemia, and identifying the cell types involved in GPR37 and GPR37L1 expression following ischemia is a crucial next step.

As GPR37L1 appeared to have differential expression in *Gpr37*$^{-/-}$ animals after MCAO, it will also be important to evaluate the interaction between Gpr37 and Gpr37L1 expression following ischemic insult. Future studies should assess Gpr37 and Gpr37L1 expression at additional time points following ischemia, as changes in receptor expression over time may shed light on the regulation of receptor expression. Additionally, future work assessing GPR37 and GPR37L1 expression within other insult and disease paradigms will be essential to determine if upregulation of GPR37 is specific to ischemia or a more general response to cell injury and damage.

We also measured the expression of hypoxia inducible factor 1α (HIF1α). HIF1α is a transcription factor regulated by oxygen availability. Under hypoxic

conditions HIF1α expression is elevated, and in turn stimulates gene transcription for several genes involved in adaptation to low oxygen conditions (Ivan et al. 2001; Jaakkola et al. 2001; Lando, Peet, Gorman, et al. 2002; Lando, Peet, Whelan, et al. 2002; Kaelin and Ratcliffe 2008; Semenza 2000, 1999). Indeed, we found a significant increase in HIF1α in the penumbra of WT mice following induction of ischemia. However, HIF1α expression was significantly reduced in *Gpr37*$^{-/-}$ compared to WT mice after ischemia. This was not due to a global reduction in HIF1α protein levels, as HIF1α expression was comparable between WT and *Gpr37*$^{-/-}$ mice in sham controls. These data suggest that GPR37 expression is essential for a normal response to ischemia. Furthermore, as HIF1a activation contributes to cell survival following an ischemic insult (Siddiq, Aminova, and Ratan 2008; Shi 2009), dysregulation of HIF1a may contribute to the increased infarct volume observed in *GPR37*$^{-/-}$ mice.

Inflammation is a characteristic response following injury. Following an ischemic insult, an inflammatory response is initiated within minutes and can persist for several weeks (Jin, Yang, and Li 2010; Kriz 2006; Amantea et al. 2009; Sofroniew 2009; Nakajima and Kohsaka 2004). Activation of microglia is the first step of an inflammatory response following ischemia (Nakajima and Kohsaka 2004; Kriz 2006; Jin et al. 2013). Microglia are the resident immune cells in the brain, and following a disruption of brain homeostasis, microglia undergo characteristic changes in morphology and gene expression (Olah et al. 2011; Ransohoff and Perry 2009; Kreutzberg 1996). This 'activation' of microglia leads to increased expression of several proteins, including ionized calcium

binding adapter molecule 1 (Iba1), a useful marker of microglia and microglial activation (Ito et al. 2001). We observed significant and comparable upregulation of Iba1 in both WT and *Gpr37*$^{-/-}$ mice following MCAO. These data suggest that loss of GPR37 does not grossly affect microglial responses *in vivo*. However, to fully characterize the microglial response in *Gpr37*$^{-/-}$ mice following ischemia, future studies will be required to assess microglial morphology, localization, and the release of cytokines and other immune modulators following ischemic stroke.

Astrocytes also contribute to the immune response within the brain. Like microglia, astrocytes can release inflammatory and cytotoxic mediators (Jin et al. 2013; Kriz 2006; Barone and Feuerstein 1999; Lakhan, Kirchgessner, and Hofer 2009; Amantea et al. 2009; Jin, Yang, and Li 2010; Wang, Tang, and Yenari 2007; Sofroniew 2009) Also like microglia, astrocyte activation is multifaceted. Astrocytic gliosis can contribute to neuronal trophic support, inhibition of apoptosis, reduction in oxygen radicals and glutamate concentration, formation of the glial scar, and exacerbation of neuronal death (Jin et al. 2013; Kriz 2006; Barone and Feuerstein 1999; Lakhan, Kirchgessner, and Hofer 2009; Amantea et al. 2009; Jin, Yang, and Li 2010; Wang, Tang, and Yenari 2007; Sofroniew 2009). As expected we observed increased expression of glial acidic fibrillary protein (GFAP), a marker of astrocytes that is upregulated with astrocytic gliosis, in the penumbra of WT mice following MCAO. Intriguingly, however, increased GFAP expression did not occur in *GPR37*$^{-/-}$ mice, and GFAP expression overall was significantly lower in the penumbra of *GPR37*$^{-/-}$ mice compared to WT littermates following MCAO. These data suggest a deficit in astrocytic (but not

microglial) responses to ischemic insults in the *GPR37*$^{-/-}$ mice. Future studies will be necessary to determine if reduced GFAP is a result of *i*) reduction in GFAP expression levels per astrocyte, *ii*) impaired proliferation or migration of astrocytes in the penumbra, and/or *iii*) an altered time course of astrocytic response. Furthermore, inhibition of HIF1α leads to attenuation of GFAP expression following ischemia (Na et al. 2015; DeNiro, Al-Mohanna, and Al-Mohanna 2011). Thus, the reduction in GFAP expression in the *GPR37*$^{-/-}$ mice could be related to the loss of HIF1α activation. As HIF1α is expressed in neurons and glia in the brain, it will be useful to assess which cell type(s) exhibit attenuated HIF1α expression following MCAO. Lastly, mice deficient for GFAP exhibit a significantly larger infarct volume following ischemic insult compared to control mice (Nawashiro et al. 2000; Li et al. 2008). These data suggest that attenuation of GFAP expression may contribute to the increased infarct volume in *Gpr37*$^{-/-}$ mice following MCAO.

4.3.4 Loss of GPR37 Reduces Astrocyte Survival in an in vitro Model of Ischemia

As we observed a specific reduction in the astrocytic marker GFAP following ischemic insult in *Gpr37*$^{-/-}$ mice, we set out to examine the role of GPR37 specifically in astrocytes. Oxygen glucose deprivation (OGD) is a commonly used *in vitro* model of stroke (Tasca, Dal-Cim, and Cimarosti 2015). Cultured astrocytes from *Gpr37*$^{-/-}$ animals were significantly more susceptible to OGD. These data suggest that the increased infarct observed in *Gpr37*$^{-/-}$ mice

following MCAO could be related to increased death of astrocytes. This idea could be tested in future studies examining the cell type(s) most affected by ischemia in the *Gpr37*$^{-/-}$ mice. Furthermore, as loss of GFAP and vimentin, another intermediate filament protein, result in increased astrocyte cell death in models of OGD/R (de Pablo et al. 2013), it will be important to investigate expression of GFAP and vimentin in cultured astrocytes from *Gpr37*$^{-/-}$ mice following OGD/R. These experiments would be useful for providing mechanistic insights that might relate to the *in vivo* situation.

4.3.5 Theoretical model of GPR37 and/or GPR37L1 contribution to seizure susceptibility and ischemic stroke

The data presented in Chapter 2, indicate that loss of Gpr37 leads to increased seizure susceptibility and spontaneous seizures. The studies described in Chapter 3 reveal that a loss of Gpr37 increases infarct volume, disrupts astrocytic response and reduces astrocyte survival following an ischemic insult. Thus, it is feasible that Gpr37 contributes to seizure susceptibility and ischemic stroke through a common mechanism. One possible mechanism is that loss of GPR37 disrupts astrocytic regulation of neuronal excitability (Figure 4-1). Increased neuronal excitability contributes to seizure susceptibility and is a major factor contributing to cell death following an ischemic insult (Dirnagl, Iadecola, and Moskowitz 1999; Hossmann 1996; Lai, Zhang, and Wang 2014). While we have no direct evidence for a role of GPR37L1 in astrocytes, GPR37L1 is one of the most highly expressed genes in astrocytes (Cahoy et al. 2008; Zhang et al.

2014), and therefore, loss of GPR37L1 might plausibly affect astrocyte function as well.

Astrocytes contribute to neuronal excitability in several ways, for example, astrocytes maintain extracellular K^+ concentrations via potassium buffering (Hertz 1965; Kofuji and Newman 2004) and even small fluctuations in the extracellular potassium concentration appreciably alter neural excitability (Wang et al. 2012). Astrocytes primarily uptake K^+ through the Na^+/ K^+ ATPase, inward rectifying channels and spatial buffering of K^+ through gap junctions (Wallraff et al. 2006; Seifert et al. 2009; Larsen et al. 2014; D'Ambrosio, Gordon, and Winn 2002). Disrupted K^+ buffering by astrocytes result in increased seizure susceptibility (Chever et al. 2010; Kofuji and Newman 2004; Kofuji et al. 2000; Haj-Yasein et al. 2011; Traynelis and Dingledine 1988; Rangroo Thrane et al. 2013). While the specific role of potassium buffering in the context of ischemia, has not been extensively studied, excitotoxicity is known to be a major factor contributing to cell death following ischemia (Dirnagl, Iadecola, and Moskowitz 1999; Hossmann 1996; Lai, Zhang, and Wang 2014), Thus, it stands to reason that increased neuronal excitability due to increased K+ concentrations could exacerbate damage following an ischemic insult. In this scenario, a role for GPR37 and/or GPR37L1 function in maintaining proper potassium buffering could explain the results described in Chapters 2 and 3.

Similarly, astrocytic uptake of glutamate and other transmitters is essential for normal neuronal excitability (Anderson and Swanson 2000). The

majority of glutamate uptake is mediated by GLT-1 (Danbolt 2001; Haugeto et al. 1996; Tanaka et al. 1997; Holmseth et al. 2012; Otis and Kavanaugh 2000). Both neurons and glia express GLT-1, however astrocytes account for majority of GLT-1 in the brain (Petr et al. 2015) . Loss of GLT-1 activity has been shown to increase seizure susceptibility (Tanaka et al. 1997; Petr et al. 2015; Seifert, Schilling, and Steinhauser 2006) and conversely, increased expression of GLT-1 has improved cell survival in models of ischemia (Chu et al. 2007; Ouyang et al. 2007; Shen et al. 2010; Harvey et al. 2011). Thus, another possible mechanism for GPR37 and/or GPR37L1 protection in models of disease is via contributions to normal GLT-1 function. Furthermore, uptake of glutamate by GLT-1 is reduced in mice lacking GFAP and vimentin (Li et al. 2008). Our data demonstrate that loss of GPR37 reduces GFAP expression following MCAO. Thus, it is possible that the attenuated GFAP expression leads to reduced GLT-1 expression and increased cell death.

Astrocytes are also essential for degradation and recycling of glutamate. As glutamate transporters are bidirectional, inhibition of glutamate degradation leading to elevated intracellular glutamate will ultimately result in glutamate release. Glutamate is converted into glutamine via glutamine sythetase (GS), an enzyme almost exclusively expressed in astrocytes (Norenberg and Martinez-Hernandez 1979). Additionally, glutamate can also be broken down into α-ketoglutarate by glutamate dehydrogenase (GDH) (Dennis, Lai, and Clark 1977). Glutamine is then shuttled to neurons, where it can be converted back into glutamate and GABA (Tani et al. 2014; Fricke, Jones-Davis, and Mathews 2007;

Bak, Schousboe, and Waagepetersen 2006). Interestingly, while glutamine is necessary for the synthesis of both glutamate and GABA (Tani et al. 2014), disruptions to the glutamate-glutamine cycle rapidly reduce synaptic release of GABA, but only minimally impact glutamate release (Liang, Carlson, and Coulter 2006; Fricke, Jones-Davis, and Mathews 2007; Yang and Cox 2011; Kam and Nicoll 2007). Therefore, another potential mechanism by which GPR37 and/or GPR37L1 could function is by promoting normal degradation and recycling of glutamate. Additionally, GPR37 and/or GPR37L1 could contribute to neuronal excitability via astrocytic regulation of osmotic balance, blood-brain barrier (BBB) stability or through the release of gliomodulators. Future studies assessing these potential mechanisms may yield interesting results.

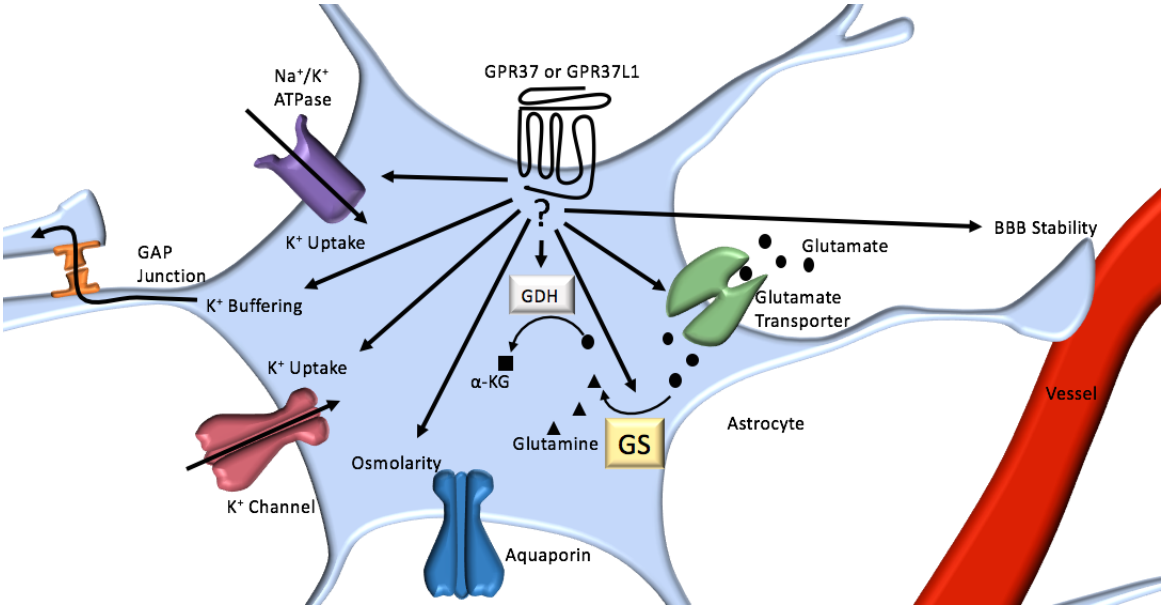

Figure 4-1. Possible Mechanisms by which GPR37 and/or GPR37L1 May Contribute to Disease

Schematic representation of possible mechanisms by which GPR37 and/or GPR37L1 be involved in the regulation of neuronal excitability by astrocytes. GPR37 and/or GPR37L1 may contribute to potassium buffering via uptake or diffusion via gap junctions, uptake of glutamate, degradation of glutamate by glutamine synthetase (GS) or glutamate dehydrogenase (GDH), osmolarity, or stability of the blood-brain-barrier (BBB).

4.3.5 Therapeutic Potential of GPR37 and GPR37L1

Ischemic stroke is a leading cause of disability and death worldwide, and though recent advances have led increased understanding of stroke pathophysiology, the only FDA approved drug for brain ischemia remains thrombolysis with tissue plasminogen activator (tPA). Unfortunately, this treatment benefits less than 10% of patients, because tPA administration must be administered within 4.5 h of stroke onset (Lansberg, Bluhmki, and Thijs 2009; Shobha et al. 2011). Therefore, research aimed to develop novel therapeutic strategies successful outside of this narrow therapeutic window is essential.

Conversely, there are more than 20 approved anti-seizure treatments for epilepsy and seizure disorders (Wilby et al. 2005; Kanner and Balabanov 2005; Lyseng-Williamson 2011; Gilioli et al. 2012; Chong and Lerman 2016; Nair 2016; Schmidt 2016; Hanaya and Arita 2016; Santulli et al. 2016; Sauro et al. 2016). The primary action for most anti-epileptic drugs (AEDs) is via inhibition of sodium and/or calcium channels, or through increased γ-Aminobutyric acid (GABA) transmission (Hanaya and Arita 2016), however AEDs targeting other proteins exist. For example, levetiracetam, a frequently prescribed AED, binds synaptic vesicle protein 2A (SV2A) (Lynch et al. 2004). Like many other AEDs, the exact mechanism of action is not completely understood. However, even with an abundance of successful AEDs, around 20% of patients are resistant to current treatments (Schuele and Luders 2008; French 2007; Kwan, Schachter, and Brodie 2011). While research aimed at novel drug discovery for treatment of drug

resistant epileptic patients is essential, research aimed at elucidating the underlying the mechanisms of epilepsies is also necessary and may lead to improvements in the treatment and quality of life for epileptic patients.

Together the studies described in this dissertation demonstrate that loss of Gpr37 and/or GPR37L1 is highly deleterious in models of seizure and stroke. The data presented here also provide evidence in support of a role for GPR37 in astrocytes as contributing to cell death following an ischemic insult. These findings suggest that GPR37 and GPR37L1 may be useful drug targets for promoting cell survival and minimizing pathology following ischemic stroke and/or seizure. Thus, future studies should be conducted to identify novel ligands for these receptors and further elucidate their fundamental biology both in health and disease.

4.4 Concluding Thoughts

The work described in this dissertation has provided new knowledge concerning the functional roles of Gpr37 and Gpr37L1 in models of disease. In these studies, we demonstrate that a variant in *GPR37L1* is associated with a novel progressive myoclonic epilepsy. Loss of *Gpr37L1* leads to increased seizure susceptibility in two seizure induction models. Additionally, we found that loss of GPR37 increases seizure susceptibility and results in spontaneous seizures. These studies also revealed a synergistic effect of both GPR37 and GPR37L1 deficiency, both in a model of seizure induction and through spontaneous seizures. In

separate studies, we demonstrated that loss of GPR37 results in increased infarct volume in a focal cerebral ischemia model. These studies also yielded the observation that GPR37 is dramatically elevated in the penumbra following ischemia, whereas GPR37L1 expression is concurrently reduced. Moreover, loss of GPR37 resulted in altered HIF1α and GFAP expression following ischemia. Finally, we found that astrocytes cultured from *Gpr37*$^{-/-}$ mice are more susceptible to an in vitro model of stroke. Given the findings described in this dissertation, we conclude that GPR37 and GPR37L1 may function as protective receptors within the central nervous system following insult and disease.

References

Alberta, J. A., S. K. Park, J. Mora, D. Yuk, I. Pawlitzky, P. Iannarelli, T. Vartanian, C. D. Stiles, and D. H. Rowitch. 2001. 'Sonic hedgehog is required during an early phase of oligodendrocyte development in mammalian brain', *Mol Cell Neurosci*, 18: 434-41.

Alieva, I. B., L. A. Gorgidze, Y. A. Komarova, O. A. Chernobelskaya, and I. A. Vorobjev. 1999. 'Experimental model for studying the primary cilia in tissue culture cells', *Membr Cell Biol*, 12: 895-905.

Amantea, D., G. Nappi, G. Bernardi, G. Bagetta, and M. T. Corasaniti. 2009. 'Post-ischemic brain damage: pathophysiology and role of inflammatory mediators', *FEBS J*, 276: 13-26.

Anderson, C. M., and R. A. Swanson. 2000. 'Astrocyte glutamate transport: review of properties, regulation, and physiological functions', *Glia*, 32: 1-14.

Bak, L. K., A. Schousboe, and H. S. Waagepetersen. 2006. 'The glutamate/GABA-glutamine cycle: aspects of transport, neurotransmitter homeostasis and ammonia transfer', *J Neurochem*, 98: 641-53.

Bao, L., S. X. Jin, C. Zhang, L. H. Wang, Z. Z. Xu, F. X. Zhang, L. C. Wang, F. S. Ning, H. J. Cai, J. S. Guan, H. S. Xiao, Z. Q. Xu, C. He, T. Hokfelt, Z. Zhou, and X. Zhang. 2003. 'Activation of delta opioid receptors induces receptor insertion and neuropeptide secretion', *Neuron*, 37: 121-33.

Barone, F. C., and G. Z. Feuerstein. 1999. 'Inflammatory mediators and stroke: new opportunities for novel therapeutics', *J Cereb Blood Flow Metab*, 19: 819-34.

Barton, M. E., B. D. Klein, H. H. Wolf, and H. S. White. 2001. 'Pharmacological characterization of the 6 Hz psychomotor seizure model of partial epilepsy', *Epilepsy Res*, 47: 217-27.

Becamel, C., G. Alonso, N. Galeotti, E. Demey, P. Jouin, C. Ullmer, A. Dumuis, J. Bockaert, and P. Marin. 2002. 'Synaptic multiprotein complexes associated with 5-HT(2C) receptors: a proteomic approach', *EMBO J*, 21: 2332-42.

Binder, D. K., X. Yao, Z. Zador, T. J. Sick, A. S. Verkman, and G. T. Manley. 2006. 'Increased seizure duration and slowed potassium kinetics in mice lacking aquaporin-4 water channels', *Glia*, 53: 631-6.

Bjarnadottir, T. K., R. Fredriksson, P. J. Hoglund, D. E. Gloriam, M. C. Lagerstrom, and H. B. Schioth. 2004. 'The human and mouse repertoire of the adhesion family of G-protein-coupled receptors', *Genomics*, 84: 23-33.

Bjarnadottir, T. K., R. Fredriksson, and H. B. Schioth. 2005. 'The gene repertoire and the common evolutionary history of glutamate, pheromone (V2R), taste(1) and other related G protein-coupled receptors', *Gene*, 362: 70-84.

Bjarnadottir, T. K., D. E. Gloriam, S. H. Hellstrand, H. Kristiansson, R. Fredriksson, and H. B. Schioth. 2006. 'Comprehensive repertoire and phylogenetic analysis of the G protein-coupled receptors in human and mouse', *Genomics*, 88: 263-73.

Bodenmuller, H., and H. C. Schaller. 1981. 'Conserved amino acid sequence of a neuropeptide, the head activator, from coelenterates to humans', *Nature*, 293: 579-80.

Boucrot, E., A. P. Ferreira, L. Almeida-Souza, S. Debard, Y. Vallis, G. Howard, L. Bertot, N. Sauvonnet, and H. T. McMahon. 2015. 'Endophilin marks and controls a clathrin-independent endocytic pathway', *Nature*, 517: 460-5.

Bouvier, M. 2001. 'Oligomerization of G-protein-coupled transmitter receptors', *Nat Rev Neurosci*, 2: 274-86.

Bozzi, Y., and E. Borrelli. 2013. 'The role of dopamine signaling in epileptogenesis', *Front Cell Neurosci*, 7: 157.

Bulenger, S., S. Marullo, and M. Bouvier. 2005. 'Emerging role of homo- and heterodimerization in G-protein-coupled receptor biosynthesis and maturation', *Trends Pharmacol Sci*, 26: 131-7.

Cahoy, J. D., B. Emery, A. Kaushal, L. C. Foo, J. L. Zamanian, K. S. Christopherson, Y. Xing, J. L. Lubischer, P. A. Krieg, S. A. Krupenko, W. J. Thompson, and B. A. Barres. 2008. 'A transcriptome database for astrocytes, neurons, and oligodendrocytes: a new resource for understanding brain development and function', *J Neurosci*, 28: 264-78.

Campana, W. M., S. J. Darin, and J. S. O'Brien. 1999. 'Phosphatidylinositol 3-kinase and Akt protein kinase mediate IGF-I- and prosaptide-induced survival in Schwann cells', *J Neurosci Res*, 57: 332-41.

Campana, W. M., N. Eskeland, N. A. Calcutt, R. Misasi, R. R. Myers, and J. S. O'Brien. 1998. 'Prosaptide prevents paclitaxel neurotoxicity', *Neurotoxicology*, 19: 237-44.

Campana, W. M., M. Hiraiwa, and J. S. O'Brien. 1998. 'Prosaptide activates the MAPK pathway by a G-protein-dependent mechanism essential for enhanced sulfatide synthesis by Schwann cells', *FASEB J*, 12: 307-14.

Campbell, S. L., and J. J. Hablitz. 2008. 'Decreased glutamate transport enhances excitability in a rat model of cortical dysplasia', *Neurobiol Dis*, 32: 254-61.

Ceulemans, A. G., T. Zgavc, R. Kooijman, S. Hachimi-Idrissi, S. Sarre, and Y. Michotte. 2010. 'The dual role of the neuroinflammatory response after ischemic stroke: modulatory effects of hypothermia', *J Neuroinflammation*, 7: 74.

Chaboub, L. S., J. M. Manalo, H. K. Lee, S. M. Glasgow, F. Chen, Y. Kawasaki, T. Akiyama, C. T. Kuo, C. J. Creighton, C. A. Mohila, and B. Deneen. 2016. 'Temporal Profiling of Astrocyte Precursors Reveals Parallel Roles for Asef during Development and after Injury', *J Neurosci*, 36: 11904-17.

Chang, D. T., A. Lopez, D. P. von Kessler, C. Chiang, B. K. Simandl, R. Zhao, M. F. Seldin, J. F. Fallon, and P. A. Beachy. 1994. 'Products, genetic linkage and limb patterning activity of a murine hedgehog gene', *Development*, 120: 3339-53.

Chever, O., B. Djukic, K. D. McCarthy, and F. Amzica. 2010. 'Implication of Kir4.1 channel in excess potassium clearance: an in vivo study on anesthetized glial-conditional Kir4.1 knock-out mice', *J Neurosci*, 30: 15769-77.

Chong, D. J., and A. M. Lerman. 2016. 'Practice Update: Review of Anticonvulsant Therapy', *Curr Neurol Neurosci Rep*, 16: 39.

Chu, K., S. T. Lee, D. I. Sinn, S. Y. Ko, E. H. Kim, J. M. Kim, S. J. Kim, D. K. Park, K. H. Jung, E. C. Song, S. K. Lee, M. Kim, and J. K. Roh. 2007.

'Pharmacological Induction of Ischemic Tolerance by Glutamate Transporter-1 (EAAT2) Upregulation', *Stroke*, 38: 177-82.

Ciechanover, A. 2006. 'The ubiquitin proteolytic system: from a vague idea, through basic mechanisms, and onto human diseases and drug targeting', *Neurology*, 66: S7-19.

Claing, A., S. A. Laporte, M. G. Caron, and R. J. Lefkowitz. 2002. 'Endocytosis of G protein-coupled receptors: roles of G protein-coupled receptor kinases and beta-arrestin proteins', *Prog Neurobiol*, 66: 61-79.

Coleman, J. L., T. Ngo, J. Schmidt, N. Mrad, C. K. Liew, N. M. Jones, R. M. Graham, and N. J. Smith. 2016. 'Metalloprotease cleavage of the N terminus of the orphan G protein-coupled receptor GPR37L1 reduces its constitutive activity', *Sci Signal*, 9: ra36.

Concha, L., C. Beaulieu, D. L. Collins, and D. W. Gross. 2009. 'White-matter diffusion abnormalities in temporal-lobe epilepsy with and without mesial temporal sclerosis', *J Neurol Neurosurg Psychiatry*, 80: 312-9.

Cubells, J. F., J. P. Schroeder, E. S. Barrie, D. F. Manvich, W. Sadee, T. Berg, K. Mercer, T. A. Stowe, L. C. Liles, K. E. Squires, A. Mezher, P. Curtin, D. L. Perdomo, P. Szot, and D. Weinshenker. 2016. 'Human Bacterial Artificial Chromosome (BAC) Transgenesis Fully Rescues Noradrenergic Function in Dopamine beta-Hydroxylase Knockout Mice', *PLoS One*, 11: e0154864.

D'Ambrosio, R., D. S. Gordon, and H. R. Winn. 2002. 'Differential role of KIR channel and Na(+)/K(+)-pump in the regulation of extracellular K(+) in rat hippocampus', *J Neurophysiol*, 87: 87-102.

Dahmane, N., and A. Ruiz i Altaba. 1999. 'Sonic hedgehog regulates the growth and patterning of the cerebellum', *Development*, 126: 3089-100.

Danbolt, N. C. 2001. 'Glutamate uptake', *Prog Neurobiol*, 65: 1-105.

Das, A., G. C. th Wallace, C. Holmes, M. L. McDowell, J. A. Smith, J. D. Marshall, L. Bonilha, J. C. Edwards, S. S. Glazier, S. K. Ray, and N. L. Banik. 2012. 'Hippocampal tissue of patients with refractory temporal lobe epilepsy is associated with astrocyte activation, inflammation, and altered expression of channels and receptors', *Neuroscience*, 220: 237-46.

Davenport, A. P., S. P. Alexander, J. L. Sharman, A. J. Pawson, H. E. Benson, A. E. Monaghan, W. C. Liew, C. P. Mpamhanga, T. I. Bonner, R. R. Neubig, J. P. Pin, M. Spedding, and A. J. Harmar. 2013. 'International Union of Basic and Clinical Pharmacology. LXXXVIII. G protein-coupled receptor list: recommendations for new pairings with cognate ligands', *Pharmacol Rev*, 65: 967-86.

De Keyser, J., M. Uyttenboogaart, M. W. Koch, J. W. Elting, G. Sulter, P. C. Vroomen, and G. J. Luijckx. 2005. 'Neuroprotection in acute ischemic stroke', *Acta Neurol Belg*, 105: 144-8.

de Lanerolle, N. C., T. S. Lee, and D. D. Spencer. 2010. 'Astrocytes and epilepsy', *Neurotherapeutics*, 7: 424-38.

de Pablo, Y., M. Nilsson, M. Pekna, and M. Pekny. 2013. 'Intermediate filaments are important for astrocyte response to oxidative stress induced by oxygen-glucose deprivation and reperfusion', *Histochem Cell Biol*, 140: 81-91.

De Vries, L., B. Zheng, T. Fischer, E. Elenko, and M. G. Farquhar. 2000. 'The regulator of G protein signaling family', *Annu Rev Pharmacol Toxicol*, 40: 235-71.

DeNiro, M., F. H. Al-Mohanna, and F. A. Al-Mohanna. 2011. 'Inhibition of reactive gliosis prevents neovascular growth in the mouse model of oxygen-induced retinopathy', *PLoS One*, 6: e22244.

Dennis, S. C., J. C. Lai, and J. B. Clark. 1977. 'Comparative studies on glutamate metabolism in synpatic and non-synaptic rat brain mitochondria', *Biochem J*, 164: 727-36.

DeWire, S. M., S. Ahn, R. J. Lefkowitz, and S. K. Shenoy. 2007. 'Beta-arrestins and cell signaling', *Annu Rev Physiol*, 69: 483-510.

Dirnagl, U., C. Iadecola, and M. A. Moskowitz. 1999. 'Pathobiology of ischaemic stroke: an integrated view', *Trends Neurosci*, 22: 391-7.

Dixon, R. A., B. K. Kobilka, D. J. Strader, J. L. Benovic, H. G. Dohlman, T. Frielle, M. A. Bolanowski, C. D. Bennett, E. Rands, R. E. Diehl, R. A. Mumford, E. E. Slater, I. S. Sigal, M. G. Caron, R. J. Lefkowitz, and C. D. Strader. 1986.

'Cloning of the gene and cDNA for mammalian beta-adrenergic receptor and homology with rhodopsin', *Nature*, 321: 75-9.

Djukic, B., K. B. Casper, B. D. Philpot, L. S. Chin, and K. D. McCarthy. 2007. 'Conditional knock-out of Kir4.1 leads to glial membrane depolarization, inhibition of potassium and glutamate uptake, and enhanced short-term synaptic potentiation', *J Neurosci*, 27: 11354-65.

Donkels, C., D. Pfeifer, P. Janz, S. Huber, J. Nakagawa, M. Prinz, A. Schulze-Bonhage, A. Weyerbrock, J. Zentner, and C. A. Haas. 2016. 'Whole Transcriptome Screening Reveals Myelination Deficits in Dysplastic Human Temporal Neocortex', *Cereb Cortex*.

Donnan, G. A., M. Fisher, M. Macleod, and S. M. Davis. 2008. 'Stroke', *Lancet*, 371: 1612-23.

Donohue, P. J., H. Shapira, S. A. Mantey, L. L. Hampton, R. T. Jensen, and J. F. Battey. 1998. 'A human gene encodes a putative G protein-coupled receptor highly expressed in the central nervous system', *Brain Res Mol Brain Res*, 54: 152-60.

Dunham, J. H., R. C. Meyer, E. L. Garcia, and R. A. Hall. 2009. 'GPR37 surface expression enhancement via N-terminal truncation or protein-protein interactions', *Biochemistry*, 48: 10286-97.

Dunn, H. A., and S. S. Ferguson. 2015. 'PDZ Protein Regulation of G Protein-Coupled Receptor Trafficking and Signaling Pathways', *Mol Pharmacol*, 88: 624-39.

Dusonchet, J., J. C. Bensadoun, B. L. Schneider, and P. Aebischer. 2009. 'Targeted overexpression of the parkin substrate Pael-R in the nigrostriatal system of adult rats to model Parkinson's disease', *Neurobiol Dis*, 35: 32-41.

Dutta, P., K. E. O'Connell, S. B. Ozkan, A. W. Sailer, and K. K. Dev. 2014. 'The protein interacting with C-kinase (PICK1) interacts with and attenuates parkin-associated endothelial-like (PAEL) receptor-mediated cell death', *J Neurochem*, 130: 360-73.

Eid, T., M. J. Thomas, D. D. Spencer, E. Runden-Pran, J. C. Lai, G. V. Malthankar, J. H. Kim, N. C. Danbolt, O. P. Ottersen, and N. C. de

Lanerolle. 2004. 'Loss of glutamine synthetase in the human epileptogenic hippocampus: possible mechanism for raised extracellular glutamate in mesial temporal lobe epilepsy', *Lancet*, 363: 28-37.

Fargin, A., J. R. Raymond, M. J. Lohse, B. K. Kobilka, M. G. Caron, and R. J. Lefkowitz. 1988. 'The genomic clone G-21 which resembles a beta-adrenergic receptor sequence encodes the 5-HT1A receptor', *Nature*, 335: 358-60.

Ferguson, S. S., J. Zhang, L. S. Barak, and M. G. Caron. 1998. 'Molecular mechanisms of G protein-coupled receptor desensitization and resensitization', *Life Sci*, 62: 1561-5.

Ferre, S., V. Casado, L. A. Devi, M. Filizola, R. Jockers, M. J. Lohse, G. Milligan, J. P. Pin, and X. Guitart. 2014. 'G protein-coupled receptor oligomerization revisited: functional and pharmacological perspectives', *Pharmacol Rev*, 66: 413-34.

Fredriksson, R., M. C. Lagerstrom, L. G. Lundin, and H. B. Schioth. 2003. 'The G-protein-coupled receptors in the human genome form five main families. Phylogenetic analysis, paralogon groups, and fingerprints', *Mol Pharmacol*, 63: 1256-72.

Fredriksson, R., and H. B. Schioth. 2005. 'The repertoire of G-protein-coupled receptors in fully sequenced genomes', *Mol Pharmacol*, 67: 1414-25.

Free, R. B., L. A. Hazelwood, D. M. Cabrera, H. N. Spalding, Y. Namkung, M. L. Rankin, and D. R. Sibley. 2007. 'D1 and D2 dopamine receptor expression is regulated by direct interaction with the chaperone protein calnexin', *J Biol Chem*, 282: 21285-300.

French, J. A. 2007. 'Refractory epilepsy: clinical overview', *Epilepsia*, 48 Suppl 1: 3-7.

Fricke, M. N., D. M. Jones-Davis, and G. C. Mathews. 2007. 'Glutamine uptake by System A transporters maintains neurotransmitter GABA synthesis and inhibitory synaptic transmission', *J Neurochem*, 102: 1895-904.

Fruttiger, M., D. Montag, M. Schachner, and R. Martini. 1995. 'Crucial role for the myelin-associated glycoprotein in the maintenance of axon-myelin integrity', *Eur J Neurosci*, 7: 511-5.

Fujita-Jimbo, E., Z. L. Yu, H. Li, T. Yamagata, M. Mori, T. Momoi, and M. Y. Momoi. 2012. 'Mutation in Parkinson disease-associated, G-protein-coupled receptor 37 (GPR37/PaelR) is related to autism spectrum disorder', *PLoS One*, 7: e51155.

Gainetdinov, R. R., R. T. Premont, L. M. Bohn, R. J. Lefkowitz, and M. G. Caron. 2004. 'Desensitization of G protein-coupled receptors and neuronal functions', *Annu Rev Neurosci*, 27: 107-44.

Galey, D., K. Becker, N. Haughey, A. Kalehua, D. Taub, J. Woodward, M. P. Mattson, and A. Nath. 2003. 'Differential transcriptional regulation by human immunodeficiency virus type 1 and gp120 in human astrocytes', *J Neurovirol*, 9: 358-71.

Gandia, J., V. Fernandez-Duenas, X. Morato, G. Caltabiano, R. Gonzalez-Muniz, L. Pardo, I. Stagljar, and F. Ciruela. 2013. 'The Parkinson's disease-associated GPR37 receptor-mediated cytotoxicity is controlled by its intracellular cysteine-rich domain', *J Neurochem*, 125: 362-72.

Gandia, J., X. Morato, I. Stagljar, V. Fernandez-Duenas, and F. Ciruela. 2015. 'Adenosine A2A receptor-mediated control of pilocarpine-induced tremulous jaw movements is Parkinson's disease-associated GPR37 receptor-dependent', *Behav Brain Res*, 288: 103-6.

Ganley, I. G., P. M. Wong, N. Gammoh, and X. Jiang. 2011. 'Distinct autophagosomal-lysosomal fusion mechanism revealed by thapsigargin-induced autophagy arrest', *Mol Cell*, 42: 731-43.

Giatti, S., M. Boraso, R. C. Melcangi, and B. Viviani. 2012. 'Neuroactive steroids, their metabolites, and neuroinflammation', *J Mol Endocrinol*, 49: R125-34.

Gilchrist, J., S. Dutton, M. Diaz-Bustamante, A. McPherson, N. Olivares, J. Kalia, A. Escayg, and F. Bosmans. 2014. 'Nav1.1 modulation by a novel triazole compound attenuates epileptic seizures in rodents', *ACS Chem Biol*, 9: 1204-12.

Gilioli, I., A. Vignoli, E. Visani, M. Casazza, L. Canafoglia, V. Chiesa, E. Gardella, F. La Briola, F. Panzica, G. Avanzini, M. P. Canevini, S. Franceschetti, and S. Binelli. 2012. 'Focal epilepsies in adult patients attending two epilepsy

centers: classification of drug-resistance, assessment of risk factors, and usefulness of "new" antiepileptic drugs', *Epilepsia*, 53: 733-40.

Gilman, A. G. 1987. 'G proteins: transducers of receptor-generated signals', *Annu Rev Biochem*, 56: 615-49.

Goodman, O. B., Jr., J. G. Krupnick, F. Santini, V. V. Gurevich, R. B. Penn, A. W. Gagnon, J. H. Keen, and J. L. Benovic. 1996. 'Beta-arrestin acts as a clathrin adaptor in endocytosis of the beta2-adrenergic receptor', *Nature*, 383: 447-50.

Grantcharova, E., J. Furkert, H. P. Reusch, H. W. Krell, G. Papsdorf, M. Beyermann, R. Schulein, W. Rosenthal, and A. Oksche. 2002. 'The extracellular N terminus of the endothelin B (ETB) receptor is cleaved by a metalloprotease in an agonist-dependent process', *J Biol Chem*, 277: 43933-41.

Haj-Yasein, N. N., V. Jensen, G. F. Vindedal, G. A. Gundersen, A. Klungland, O. P. Ottersen, O. Hvalby, and E. A. Nagelhus. 2011. 'Evidence that compromised K+ spatial buffering contributes to the epileptogenic effect of mutations in the human Kir4.1 gene (KCNJ10)', *Glia*, 59: 1635-42.

Hanaya, R., and K. Arita. 2016. 'The New Antiepileptic Drugs: Their Neuropharmacology and Clinical Indications', *Neurol Med Chir (Tokyo)*, 56: 205-20.

Hargrave, P. A., J. H. McDowell, D. R. Curtis, J. K. Wang, E. Juszczak, S. L. Fong, J. K. Rao, and P. Argos. 1983. 'The structure of bovine rhodopsin', *Biophys Struct Mech*, 9: 235-44.

Harvey, B. K., M. Airavaara, J. Hinzman, E. M. Wires, M. J. Chiocco, D. B. Howard, H. Shen, G. Gerhardt, B. J. Hoffer, and Y. Wang. 2011. 'Targeted over-expression of glutamate transporter 1 (GLT-1) reduces ischemic brain injury in a rat model of stroke', *PLoS One*, 6: e22135.

Haugeto, O., K. Ullensvang, L. M. Levy, F. A. Chaudhry, T. Honore, M. Nielsen, K. P. Lehre, and N. C. Danbolt. 1996. 'Brain glutamate transporter proteins form homomultimers', *J Biol Chem*, 271: 27715-22.

Hausdorff, W. P., M. G. Caron, and R. J. Lefkowitz. 1990. 'Turning off the signal: desensitization of beta-adrenergic receptor function', *FASEB J*, 4: 2881-9.

Hay, D. L., and A. A. Pioszak. 2016. 'Receptor Activity-Modifying Proteins (RAMPs): New Insights and Roles', *Annu Rev Pharmacol Toxicol*, 56: 469-87.

Heinzen, E. L., R. A. Radtke, T. J. Urban, G. L. Cavalleri, C. Depondt, A. C. Need, N. M. Walley, P. Nicoletti, D. Ge, C. B. Catarino, J. S. Duncan, D. Kasperaviciute, S. K. Tate, L. O. Caboclo, J. W. Sander, L. Clayton, K. N. Linney, K. V. Shianna, C. E. Gumbs, J. Smith, K. D. Cronin, J. M. Maia, C. P. Doherty, M. Pandolfo, D. Leppert, L. T. Middleton, R. A. Gibson, M. R. Johnson, P. M. Matthews, D. Hosford, R. Kalviainen, K. Eriksson, A. M. Kantanen, T. Dorn, J. Hansen, G. Kramer, B. J. Steinhoff, H. G. Wieser, D. Zumsteg, M. Ortega, N. W. Wood, J. Huxley-Jones, M. Mikati, W. B. Gallentine, A. M. Husain, P. G. Buckley, R. L. Stallings, M. V. Podgoreanu, N. Delanty, S. M. Sisodiya, and D. B. Goldstein. 2010. 'Rare deletions at 16p13.11 predispose to a diverse spectrum of sporadic epilepsy syndromes', *Am J Hum Genet*, 86: 707-18.

Heng, B. C., D. Aubel, and M. Fussenegger. 2013. 'An overview of the diverse roles of G-protein coupled receptors (GPCRs) in the pathophysiology of various human diseases', *Biotechnol Adv*, 31: 1676-94.

Hertz, L. 1965. 'Possible role of neuroglia: a potassium-mediated neuronal--neuroglial--neuronal impulse transmission system', *Nature*, 206: 1091-4.

Hineno, T., A. Sano, K. Kondoh, S. Ueno, Y. Kakimoto, and K. Yoshida. 1991. 'Secretion of sphingolipid hydrolase activator precursor, prosaposin', *Biochem Biophys Res Commun*, 176: 668-74.

Hiraiwa, M., W. M. Campana, A. P. Mizisin, L. Mohiuddin, and J. S. O'Brien. 1999. 'Prosaposin: a myelinotrophic protein that promotes expression of myelin constituents and is secreted after nerve injury', *Glia*, 26: 353-60.

Hiraiwa, M., W. M. Campana, C. Y. Wang, D. A. Otero, and J. S. O'Brien. 2001. 'A retro-inverso Prosaptide D5 promotes a myelination process in developing rats', *Brain Res Dev Brain Res*, 128: 73-6.

Hiraiwa, M., E. M. Taylor, W. M. Campana, S. J. Darin, and J. S. O'Brien. 1997. 'Cell death prevention, mitogen-activated protein kinase stimulation, and

increased sulfatide concentrations in Schwann cells and oligodendrocytes by prosaposin and prosaptides', *Proc Natl Acad Sci U S A*, 94: 4778-81.

Holmseth, S., Y. Dehnes, Y. H. Huang, V. V. Follin-Arbelet, N. J. Grutle, M. N. Mylonakou, C. Plachez, Y. Zhou, D. N. Furness, D. E. Bergles, K. P. Lehre, and N. C. Danbolt. 2012. 'The density of EAAC1 (EAAT3) glutamate transporters expressed by neurons in the mammalian CNS', *J Neurosci*, 32: 6000-13.

Hossmann, K. A. 1994. 'Viability thresholds and the penumbra of focal ischemia', *Ann Neurol*, 36: 557-65.

———. 1996. 'Periinfarct depolarizations', *Cerebrovasc Brain Metab Rev*, 8: 195-208.

———. 2006. 'Pathophysiology and therapy of experimental stroke', *Cell Mol Neurobiol*, 26: 1057-83.

Hubbard, J. A., and D. K. Binder. 2016. *Astrocytes and Epilepsy* (Academic Press).

Husi, H., M. A. Ward, J. S. Choudhary, W. P. Blackstock, and S. G. Grant. 2000. 'Proteomic analysis of NMDA receptor-adhesion protein signaling complexes', *Nat Neurosci*, 3: 661-9.

Imai, Y., H. Inoue, A. Kataoka, W. Hua-Qin, M. Masuda, T. Ikeda, K. Tsukita, M. Soda, T. Kodama, T. Fuwa, Y. Honda, S. Kaneko, S. Matsumoto, K. Wakamatsu, S. Ito, M. Miura, T. Aosaki, S. Itohara, and R. Takahashi. 2007. 'Pael receptor is involved in dopamine metabolism in the nigrostriatal system', *Neurosci Res*, 59: 413-25.

Imai, Y., M. Soda, H. Inoue, N. Hattori, Y. Mizuno, and R. Takahashi. 2001. 'An unfolded putative transmembrane polypeptide, which can lead to endoplasmic reticulum stress, is a substrate of Parkin', *Cell*, 105: 891-902.

Imai, Y., M. Soda, and R. Takahashi. 2000. 'Parkin suppresses unfolded protein stress-induced cell death through its E3 ubiquitin-protein ligase activity', *J Biol Chem*, 275: 35661-4.

Ito, D., K. Tanaka, S. Suzuki, T. Dembo, and Y. Fukuuchi. 2001. 'Enhanced expression of Iba1, ionized calcium-binding adapter molecule 1, after transient focal cerebral ischemia in rat brain', *Stroke*, 32: 1208-15.

Ivan, M., K. Kondo, H. Yang, W. Kim, J. Valiando, M. Ohh, A. Salic, J. M. Asara, W. S. Lane, and W. G. Kaelin, Jr. 2001. 'HIFalpha targeted for VHL-mediated destruction by proline hydroxylation: implications for O2 sensing', *Science*, 292: 464-8.

Jaakkola, P., D. R. Mole, Y. M. Tian, M. I. Wilson, J. Gielbert, S. J. Gaskell, A. von Kriegsheim, H. F. Hebestreit, M. Mukherji, C. J. Schofield, P. H. Maxwell, C. W. Pugh, and P. J. Ratcliffe. 2001. 'Targeting of HIF-alpha to the von Hippel-Lindau ubiquitylation complex by O2-regulated prolyl hydroxylation', *Science*, 292: 468-72.

Jiang, M. Q., Y. Y. Zhao, W. Cao, Z. Z. Wei, X. Gu, L. Wei, and S. P. Yu. 2016. 'Long-term survival and regeneration of neuronal and vasculature cells inside the core region after ischemic stroke in adult mice', *Brain Pathol*.

Jin, R., L. Liu, S. Zhang, A. Nanda, and G. Li. 2013. 'Role of inflammation and its mediators in acute ischemic stroke', *J Cardiovasc Transl Res*, 6: 834-51.

Jin, R., G. Yang, and G. Li. 2010. 'Inflammatory mechanisms in ischemic stroke: role of inflammatory cells', *J Leukoc Biol*, 87: 779-89.

Junaid, M. A., S. Kuizon, J. Cardona, T. Azher, N. Murakami, R. K. Pullarkat, and W. T. Brown. 2011. 'Folic acid supplementation dysregulates gene expression in lymphoblastoid cells--implications in nutrition', *Biochem Biophys Res Commun*, 412: 688-92.

Kaelin, W. G., Jr., and P. J. Ratcliffe. 2008. 'Oxygen sensing by metazoans: the central role of the HIF hydroxylase pathway', *Mol Cell*, 30: 393-402.

Kam, K., and R. Nicoll. 2007. 'Excitatory synaptic transmission persists independently of the glutamate-glutamine cycle', *J Neurosci*, 27: 9192-200.

Kanner, A. M., and A. J. Balabanov. 2005. 'The use of monotherapy in patients with epilepsy: an appraisal of the new antiepileptic drugs', *Curr Neurol Neurosci Rep*, 5: 322-8.

Kaupp, U. B., and R. Seifert. 2002. 'Cyclic nucleotide-gated ion channels', *Physiol Rev*, 82: 769-824.

Khan, S. M., R. Sleno, S. Gora, P. Zylbergold, J. P. Laverdure, J. C. Labbe, G. J. Miller, and T. E. Hebert. 2013. 'The expanding roles of Gbetagamma

subunits in G protein-coupled receptor signaling and drug action', *Pharmacol Rev*, 65: 545-77.

Kim, M., L. H. Jiang, H. L. Wilson, R. A. North, and A. Surprenant. 2001. 'Proteomic and functional evidence for a P2X7 receptor signalling complex', *EMBO J*, 20: 6347-58.

Kishimoto, Y., M. Hiraiwa, and J. S. O'Brien. 1992. 'Saposins: structure, function, distribution, and molecular genetics', *J Lipid Res*, 33: 1255-67.

Kitao, Y., Y. Imai, K. Ozawa, A. Kataoka, T. Ikeda, M. Soda, K. Nakimawa, H. Kiyama, D. M. Stern, O. Hori, K. Wakamatsu, S. Ito, S. Itohara, R. Takahashi, and S. Ogawa. 2007. 'Pael receptor induces death of dopaminergic neurons in the substantia nigra via endoplasmic reticulum stress and dopamine toxicity, which is enhanced under condition of parkin inactivation', *Hum Mol Genet*, 16: 50-60.

Klein, K. R., B. C. Matson, and K. M. Caron. 2016. 'The expanding repertoire of receptor activity modifying protein (RAMP) function', *Crit Rev Biochem Mol Biol*, 51: 65-71.

Kniazeff, J., L. Prezeau, P. Rondard, J. P. Pin, and C. Goudet. 2011. 'Dimers and beyond: The functional puzzles of class C GPCRs', *Pharmacol Ther*, 130: 9-25.

Kobilka, B. K., H. Matsui, T. S. Kobilka, T. L. Yang-Feng, U. Francke, M. G. Caron, R. J. Lefkowitz, and J. W. Regan. 1987. 'Cloning, sequencing, and expression of the gene coding for the human platelet alpha 2-adrenergic receptor', *Science*, 238: 650-6.

Kofuji, P., P. Ceelen, K. R. Zahs, L. W. Surbeck, H. A. Lester, and E. A. Newman. 2000. 'Genetic inactivation of an inwardly rectifying potassium channel (Kir4.1 subunit) in mice: phenotypic impact in retina', *J Neurosci*, 20: 5733-40.

Kofuji, P., and E. A. Newman. 2004. 'Potassium buffering in the central nervous system', *Neuroscience*, 129: 1045-56.

Kolakowski, L. F., Jr. 1994. 'GCRDb: a G-protein-coupled receptor database', *Receptors Channels*, 2: 1-7.

Krasnoperov, V. G., M. A. Bittner, R. Beavis, Y. Kuang, K. V. Salnikow, O. G. Chepurny, A. R. Little, A. N. Plotnikov, D. Wu, R. W. Holz, and A. G. Petrenko. 1997. 'alpha-Latrotoxin stimulates exocytosis by the interaction with a neuronal G-protein-coupled receptor', *Neuron*, 18: 925-37.

Kreutzberg, G. W. 1996. 'Microglia: a sensor for pathological events in the CNS', *Trends Neurosci*, 19: 312-8.

Kriz, J. 2006. 'Inflammation in ischemic brain injury: timing is important', *Crit Rev Neurobiol*, 18: 145-57.

Kwan, P., S. C. Schachter, and M. J. Brodie. 2011. 'Drug-resistant epilepsy', *N Engl J Med*, 365: 919-26.

La Sala, G., D. Marazziti, C. Di Pietro, E. Golini, R. Matteoni, and G. P. Tocchini-Valentini. 2015. 'Modulation of Dhh signaling and altered Sertoli cell function in mice lacking the GPR37-prosaposin receptor', *FASEB J*, 29: 2059-69.

Lagerstrom, M. C., and H. B. Schioth. 2008. 'Structural diversity of G protein-coupled receptors and significance for drug discovery', *Nat Rev Drug Discov*, 7: 339-57.

Lai, T. W., S. Zhang, and Y. T. Wang. 2014. 'Excitotoxicity and stroke: identifying novel targets for neuroprotection', *Prog Neurobiol*, 115: 157-88.

Lakhan, S. E., A. Kirchgessner, and M. Hofer. 2009. 'Inflammatory mechanisms in ischemic stroke: therapeutic approaches', *J Transl Med*, 7: 97.

Lando, D., D. J. Peet, J. J. Gorman, D. A. Whelan, M. L. Whitelaw, and R. K. Bruick. 2002. 'FIH-1 is an asparaginyl hydroxylase enzyme that regulates the transcriptional activity of hypoxia-inducible factor', *Genes Dev*, 16: 1466-71.

Lando, D., D. J. Peet, D. A. Whelan, J. J. Gorman, and M. L. Whitelaw. 2002. 'Asparagine hydroxylation of the HIF transactivation domain a hypoxic switch', *Science*, 295: 858-61.

Lansberg, M. G., E. Bluhmki, and V. N. Thijs. 2009. 'Efficacy and safety of tissue plasminogen activator 3 to 4.5 hours after acute ischemic stroke: a metaanalysis', *Stroke*, 40: 2438-41.

Larsen, B. R., M. Assentoft, M. L. Cotrina, S. Z. Hua, M. Nedergaard, K. Kaila, J. Voipio, and N. MacAulay. 2014. 'Contributions of the Na(+)/K(+)-ATPase, NKCC1, and Kir4.1 to hippocampal K(+) clearance and volume responses', *Glia*, 62: 608-22.

Lee, T. J., O. Sartor, R. B. Luftig, and S. Koochekpour. 2004. 'Saposin C promotes survival and prevents apoptosis via PI3K/Akt-dependent pathway in prostate cancer cells', *Mol Cancer*, 3: 31.

Lefkowitz, R. J. 1998. 'G protein-coupled receptors. III. New roles for receptor kinases and beta-arrestins in receptor signaling and desensitization', *J Biol Chem*, 273: 18677-80.

Lefkowitz, R. J., and M. G. Caron. 1990. 'The adrenergic receptors', *Adv Second Messenger Phosphoprotein Res*, 24: 1-8.

Leng, N., G. Gu, R. B. Simerly, and E. R. Spindel. 1999. 'Molecular cloning and characterization of two putative G protein-coupled receptors which are highly expressed in the central nervous system', *Brain Res Mol Brain Res*, 69: 73-83.

Li, L., A. Lundkvist, D. Andersson, U. Wilhelmsson, N. Nagai, A. C. Pardo, C. Nodin, A. Stahlberg, K. Aprico, K. Larsson, T. Yabe, L. Moons, A. Fotheringham, I. Davies, P. Carmeliet, J. P. Schwartz, M. Pekna, M. Kubista, F. Blomstrand, N. Maragakis, M. Nilsson, and M. Pekny. 2008. 'Protective role of reactive astrocytes in brain ischemia', *J Cereb Blood Flow Metab*, 28: 468-81.

Liang, S. L., G. C. Carlson, and D. A. Coulter. 2006. 'Dynamic regulation of synaptic GABA release by the glutamate-glutamine cycle in hippocampal area CA1', *J Neurosci*, 26: 8537-48.

Liu, F., C. Zhu, X. Huang, J. Cai, H. Wang, X. Wang, S. He, C. Liu, X. Yang, Y. Zhang, and T. Zhang. 2014. 'A low level of GPR37 is associated with human hepatocellular carcinoma progression and poor patient survival', *Pathol Res Pract*, 210: 885-92.

Liu, Z., Y. Li, Y. Cui, C. Roberts, M. Lu, U. Wilhelmsson, M. Pekny, and M. Chopp. 2014. 'Beneficial effects of gfap/vimentin reactive astrocytes for

axonal remodeling and motor behavioral recovery in mice after stroke', *Glia*, 62: 2022-33.

Llovera, G., S. Roth, N. Plesnila, R. Veltkamp, and A. Liesz. 2014. 'Modeling stroke in mice: permanent coagulation of the distal middle cerebral artery', *J Vis Exp*: e51729.

Lohse, M. J., J. L. Benovic, J. Codina, M. G. Caron, and R. J. Lefkowitz. 1990. 'beta-Arrestin: a protein that regulates beta-adrenergic receptor function', *Science*, 248: 1547-50.

Lopes, J. P., X. Morato, C. Souza, C. Pinhal, N. J. Machado, P. M. Canas, H. B. Silva, I. Stagljar, J. Gandia, V. Fernandez-Duenas, R. Lujan, R. A. Cunha, and F. Ciruela. 2015. 'The role of parkinson's disease-associated receptor GPR37 in the hippocampus: functional interplay with the adenosinergic system', *J Neurochem*, 134: 135-46.

Lopez, P. H., A. S. Ahmad, N. R. Mehta, M. Toner, E. A. Rowland, J. Zhang, S. Dore, and R. L. Schnaar. 2011. 'Myelin-associated glycoprotein protects neurons from excitotoxicity', *J Neurochem*, 116: 900-8.

Lucas, S. M., N. J. Rothwell, and R. M. Gibson. 2006. 'The role of inflammation in CNS injury and disease', *Br J Pharmacol*, 147 Suppl 1: S232-40.

Lundius, E. G., N. Stroth, V. Vukojevic, L. Terenius, and P. Svenningsson. 2013. 'Functional GPR37 trafficking protects against toxicity induced by 6-OHDA, MPP+ or rotenone in a catecholaminergic cell line', *J Neurochem*, 124: 410-7.

Lundius, E. G., V. Vukojevic, E. Hertz, N. Stroth, A. Cederlund, M. Hiraiwa, L. Terenius, and P. Svenningsson. 2014. 'GPR37 protein trafficking to the plasma membrane regulated by prosaposin and GM1 gangliosides promotes cell viability', *J Biol Chem*, 289: 4660-73.

Luttrell, L. M., S. S. Ferguson, Y. Daaka, W. E. Miller, S. Maudsley, G. J. Della Rocca, F. Lin, H. Kawakatsu, K. Owada, D. K. Luttrell, M. G. Caron, and R. J. Lefkowitz. 1999. 'Beta-arrestin-dependent formation of beta2 adrenergic receptor-Src protein kinase complexes', *Science*, 283: 655-61.

Lynch, B. A., N. Lambeng, K. Nocka, P. Kensel-Hammes, S. M. Bajjalieh, A. Matagne, and B. Fuks. 2004. 'The synaptic vesicle protein SV2A is the

binding site for the antiepileptic drug levetiracetam', *Proc Natl Acad Sci U S A*, 101: 9861-6.

Lyseng-Williamson, K. A. 2011. 'Spotlight on levetiracetam in epilepsy', *CNS Drugs*, 25: 901-5.

Magalhaes, A. C., H. Dunn, and S. S. Ferguson. 2012. 'Regulation of GPCR activity, trafficking and localization by GPCR-interacting proteins', *Br J Pharmacol*, 165: 1717-36.

Mahoney, J. P., and R. K. Sunahara. 2016. 'Mechanistic insights into GPCR-G protein interactions', *Curr Opin Struct Biol*, 41: 247-54.

Mandillo, S., E. Golini, D. Marazziti, C. Di Pietro, R. Matteoni, and G. P. Tocchini-Valentini. 2013. 'Mice lacking the Parkinson's related GPR37/PAEL receptor show non-motor behavioral phenotypes: age and gender effect', *Genes Brain Behav*, 12: 465-77.

Marazziti, D., C. Di Pietro, E. Golini, S. Mandillo, G. La Sala, R. Matteoni, and G. P. Tocchini-Valentini. 2013. 'Precocious cerebellum development and improved motor functions in mice lacking the astrocyte cilium-, patched 1-associated Gpr37l1 receptor', *Proc Natl Acad Sci U S A*, 110: 16486-91.

Marazziti, D., C. Di Pietro, E. Golini, S. Mandillo, R. Matteoni, and G. P. Tocchini-Valentini. 2009. 'Macroautophagy of the GPR37 orphan receptor and Parkinson disease-associated neurodegeneration', *Autophagy*, 5: 741-2.

Marazziti, D., C. Di Pietro, S. Mandillo, E. Golini, R. Matteoni, and G. P. Tocchini-Valentini. 2011. 'Absence of the GPR37/PAEL receptor impairs striatal Akt and ERK2 phosphorylation, DeltaFosB expression, and conditioned place preference to amphetamine and cocaine', *FASEB J*, 25: 2071-81.

Marazziti, D., A. Gallo, E. Golini, R. Matteoni, and G. P. Tocchini-Valentini. 1998. 'Molecular cloning and chromosomal localization of the mouse Gpr37 gene encoding an orphan G-protein-coupled peptide receptor expressed in brain and testis', *Genomics*, 53: 315-24.

Marazziti, D., E. Golini, A. Gallo, M. S. Lombardi, R. Matteoni, and G. P. Tocchini-Valentini. 1997. 'Cloning of GPR37, a gene located on

chromosome 7 encoding a putative G-protein-coupled peptide receptor, from a human frontal brain EST library', *Genomics*, 45: 68-77.

Marazziti, D., E. Golini, S. Mandillo, A. Magrelli, W. Witke, R. Matteoni, and G. P. Tocchini-Valentini. 2004. 'Altered dopamine signaling and MPTP resistance in mice lacking the Parkinson's disease-associated GPR37/parkin-associated endothelin-like receptor', *Proc Natl Acad Sci U S A*, 101: 10189-94.

Marazziti, D., S. Mandillo, C. Di Pietro, E. Golini, R. Matteoni, and G. P. Tocchini-Valentini. 2007. 'GPR37 associates with the dopamine transporter to modulate dopamine uptake and behavioral responses to dopaminergic drugs', *Proc Natl Acad Sci U S A*, 104: 9846-51.

Marchese, A., M. M. Paing, B. R. Temple, and J. Trejo. 2008. 'G protein-coupled receptor sorting to endosomes and lysosomes', *Annu Rev Pharmacol Toxicol*, 48: 601-29.

Mattila, S. O., J. T. Tuusa, and U. E. Petaja-Repo. 2016. 'The Parkinson's-disease-associated receptor GPR37 undergoes metalloproteinase-mediated N-terminal cleavage and ectodomain shedding', *J Cell Sci*, 129: 1366-77.

McGarrigle, D., and X. Y. Huang. 2007. 'GPCRs signaling directly through Src-family kinases', *Sci STKE*, 2007: pe35.

McKee, E. E., A. T. Bentley, R. M. Smith, Jr., and C. E. Ciaccio. 1999. 'Origin of guanine nucleotides in isolated heart mitochondria', *Biochem Biophys Res Commun*, 257: 466-72.

McLatchie, L. M., N. J. Fraser, M. J. Main, A. Wise, J. Brown, N. Thompson, R. Solari, M. G. Lee, and S. M. Foord. 1998. 'RAMPs regulate the transport and ligand specificity of the calcitonin-receptor-like receptor', *Nature*, 393: 333-9.

Meyer, R. C. 2014. 'GPR37 & GPR37L1: Ligand Identification, Cell Protective Signaling & Dopaminergic Cross-Talk', Emory University.

Meyer, R. C., M. M. Giddens, B. M. Coleman, and R. A. Hall. 2014. 'The protective role of prosaposin and its receptors in the nervous system', *Brain Res*, 1585: 1-12.

Meyer, R. C., M. M. Giddens, S. A. Schaefer, and R. A. Hall. 2013. 'GPR37 and GPR37L1 are receptors for the neuroprotective and glioprotective factors prosaptide and prosaposin', *Proc Natl Acad Sci U S A*, 110: 9529-34.

Montag, D., K. P. Giese, U. Bartsch, R. Martini, Y. Lang, H. Bluthmann, J. Karthigasan, D. A. Kirschner, E. S. Wintergerst, K. A. Nave, and et al. 1994. 'Mice deficient for the myelin-associated glycoprotein show subtle abnormalities in myelin', *Neuron*, 13: 229-46.

Munk, C., V. Isberg, S. Mordalski, K. Harpsoe, K. Rataj, A. S. Hauser, P. Kolb, A. J. Bojarski, G. Vriend, and D. E. Gloriam. 2016. 'GPCRdb: the G protein-coupled receptor database - an introduction', *Br J Pharmacol*, 173: 2195-207.

Murakami, T., M. Shoji, Y. Imai, H. Inoue, T. Kawarabayashi, E. Matsubara, Y. Harigaya, A. Sasaki, R. Takahashi, and K. Abe. 2004. 'Pael-R is accumulated in Lewy bodies of Parkinson's disease', *Ann Neurol*, 55: 439-42.

Na, J. I., J. Y. Na, W. Y. Choi, M. C. Lee, M. S. Park, K. H. Choi, J. K. Lee, K. T. Kim, J. T. Park, and H. S. Kim. 2015. 'The HIF-1 inhibitor YC-1 decreases reactive astrocyte formation in a rodent ischemia model', *Am J Transl Res*, 7: 751-60.

Nair, D. R. 2016. 'Management of Drug-Resistant Epilepsy', *Continuum (Minneap Minn)*, 22: 157-72.

Nakajima, K., and S. Kohsaka. 2004. 'Microglia: neuroprotective and neurotrophic cells in the central nervous system', *Curr Drug Targets Cardiovasc Haematol Disord*, 4: 65-84.

Nawashiro, H., M. Brenner, S. Fukui, K. Shima, and J. M. Hallenbeck. 2000. 'High susceptibility to cerebral ischemia in GFAP-null mice', *J Cereb Blood Flow Metab*, 20: 1040-4.

Nery, S., H. Wichterle, and G. Fishell. 2001. 'Sonic hedgehog contributes to oligodendrocyte specification in the mammalian forebrain', *Development*, 128: 527-40.

Neves, S. R., P. T. Ram, and R. Iyengar. 2002. 'G protein pathways', *Science*, 296: 1636-9.

Ng, P. C., and S. Henikoff. 2001. 'Predicting deleterious amino acid substitutions', *Genome Res*, 11: 863-74.

Ngo, T., A. V. Ilatovskiy, A. G. Stewart, J. L. Coleman, F. M. McRobb, R. P. Riek, R. M. Graham, R. Abagyan, I. Kufareva, and N. J. Smith. 2016. 'Orphan receptor ligand discovery by pickpocketing pharmacological neighbors', *Nat Chem Biol*.

Nickols, H. H., and P. J. Conn. 2014. 'Development of allosteric modulators of GPCRs for treatment of CNS disorders', *Neurobiol Dis*, 61: 55-71.

Nilsson, D., C. Go, J. T. Rutka, B. Rydenhag, D. J. Mabbott, O. C. Snead, 3rd, C. R. Raybaud, and E. Widjaja. 2008. 'Bilateral diffusion tensor abnormalities of temporal lobe and cingulate gyrus white matter in children with temporal lobe epilepsy', *Epilepsy Res*, 81: 128-35.

Norenberg, M. D., and A. Martinez-Hernandez. 1979. 'Fine structural localization of glutamine synthetase in astrocytes of rat brain', *Brain Res*, 161: 303-10.

O'Brien, J. S., G. S. Carson, H. C. Seo, M. Hiraiwa, and Y. Kishimoto. 1994. 'Identification of prosaposin as a neurotrophic factor', *Proc Natl Acad Sci U S A*, 91: 9593-6.

O'Brien, J. S., G. S. Carson, H. C. Seo, M. Hiraiwa, S. Weiler, J. M. Tomich, J. A. Barranger, M. Kahn, N. Azuma, and Y. Kishimoto. 1995. 'Identification of the neurotrophic factor sequence of prosaposin', *FASEB J*, 9: 681-5.

Ochiai, T., Y. Takenaka, Y. Kuramoto, M. Kasuya, K. Fukuda, M. Kimura, H. Shimeno, R. Misasi, M. Hiraiwa, and S. Soeda. 2008. 'Molecular mechanism for neuro-protective effect of prosaposin against oxidative stress: its regulation of dimeric transcription factor formation', *Biochim Biophys Acta*, 1780: 1441-7.

Olah, M., K. Biber, J. Vinet, and H. W. Boddeke. 2011. 'Microglia phenotype diversity', *CNS Neurol Disord Drug Targets*, 10: 108-18.

Oldham, M. C., G. Konopka, K. Iwamoto, P. Langfelder, T. Kato, S. Horvath, and D. H. Geschwind. 2008. 'Functional organization of the transcriptome in human brain', *Nat Neurosci*, 11: 1271-82.

Omura, T., M. Kaneko, M. Onoguchi, S. Koizumi, M. Itami, M. Ueyama, Y. Okuma, and Y. Nomura. 2008. 'Novel functions of ubiquitin ligase HRD1

with transmembrane and proline-rich domains', *J Pharmacol Sci*, 106: 512-9.

Orth, J. M., G. L. Gunsalus, and A. A. Lamperti. 1988. 'Evidence from Sertoli cell-depleted rats indicates that spermatid number in adults depends on numbers of Sertoli cells produced during perinatal development', *Endocrinology*, 122: 787-94.

Otis, T. S., and M. P. Kavanaugh. 2000. 'Isolation of current components and partial reaction cycles in the glial glutamate transporter EAAT2', *J Neurosci*, 20: 2749-57.

Ouyang, Y. B., L. A. Voloboueva, L. J. Xu, and R. G. Giffard. 2007. 'Selective dysfunction of hippocampal CA1 astrocytes contributes to delayed neuronal damage after transient forebrain ischemia', *J Neurosci*, 27: 4253-60.

Ovchinnikov Iu, A., N. G. Abdulaev, MIu Feigina, I. D. Artamonov, and A. S. Bogachuk. 1983. '[Visual rhodopsin. III. Complete amino acid sequence and topography in a membrane]', *Bioorg Khim*, 9: 1331-40.

Pan, B., S. E. Fromholt, E. J. Hess, T. O. Crawford, J. W. Griffin, K. A. Sheikh, and R. L. Schnaar. 2005. 'Myelin-associated glycoprotein and complementary axonal ligands, gangliosides, mediate axon stability in the CNS and PNS: neuropathology and behavioral deficits in single- and double-null mice', *Exp Neurol*, 195: 208-17.

Perry, S. J., and R. J. Lefkowitz. 2002. 'Arresting developments in heptahelical receptor signaling and regulation', *Trends Cell Biol*, 12: 130-8.

Petr, G. T., Y. Sun, N. M. Frederick, Y. Zhou, S. C. Dhamne, M. Q. Hameed, C. Miranda, E. A. Bedoya, K. D. Fischer, W. Armsen, J. Wang, N. C. Danbolt, A. Rotenberg, C. J. Aoki, and P. A. Rosenberg. 2015. 'Conditional deletion of the glutamate transporter GLT-1 reveals that astrocytic GLT-1 protects against fatal epilepsy while neuronal GLT-1 contributes significantly to glutamate uptake into synaptosomes', *J Neurosci*, 35: 5187-201.

Pickrell, A. M., and R. J. Youle. 2015. 'The roles of PINK1, parkin, and mitochondrial fidelity in Parkinson's disease', *Neuron*, 85: 257-73.

Pierce, K. L., R. T. Premont, and R. J. Lefkowitz. 2002. 'Seven-transmembrane receptors', *Nat Rev Mol Cell Biol*, 3: 639-50.

Poncet, C., C. Soula, F. Trousse, P. Kan, E. Hirsinger, O. Pourquie, A. M. Duprat, and P. Cochard. 1996. 'Induction of oligodendrocyte progenitors in the trunk neural tube by ventralizing signals: effects of notochord and floor plate grafts, and of sonic hedgehog', *Mech Dev*, 60: 13-32.

Poyner, D. R., P. M. Sexton, I. Marshall, D. M. Smith, R. Quirion, W. Born, R. Muff, J. A. Fischer, and S. M. Foord. 2002. 'International Union of Pharmacology. XXXII. The mammalian calcitonin gene-related peptides, adrenomedullin, amylin, and calcitonin receptors', *Pharmacol Rev*, 54: 233-46.

Premont, R. T., J. Inglese, and R. J. Lefkowitz. 1995. 'Protein kinases that phosphorylate activated G protein-coupled receptors', *FASEB J*, 9: 175-82.

Rangroo Thrane, V., A. S. Thrane, F. Wang, M. L. Cotrina, N. A. Smith, M. Chen, Q. Xu, N. Kang, T. Fujita, E. A. Nagelhus, and M. Nedergaard. 2013. 'Ammonia triggers neuronal disinhibition and seizures by impairing astrocyte potassium buffering', *Nat Med*, 19: 1643-8.

Ransohoff, R. M., and V. H. Perry. 2009. 'Microglial physiology: unique stimuli, specialized responses', *Annu Rev Immunol*, 27: 119-45.

Rask-Andersen, M., S. Masuram, and H. B. Schioth. 2014. 'The druggable genome: Evaluation of drug targets in clinical trials suggests major shifts in molecular class and indication', *Annu Rev Pharmacol Toxicol*, 54: 9-26.

Reddy, A. S., D. O'Brien, N. Pisat, C. T. Weichselbaum, K. Sakers, M. Lisci, J. S. Dalal, and J. D. Dougherty. 2017. 'A Comprehensive Analysis of Cell Type-Specific Nuclear RNA From Neurons and Glia of the Brain', *Biol Psychiatry*, 81: 252-64.

Regard, J. B., I. T. Sato, and S. R. Coughlin. 2008. 'Anatomical profiling of G protein-coupled receptor expression', *Cell*, 135: 561-71.

Rezgaoui, M., U. Susens, A. Ignatov, M. Gelderblom, G. Glassmeier, I. Franke, J. Urny, Y. Imai, R. Takahashi, and H. C. Schaller. 2006. 'The neuropeptide head activator is a high-affinity ligand for the orphan G-protein-coupled receptor GPR37', *J Cell Sci*, 119: 542-9.

Richards, S., N. Aziz, S. Bale, D. Bick, S. Das, J. Gastier-Foster, W. W. Grody, M. Hegde, E. Lyon, E. Spector, K. Voelkerding, H. L. Rehm, and Acmg Laboratory Quality Assurance Committee. 2015. 'Standards and guidelines for the interpretation of sequence variants: a joint consensus recommendation of the American College of Medical Genetics and Genomics and the Association for Molecular Pathology', *Genet Med*, 17: 405-24.

Ritter, S. L., and R. A. Hall. 2009. 'Fine-tuning of GPCR activity by receptor-interacting proteins', *Nat Rev Mol Cell Biol*, 10: 819-30.

Rockman, H. A., W. J. Koch, and R. J. Lefkowitz. 2002. 'Seven-transmembrane-spanning receptors and heart function', *Nature*, 415: 206-12.

Roesch, K., A. P. Jadhav, J. M. Trimarchi, M. B. Stadler, B. Roska, B. B. Sun, and C. L. Cepko. 2008. 'The transcriptome of retinal Muller glial cells', *J Comp Neurol*, 509: 225-38.

Roger, V. L., A. S. Go, D. M. Lloyd-Jones, E. J. Benjamin, J. D. Berry, W. B. Borden, D. M. Bravata, S. Dai, E. S. Ford, C. S. Fox, H. J. Fullerton, C. Gillespie, S. M. Hailpern, J. A. Heit, V. J. Howard, B. M. Kissela, S. J. Kittner, D. T. Lackland, J. H. Lichtman, L. D. Lisabeth, D. M. Makuc, G. M. Marcus, A. Marelli, D. B. Matchar, C. S. Moy, D. Mozaffarian, M. E. Mussolino, G. Nichol, N. P. Paynter, E. Z. Soliman, P. D. Sorlie, N. Sotoodehnia, T. N. Turan, S. S. Virani, N. D. Wong, D. Woo, M. B. Turner, Committee American Heart Association Statistics, and Subcommittee Stroke Statistics. 2012. 'Heart disease and stroke statistics--2012 update: a report from the American Heart Association', *Circulation*, 125: e2-e220.

Rondard, P., C. Goudet, J. Kniazeff, J. P. Pin, and L. Prezeau. 2011. 'The complexity of their activation mechanism opens new possibilities for the modulation of mGlu and GABAB class C G protein-coupled receptors', *Neuropharmacology*, 60: 82-92.

Ruat, M., H. Roudaut, J. Ferent, and E. Traiffort. 2012. 'Hedgehog trafficking, cilia and brain functions', *Differentiation*, 83: S97-104.

Santos, R., O. Ursu, A. Gaulton, A. P. Bento, R. S. Donadi, C. G. Bologa, A. Karlsson, B. Al-Lazikani, A. Hersey, T. I. Oprea, and J. P. Overington.

2017. 'A comprehensive map of molecular drug targets', *Nat Rev Drug Discov*, 16: 19-34.

Santulli, L., A. Coppola, S. Balestrini, and S. Striano. 2016. 'The challenges of treating epilepsy with 25 antiepileptic drugs', *Pharmacol Res*, 107: 211-9.

Sanz, E., R. Evanoff, A. Quintana, E. Evans, J. A. Miller, C. Ko, P. S. Amieux, M. D. Griswold, and G. S. McKnight. 2013. 'RiboTag analysis of actively translated mRNAs in Sertoli and Leydig cells in vivo', *PLoS One*, 8: e66179.

Sauro, K. M., S. Wiebe, C. Dunkley, J. Janszky, E. Kumlien, S. Moshe, N. Nakasato, T. A. Pedley, E. Perucca, H. Senties, S. V. Thomas, Y. Wang, J. Wilmshurst, and N. Jette. 2016. 'The current state of epilepsy guidelines: A systematic review', *Epilepsia*, 57: 13-23.

Scanlon, C., S. G. Mueller, I. Cheong, M. Hartig, M. W. Weiner, and K. D. Laxer. 2013. 'Grey and white matter abnormalities in temporal lobe epilepsy with and without mesial temporal sclerosis', *J Neurol*, 260: 2320-9.

Schmidt, D. 2016. 'Starting, Choosing, Changing, and Discontinuing Drug Treatment for Epilepsy Patients', *Neurol Clin*, 34: 363-81, viii.

Schoene-Bake, J. C., J. Faber, P. Trautner, S. Kaaden, M. Tittgemeyer, C. E. Elger, and B. Weber. 2009. 'Widespread affections of large fiber tracts in postoperative temporal lobe epilepsy', *Neuroimage*, 46: 569-76.

Schuele, S. U., and H. O. Luders. 2008. 'Intractable epilepsy: management and therapeutic alternatives', *Lancet Neurol*, 7: 514-24.

Schulte, G. 2010. 'International Union of Basic and Clinical Pharmacology. LXXX. The class Frizzled receptors', *Pharmacol Rev*, 62: 632-67.

Schwarz, J. M., D. N. Cooper, M. Schuelke, and D. Seelow. 2014. 'MutationTaster2: mutation prediction for the deep-sequencing age', *Nat Methods*, 11: 361-2.

Seifert, G., K. Huttmann, D. K. Binder, C. Hartmann, A. Wyczynski, C. Neusch, and C. Steinhauser. 2009. 'Analysis of astroglial K+ channel expression in the developing hippocampus reveals a predominant role of the Kir4.1 subunit', *J Neurosci*, 29: 7474-88.

Seifert, G., K. Schilling, and C. Steinhauser. 2006. 'Astrocyte dysfunction in neurological disorders: a molecular perspective', *Nat Rev Neurosci*, 7: 194-206.

Semenza, G. L. 1999. 'Regulation of mammalian O2 homeostasis by hypoxia-inducible factor 1', *Annu Rev Cell Dev Biol*, 15: 551-78.

———. 2000. 'HIF-1: mediator of physiological and pathophysiological responses to hypoxia', *J Appl Physiol (1985)*, 88: 1474-80.

Shen, Y., P. He, Y. Y. Fan, J. X. Zhang, H. J. Yan, W. W. Hu, H. Ohtsu, and Z. Chen. 2010. 'Carnosine protects against permanent cerebral ischemia in histidine decarboxylase knockout mice by reducing glutamate excitotoxicity', *Free Radic Biol Med*, 48: 727-35.

Shi, H. 2009. 'Hypoxia inducible factor 1 as a therapeutic target in ischemic stroke', *Curr Med Chem*, 16: 4593-600.

Shi, L., Z. Zhang, and B. Su. 2016. 'Sex Biased Gene Expression Profiling of Human Brains at Major Developmental Stages', *Sci Rep*, 6: 21181.

Shimura, H., N. Hattori, Si Kubo, Y. Mizuno, S. Asakawa, S. Minoshima, N. Shimizu, K. Iwai, T. Chiba, K. Tanaka, and T. Suzuki. 2000. 'Familial Parkinson disease gene product, parkin, is a ubiquitin-protein ligase', *Nat Genet*, 25: 302-5.

Shobha, N., A. M. Buchan, M. D. Hill, and Study Canadian Alteplase for Stroke Effectiveness. 2011. 'Thrombolysis at 3-4.5 hours after acute ischemic stroke onset--evidence from the Canadian Alteplase for Stroke Effectiveness Study (CASES) registry', *Cerebrovasc Dis*, 31: 223-8.

Siddiq, A., L. R. Aminova, and R. R. Ratan. 2008. 'Prolyl 4-hydroxylase activity-responsive transcription factors: from hydroxylation to gene expression and neuroprotection', *Front Biosci*, 13: 2875-87.

Smith, J. S., and S. Rajagopal. 2016. 'The beta-Arrestins: Multifunctional Regulators of G Protein-coupled Receptors', *J Biol Chem*, 291: 8969-77.

Smith, N. J. 2015. 'Drug Discovery Opportunities at the Endothelin B Receptor-Related Orphan G Protein-Coupled Receptors, GPR37 and GPR37L1', *Front Pharmacol*, 6: 275.

Smith, N. J., and L. M. Luttrell. 2006. 'Signal switching, crosstalk, and arrestin scaffolds: novel G protein-coupled receptor signaling in cardiovascular disease', *Hypertension*, 48: 173-9.

Soden, S. E., C. J. Saunders, L. K. Willig, E. G. Farrow, L. D. Smith, J. E. Petrikin, J. B. LePichon, N. A. Miller, I. Thiffault, D. L. Dinwiddie, G. Twist, A. Noll, B. A. Heese, L. Zellmer, A. M. Atherton, A. T. Abdelmoity, N. Safina, S. S. Nyp, B. Zuccarelli, I. A. Larson, A. Modrcin, S. Herd, M. Creed, Z. Ye, X. Yuan, R. A. Brodsky, and S. F. Kingsmore. 2014. 'Effectiveness of exome and genome sequencing guided by acuity of illness for diagnosis of neurodevelopmental disorders', *Sci Transl Med*, 6: 265ra168.

Sofroniew, M. V. 2009. 'Molecular dissection of reactive astrogliosis and glial scar formation', *Trends Neurosci*, 32: 638-47.

Southern, C., J. M. Cook, Z. Neetoo-Isseljee, D. L. Taylor, C. A. Kettleborough, A. Merritt, D. L. Bassoni, W. J. Raab, E. Quinn, T. S. Wehrman, A. P. Davenport, A. J. Brown, A. Green, M. J. Wigglesworth, and S. Rees. 2013. 'Screening beta-arrestin recruitment for the identification of natural ligands for orphan G-protein-coupled receptors', *J Biomol Screen*, 18: 599-609.

Stark, M., O. Danielsson, W. J. Griffiths, H. Jornvall, and J. Johansson. 2001. 'Peptide repertoire of human cerebrospinal fluid: novel proteolytic fragments of neuroendocrine proteins', *J Chromatogr B Biomed Sci Appl*, 754: 357-67.

Starr, M. S. 1996. 'The role of dopamine in epilepsy', *Synapse*, 22: 159-94.

Steinhauser, C., and G. Seifert. 2002. 'Glial membrane channels and receptors in epilepsy: impact for generation and spread of seizure activity', *Eur J Pharmacol*, 447: 227-37.

Sterne-Marr, R., and J. L. Benovic. 1995. 'Regulation of G protein-coupled receptors by receptor kinases and arrestins', *Vitam Horm*, 51: 193-234.

Sunyaev, S., V. Ramensky, I. Koch, W. Lathe, 3rd, A. S. Kondrashov, and P. Bork. 2001. 'Prediction of deleterious human alleles', *Hum Mol Genet*, 10: 591-7.

Syrovatkina, V., K. O. Alegre, R. Dey, and X. Y. Huang. 2016. 'Regulation, Signaling, and Physiological Functions of G-Proteins', *J Mol Biol*, 428: 3850-68.

Szot, P., D. Weinshenker, S. S. White, C. A. Robbins, N. C. Rust, P. A. Schwartzkroin, and R. D. Palmiter. 1999. 'Norepinephrine-deficient mice have increased susceptibility to seizure-inducing stimuli', *J Neurosci*, 19: 10985-92.

Takahashi, R., and Y. Imai. 2003. 'Pael receptor, endoplasmic reticulum stress, and Parkinson's disease', *J Neurol*, 250 Suppl 3: III25-9.

Tanabe, Y., E. Fujita-Jimbo, M. Y. Momoi, and T. Momoi. 2015. 'CASPR2 forms a complex with GPR37 via MUPP1 but not with GPR37(R558Q), an autism spectrum disorder-related mutation', *J Neurochem*, 134: 783-93.

Tanaka, K., K. Watase, T. Manabe, K. Yamada, M. Watanabe, K. Takahashi, H. Iwama, T. Nishikawa, N. Ichihara, T. Kikuchi, S. Okuyama, N. Kawashima, S. Hori, M. Takimoto, and K. Wada. 1997. 'Epilepsy and exacerbation of brain injury in mice lacking the glutamate transporter GLT-1', *Science*, 276: 1699-702.

Tang, X. L., Y. Wang, D. L. Li, J. Luo, and M. Y. Liu. 2012. 'Orphan G protein-coupled receptors (GPCRs): biological functions and potential drug targets', *Acta Pharmacol Sin*, 33: 363-71.

Tani, H., C. G. Dulla, Z. Farzampour, A. Taylor-Weiner, J. R. Huguenard, and R. J. Reimer. 2014. 'A local glutamate-glutamine cycle sustains synaptic excitatory transmitter release', *Neuron*, 81: 888-900.

Tasca, C. I., T. Dal-Cim, and H. Cimarosti. 2015. 'In vitro oxygen-glucose deprivation to study ischemic cell death', *Methods Mol Biol*, 1254: 197-210.

Terrillon, S., and M. Bouvier. 2004. 'Roles of G-protein-coupled receptor dimerization', *EMBO Rep*, 5: 30-4.

Tomita, H., M. E. Ziegler, H. B. Kim, S. J. Evans, P. V. Choudary, J. Z. Li, F. Meng, M. Dai, R. M. Myers, C. R. Neal, T. P. Speed, J. D. Barchas, A. F. Schatzberg, S. J. Watson, H. Akil, E. G. Jones, W. E. Bunney, and M. P. Vawter. 2013. 'G protein-linked signaling pathways in bipolar and major depressive disorders', *Front Genet*, 4: 297.

Toyota, M., K. J. Kopecky, M. O. Toyota, K. W. Jair, C. L. Willman, and J. P. Issa. 2001. 'Methylation profiling in acute myeloid leukemia', *Blood*, 97: 2823-9.

Traynelis, S. F., and R. Dingledine. 1988. 'Potassium-induced spontaneous electrographic seizures in the rat hippocampal slice', *J Neurophysiol*, 59: 259-76.

Tsao, P., and M. von Zastrow. 2000. 'Downregulation of G protein-coupled receptors', *Curr Opin Neurobiol*, 10: 365-9.

Tsvetanova, N. G., R. Irannejad, and M. von Zastrow. 2015. 'G protein-coupled receptor (GPCR) signaling via heterotrimeric G proteins from endosomes', *J Biol Chem*, 290: 6689-96.

Vaillant, C., and D. Monard. 2009. 'SHH pathway and cerebellar development', *Cerebellum*, 8: 291-301.

Valdenaire, O., T. Giller, V. Breu, A. Ardati, A. Schweizer, and J. G. Richards. 1998. 'A new family of orphan G protein-coupled receptors predominantly expressed in the brain', *FEBS Lett*, 424: 193-6.

Vassart, G., and S. Costagliola. 2011. 'G protein-coupled receptors: mutations and endocrine diseases', *Nat Rev Endocrinol*, 7: 362-72.

Verkhratsky, A., L. Steardo, V. Parpura, and V. Montana. 2016. 'Translational potential of astrocytes in brain disorders', *Prog Neurobiol*, 144: 188-205.

Vinson, C. R., and P. N. Adler. 1987. 'Directional non-cell autonomy and the transmission of polarity information by the frizzled gene of Drosophila', *Nature*, 329: 549-51.

Violin, J. D., and R. J. Lefkowitz. 2007. 'Beta-arrestin-biased ligands at seven-transmembrane receptors', *Trends Pharmacol Sci*, 28: 416-22.

Wallace, V. A. 1999. 'Purkinje-cell-derived Sonic hedgehog regulates granule neuron precursor cell proliferation in the developing mouse cerebellum', *Curr Biol*, 9: 445-8.

Wallraff, A., R. Kohling, U. Heinemann, M. Theis, K. Willecke, and C. Steinhauser. 2006. 'The impact of astrocytic gap junctional coupling on potassium buffering in the hippocampus', *J Neurosci*, 26: 5438-47.

Wang, F., N. A. Smith, Q. Xu, T. Fujita, A. Baba, T. Matsuda, T. Takano, L. Bekar, and M. Nedergaard. 2012. 'Astrocytes modulate neural network activity by Ca(2)+-dependent uptake of extracellular K+', *Sci Signal*, 5: ra26.

Wang, H., L. Hu, M. Zang, B. Zhang, Y. Duan, Z. Fan, J. Li, L. Su, M. Yan, Z. Zhu, B. Liu, and Q. Yang. 2016. 'REG4 promotes peritoneal metastasis of gastric cancer through GPR37', *Oncotarget*, 7: 27874-88.

Wang, H. Q., Y. Imai, H. Inoue, A. Kataoka, S. Iita, N. Nukina, and R. Takahashi. 2008. 'Pael-R transgenic mice crossed with parkin deficient mice displayed progressive and selective catecholaminergic neuronal loss', *J Neurochem*, 107: 171-85.

Wang, Q., X. N. Tang, and M. A. Yenari. 2007. 'The inflammatory response in stroke', *J Neuroimmunol*, 184: 53-68.

Watson, N., M. E. Linder, K. M. Druey, J. H. Kehrl, and K. J. Blumer. 1996. 'RGS family members: GTPase-activating proteins for heterotrimeric G-protein alpha-subunits', *Nature*, 383: 172-5.

Wechsler-Reya, R. J., and M. P. Scott. 1999. 'Control of neuronal precursor proliferation in the cerebellum by Sonic Hedgehog', *Neuron*, 22: 103-14.

Wilby, J., A. Kainth, N. Hawkins, D. Epstein, H. McIntosh, C. McDaid, A. Mason, S. Golder, S. O'Meara, M. Sculpher, M. Drummond, and C. Forbes. 2005. 'Clinical effectiveness, tolerability and cost-effectiveness of newer drugs for epilepsy in adults: a systematic review and economic evaluation', *Health Technol Assess*, 9: 1-157, iii-iv.

Willig, L. K., J. E. Petrikin, L. D. Smith, C. J. Saunders, I. Thiffault, N. A. Miller, S. E. Soden, J. A. Cakici, S. M. Herd, G. Twist, A. Noll, M. Creed, P. M. Alba, S. L. Carpenter, M. A. Clements, R. T. Fischer, J. A. Hays, H. Kilbride, R. J. McDonough, J. L. Rosterman, S. L. Tsai, L. Zellmer, E. G. Farrow, and S. F. Kingsmore. 2015. 'Whole-genome sequencing for identification of Mendelian disorders in critically ill infants: a retrospective analysis of diagnostic and clinical findings', *Lancet Respir Med*, 3: 377-87.

Wisler, J. W., K. Xiao, A. R. Thomsen, and R. J. Lefkowitz. 2014. 'Recent developments in biased agonism', *Curr Opin Cell Biol*, 27: 18-24.

Wong, C. H., and P. J. Crack. 2008. 'Modulation of neuro-inflammation and vascular response by oxidative stress following cerebral ischemia-reperfusion injury', *Curr Med Chem*, 15: 1-14.

Wong, J. C., S. B. Dutton, S. D. Collins, S. Schachter, and A. Escayg. 2016. 'Huperzine A Provides Robust and Sustained Protection against Induced Seizures in Scn1a Mutant Mice', *Front Pharmacol*, 7: 357.

Yang, H. J., A. Vainshtein, G. Maik-Rachline, and E. Peles. 2016. 'G protein-coupled receptor 37 is a negative regulator of oligodendrocyte differentiation and myelination', *Nat Commun*, 7: 10884.

Yang, S., and C. L. Cox. 2011. 'Attenuation of inhibitory synaptic transmission by glial dysfunction in rat thalamus', *Synapse*, 65: 1298-308.

Yang, Y., I. Nishimura, Y. Imai, R. Takahashi, and B. Lu. 2003. 'Parkin suppresses dopaminergic neuron-selective neurotoxicity induced by Pael-R in Drosophila', *Neuron*, 37: 911-24.

Yorimitsu, T., and D. J. Klionsky. 2005. 'Autophagy: molecular machinery for self-eating', *Cell Death Differ*, 12 Suppl 2: 1542-52.

Zeng, Z., K. Su, H. Kyaw, and Y. Li. 1997. 'A novel endothelin receptor type-B-like gene enriched in the brain', *Biochem Biophys Res Commun*, 233: 559-67.

Zhang, Y., K. Chen, S. A. Sloan, M. L. Bennett, A. R. Scholze, S. O'Keeffe, H. P. Phatnani, P. Guarnieri, C. Caneda, N. Ruderisch, S. Deng, S. A. Liddelow, C. Zhang, R. Daneman, T. Maniatis, B. A. Barres, and J. Q. Wu. 2014. 'An RNA-sequencing transcriptome and splicing database of glia, neurons, and vascular cells of the cerebral cortex', *J Neurosci*, 34: 11929-47.

Zhang, Y., J. Gao, K. K. Chung, H. Huang, V. L. Dawson, and T. M. Dawson. 2000. 'Parkin functions as an E2-dependent ubiquitin- protein ligase and promotes the degradation of the synaptic vesicle-associated protein, CDCrel-1', *Proc Natl Acad Sci U S A*, 97: 13354-9.

Zhao, X., K. Southwick, H. L. Cardasis, Y. Du, M. E. Lassman, D. Xie, M. El-Sherbeini, W. M. Geissler, K. D. Pryor, A. Verras, M. Garcia-Calvo, D. M. Shen, N. A. Yates, S. Pinto, and R. C. Hendrickon. 2010. 'Peptidomic profiling of human cerebrospinal fluid identifies YPRPIHPA as a novel substrate for prolylcarboxypeptidase', *Proteomics*, 10: 2882-6.

Zou, T., X. Tang, Z. Huang, N. Xu, and Z. Hu. 2014. 'The Pael-R gene does not mediate the changes in rotenone-induced Parkinson's disease model cells', *Neural Regen Res*, 9: 402-6.

Zou, T., B. Xiao, J. Tang, H. Zhang, and X. Tang. 2012. 'Downregulation of Pael-R expression in a Parkinson's disease cell model reduces apoptosis', *J Clin Neurosci*, 19: 1433-6.

APPENDIX I:

GPR37 and GPR37L1: Protein Interaction

Section I.1 Rationale

Loss of Gpr37 and/or Gpr37L1 contributes to increased susceptibility in models of seizure and stroke. However, the mechanisms underlying these observations have yet to be completely understood. One method for improving our understanding of the protective actions of G protein-coupled receptors (GPCRs) is to identify relevant interacting proteins involved in the regulation and signaling of these receptors. To achieve this goal, we pursued a two-pronged approach. First, GPR37 and GPR37L1 were immunoprecipitated from whole brain samples of wild-type (WT) mice vs. mice lacking both GPR37 and GPR37L1 (DKO), as a control. Co-immunoprecipitated proteins were identified through mass spectrometry. This proteomic-based method has been successfully used for a number of other receptors, including NMDA (Husi et al. 2000), $P2X_7$ (Kim et al. 2001), 5-HT_{2C} (Becamel et al. 2002), and D_1 and D_2 (Free et al. 2007) receptors. Secondly, we compared the brain-specific proteome of WT and DKO mice to identify significant alterations in protein expression in mice lacking both Gpr37 and Gpr37L1. The studies described in this appendix, provide a major step forward in the identification of interaction partners of Gpr37 and/or Gpr37L1 and set the stage for achieving a deeper understanding of the signaling and regulation of these receptors.

Section I.2 Materials and Methods

I.2.1 Tissue Homogenization

The sample was vortex in 300 uL of urea lysis buffer (8M urea, 100 mM NaHPO4, pH 8.5), including 3 uL (100x stock) HALT protease and phosphatase inhibitor cocktail (Pierce). All homogenization was performed using a Bullet Blender (Next Advance) according to manufacturer protocols. Protein supernatants were transferred to 1.5 mL Eppendorf tubes, centrifuged at 14,000 rpm for 1 minute and sonicated (Sonic Dismembrator, Fisher Scientific) 3 times for 5 s with 15 s intervals of rest at 30% amplitude to disrupt nucleic acids and subsequently vortexed. Protein concentration was determined by the bicinchoninic acid (BCA) method, and samples were frozen in aliquots at −80°C. Protein homogenates (100 ug) is then treated with 1 mM dithiothreitol (DTT) at 25°C for 30 minutes, followed by 5 mM iodoacetimide (IAA) at 25°C for 30 minutes in the dark. Protein was digested with 1:100 (w/w) lysyl endopeptidase (Wako) at 25°C overnight. Samples were then diluted with 50 mM NH4HCO3 to a final concentration of less than 2M urea and further digested overnight with 1:50 (w/w) trypsin (Promega) at 25°C. Resulting peptides were desalted with a Sep-Pak C18 column (Waters) and dried under vacuum.

I.2.2 LC-MS/MS analysis

Derived peptides were resuspended in peptide 10 uL of loading buffer (0.1% formic acid, 0.03% trifluoroacetic acid, 1% acetonitrile). Peptide mixtures (2 uL) were separated on a self-packed C18 (1.9 um Dr. Maisch, Germany) fused

silica column (25 cm x 75 uM internal diameter (ID); New Objective, Woburn, MA) by a Dionex Ultimate 3000 RSLCNano and monitored on a Fusion mass spectrometer (ThermoFisher Scientific , San Jose, CA). Elution was performed over a 120 minute gradient at a rate of 300nl/min with buffer B ranging from 3% to 80% (buffer A: 0.1% formic acid in water, buffer B: 0.1 % formic in acetonitrile). The mass spectrometer cycle was programmed to collect at the top speed for 3 second cycles. The MS scans (400-1500 m/z range, 200,000 AGC, 50 ms maximum ion time) were collected at a resolution of 120,000 at m/z 200 in profile mode and the HCD MS/MS spectra (1.6 m/z isolation width, 32% collision energy, 10,000 AGC target, 35 ms maximum ion time) were detected in the ion trap. Dynamic exclusion was set to exclude previous sequenced precursor ions for 20 seconds within a 10 ppm window. Precursor ions with +1, and +8 or higher charge states were excluded from sequencing.

I.2.3 Data Analysis

RAW data for the samples was analyzed using MaxQuant v1.5.4.1 with Thermo Foundation 2.0 for RAW file reading capability. The search engine Andromeda, integrated into MaxQuant, was used to build and search a concatenated target-decoy Uniprot mouse reference protein database (retrieved April 20, 2015; 53,289 target sequences), plus 245 contaminant proteins from the common repository of adventitious proteins (cRAP) built into MaxQuant. Methionine oxidation (+15.9949 Da), asparagine and glutamine deamidation (+0.9840 Da), and protein N-terminal acetylation (+42.0106 Da) were variable

modifications (up to 5 allowed per peptide); cysteine was assigned a fixed carbamidomethyl modification (+57.0215 Da). Only fully tryptic peptides were considered with up to 2 miscleavages in the database search. A precursor mass tolerance of ±20 ppm was applied prior to mass accuracy calibration and ±4.5 ppm after internal MaxQuant calibration. Other search settings included a maximum peptide mass of 6,000 Da, a minimum peptide length of 6 residues, 0.50 Da tolerance for low resolution MS/MS scans. Co-fragmented peptide search was enabled to deconvolute multiplex spectra. The false discovery rate (FDR) for peptide spectral matches, proteins, and site decoy fraction were all set to 1 percent. Quantification settings were as follows: requantify with a second peak finding attempt after protein identification has completed; match MS1 peaks between runs; a 0.7 min retention time match window was used after an alignment function was found with a 20 minute RT search space. Quantitation of proteins was performed using summed peptide intensities given by MaxQuant. The quantitation method only considered razor plus unique peptides for protein level quantitation.

I.2.4 Endogenous Pulldown

Whole brain samples from wild-type or double knowkout animals 3-4 months of age were homogenized in 10mL lysis buffer (10 mM Hepes, 50 mM NaCl, 5 mM EDTA, and protease inhibitor cocktail (Roche Diagnostics)) with a dounce homogenizer. Samples were centrifuged for 20 minutes at 4^{o}C at 16,000 rpm and resuspended in 10 lysis buffer + 1% Triton-X, and solubilized by rotating

end-over-end for 30 minutes at 4˚C. Samples were centrifuged at 16,000 rpm at 4°C for 20 minutes. The supernatant was collected into new, clean tubes and centrifuged again at 16,000 rpm at 4°C for 20 minutes to clear membranes. Samples were pre-cleared with 30µL of beads (no antibody) while rotating end-over-end for 1 hour at 4°C. The beads were pelleted with a 10 minute centrifugation at 1000 rpm and the supernatant was transferred into a new tube with 25uL of GPR37 or GPR37L1 antibody (Mab Technologies) and incubated at 4˚C for 24-48h, rotating end-over-end. Following antibody incubation, 60uL of Pierce Protein A/G Agarose beads (Thermo Sceintific) were added and incubated rotating end-over-end for 2 hours. Beads were washed 5X in LSHB + Triton X and resuspended in lysis buffer for digestion.

I.2.5 Sample Digestion

The IP beads were spun down and residual wash buffer was removed. Ddigestion buffer (300 ul of 50 mM NH_4HCO_3) was added and the bead solution was then treated with 1 mM dithiothreitol (DTT) at 25°C for 30 minutes, followed by 5 mM iodoacetimide (IAA) at 25°C for 30 minutes in the dark. Proteins were digested with 1ug of lysyl endopeptidase (Wako) at room temperature for 2 hours and further digested overnight with 1:50 (w/w) trypsin (Promega) at room temperature. Resulting peptides were desalted with a Sep-Pak C18 column (Waters) and dried under vacuum. LC-MS/MS analysis: The dried peptides were resuspended in 10 uL of loading buffer (0.1% formic acid, 0.03% trifluoroacetic acid, 1% acetonitrile). Peptide mixtures (2 uL) were separated on a self-packed C18 (1.9 um Dr. Maisch, Germany) fused silica column (25 cm x 75 uM internal

diameter (ID); New Objective, Woburn, MA) by a Dionex Ultimate 3000 RSLCNano and monitored on a Fusion mass spectrometer (ThermoFisher Scientific , San Jose, CA). Elution was performed over a 120 minute gradient at a rate of 350nl/min with buffer B ranging from 3% to 80% (buffer A: 0.1% formic acid in water, buffer B: 0.1 % formic in acetonitrile). The mass spectrometer cycle was programmed to collect at the top speed for 3 second cycles. The MS scans (400-1600 m/z range, 200,000 AGC, 50 ms maximum ion time) were collected at a resolution of 120,000 at m/z 200 in profile mode and the HCD MS/MS spectra (0.7 m/z isolation width, 30% collision energy, 10,000 AGC target, 35 ms maximum ion time) were detected in the ion trap. Dynamic exclusion was set to exclude previous sequenced precursor ions for 20 seconds within a 10 ppm window. Precursor ions with +1, and +8 or higher charge states were excluded from sequencing.

I.2.6 Database search:

Spectra were searched using Proteome Discoverer 2.0 against mouse Uniprot database (53289 target sequences). Searching parameters included fully tryptic restriction and a parent ion mass tolerance (± 20 ppm). Methionine oxidation (+15.99492 Da), asaparagine and glutamine deamidation (+0.98402 Da), and protein N-terminal acetylation (+42.03670) were variable modifications (up to 3 allowed per peptide); cysteine was assigned a fixed carbamidomethyl modification (+57.021465 Da). Percolator was used to filter the peptide spectrum matches to a false discovery rate of 1%.

Section I.3 Results

To determine potential interacting partners for GPR37 and GPR37L1, we assessed the severity of a cortical ischemic stroke model in mice lacking *Gpr37*$^{-/-}$ compared to wild-type (WT) littermates. Permanent middle cerebral artery occlusion (MCAO) combined with seven minutes of common carotid artery (CCA) occlusion was used to induce a cortical ischemic stroke (Figure 3-1). Animals were sacrificed 72h after MCAO and the size of the infarct was assessed via 2,3,5-triphenyltetrazolium chloride (TTC), a measure of cell death. *Gpr37*$^{-/-}$ mice had a significantly larger infarct size than their WT littermates at 72h post MCAO (Figure 3-2A & B)

Table I-1. Potential Interacting Partners of GPR37

Protein Name	Gene Name	Log2 Ratio (WT/DKO)	# PSMs WT	# PSMs DKO
Rabphilin-3A	Rph3a	6.64	30	0
AP-2 complex subunit alpha-2	Ap2a2	6.64	25	0
Peroxisomal multifunctional enzyme type 2	Hsd17b4	6.64	23	0
Disco-interacting protein 2 homolog B	Dip2b	6.64	22	0
Breast carcinoma-amplified sequence 1	Bcas1	6.64	18	0
Serine/threonine-protein kinase DCLK1	Dclk1	6.64	15	0
Methylglutaconyl-CoA hydratase, mitochondrial	Auh	6.64	13	0
Serine/threonine-protein kinase BRSK1	Brsk1	6.64	13	0
Serine/arginine-rich splicing factor 3	Srsf3	6.64	12	0
Zinc finger C2HC domain-containing protein 1A	Zc2hc1a	6.64	11	0
Acyl-coenzyme A thioesterase 11	Acot11	6.64	11	0
AP-3 complex subunit delta-1	Ap3d1	6.64	11	0
Microtubule-associated protein (Fragment)	Map2	6.64	10	0
Microtubule-associated protein 4	Map4	6.64	10	0
Creatine kinase U-type, mitochondrial	Ckmt1	6.64	10	0
Protein-glutamine gamma-glutamyltransferase K	Tgm1	6.64	10	0
Alpha-tubulin N-acetyltransferase 1	Atat1	6.64	10	0
AMP deaminase 3	Ampd3	6.64	9	0
Serine/threonine-protein kinase BRSK2	Brsk2	6.64	9	0
Saccharopine dehydrogenase-like oxidoreductase	Sccpdh	6.64	9	0
AP-2 complex subunit mu	Ap2m1	6.64	9	0

Table I-1. Potential Interacting Partners of GPR37 contd.

Protein Name	Gene Name	Log2 Ratio (WT/DKO)	# PSMs WT	# PSMs DKO
Microtubule-associated protein 6	Map6	4.29	39	2
Isoform 2 of AP-2 complex subunit beta	Ap2b1	4.17	18	1
Elongation factor 2	Eef2	3.70	13	1
RNA-binding protein FUS	Fus	3.58	12	1
Mitochondrial pyruvate carrier 2	Mpc2	3.58	12	1
Microtubule-associated protein 2	Map2	3.52	23	2
Synapsin-1	Syn1	3.41	85	8
Glioblastoma amplified sequence	Gbas	3.32	30	3
Synaptotagmin-1	Syt1	3.25	19	2
ATP-dependent 6-phosphofructokinase, liver type	Pfkl	3.25	19	2
Succinyl-CoA ligase [ADP/GDP-forming] subunit alpha, mitochondrial	Suclg1	3.17	18	2
Tricarboxylate transport protein, mitochondrial	Slc25a1	3.17	9	1
Histidine ammonia-lyase	Hal	3.17	9	1
Protein NipSnap homolog 2	Gbas	3.00	24	3
ATPase inhibitor, mitochondrial	Atpif1	3.00	8	1
Prosaposin receptor GPR37	Gpr37	3.00	8	1
THO complex subunit 4	Alyref	3.00	8	1
Mitogen-activated protein kinase 1	Mapk1	3.00	8	1
Isoform 3 of ATP-dependent 6-phosphofructokinase, muscle type	Pfkm	2.96	39	5
Myelin basic protein (Fragment)	Mbp	2.89	111	15
Myelin basic protein (Fragment)	Mbp	2.86	109	15
Protein NipSnap homolog 1	Nipsnap1	2.81	35	5
Tubulin polymerization-promoting protein	Tppp	2.81	21	3

Table I-1. Potential Interacting Partners of GPR37 contd.

Protein Name	Gene Name	Log2 Ratio (WT/DKO)	# PSMs WT	# PSMs DKO
Synapsin-2	Syn2	2.58	18	3
MCG1048875, isoform CRA_c	Gm9755	2.42	16	3
Sideroflexin-5	Sfxn5	2.32	10	2
Elongation factor 1-alpha 2	Eef1a2	2.17	54	12
Enoyl-CoA hydratase, mitochondrial	Echs1	2.17	9	2
Microtubule-associated protein	Mapt	2.12	39	9
Filaggrin-2	Flg2	2.12	13	3
Isoform Tau-A of Microtubule-associated protein tau	Mapt	2.05	29	7
Mitochondrial 2-oxoglutarate/malate carrier protein	Slc25a11	2.00	24	6
Isoform 2 of Dynamin-like 120 kDa protein, mitochondrial	Opa1	2.00	12	3
ADP-ribosylation factor 3	Arf3	2.00	8	2
ADP/ATP translocase 1	Slc25a4	1.77	92	27
Desmoglein-1-beta	Dsg1b	1.74	10	3
Glutamate dehydrogenase 1, mitochondrial	Glud1	1.74	10	3
ATP synthase subunit O, mitochondrial	Atp5o	1.71	36	11
ADP/ATP translocase 2	Slc25a5	1.70	78	24
Aldolase A splice variant 2	Aldoa	1.68	16	5
Junction plakoglobin	Jup	1.64	75	24
Sideroflexin	Sfxn3	1.58	9	3
Dynamin-1	Dnm1	1.58	9	3
Beta-enolase	Eno3	1.58	9	3
Desmoplakin	Dsp	1.52	89	31
Elongation factor 1-alpha 1	Eef1a1	1.52	43	15

Table I-1. Potential Interacting Partners of GPR37 contd.

Protein Name	Gene Name	Log2 Ratio (WT/DKO)	# PSMs WT	# PSMs DKO
Annexin A2	Anxa2	1.50	17	6
Isocitrate dehydrogenase 3 (NAD+) beta	Idh3b	1.44	19	7
Histone H2A type 1	Hist1h2ab	1.42	8	3
Gamma-enolase	Eno2	1.42	8	3
Tubulin beta-4A chain	Tubb4a	1.38	86	33
Tubulin beta-4B chain	Tubb4b	1.37	88	34
Tubulin beta-5 chain	Tubb5	1.34	86	34
Septin-7	Sept7	1.32	10	4
Glyceraldehyde-3-phosphate dehydrogenase	Gapdh	1.29	44	18
Vesicle-fusing ATPase	Nsf	1.22	28	12
14-3-3 protein beta/alpha	Ywhab	1.17	9	4
Tubulin beta-2A chain	Tubb2a	1.12	85	39
Mitochondrial glutamate carrier 1	Slc25a22	1.12	13	6
Plakophilin-1	Pkp1	1.10	15	7
2',3'-cyclic-nucleotide 3'-phosphodiesterase	Cnp	1.07	40	19
Calcium-binding mitochondrial carrier protein Aralar1	Slc25a12	1	16	8
Phosphate carrier protein, mitochondrial	Slc25a3	1	10	5

Table I-1. Potential GPR37 Interacting Partners

Proteins immunoprecipitated with GPR37 in wild-type (WT) and double knockout (DKO) mice lacking GPR37 and GPR37L1 as identified with mass spectrometry. Specific protein interactions were determined as having a log2 ratio score of ≥ 1 and at least 8 peptide spectrum matches (PSMs) in WT mice. Common contaminant, keratin, was removed from results.

Table I-2. Potential Interacting Partners of GPR37L1

Protein Name	Gene Name	Log2 Ratio (WT/DKO)	# PSMs WT	# PSMs DKO
Synapsin-1 OS	Syn1	6.64	37	0
Cysteine and glycine-rich protein 1	Csrp1	6.64	9	0
Synapsin-2	Syn2	6.64	8	0
Prosaposin receptor GPR37L1	Gpr37l1	3.39	21	2
14-3-3 protein theta (Fragment)	Ywhaq	1.46	11	4
Actin, cytoplasmic 1	Actb	1.42	72	27
Guanine nucleotide-binding protein G(o) subunit alpha	Gnao1	1.42	16	6
Excitatory amino acid transporter 2	Slc1a2	1.32	50	20
Dynamin-3	Dnm3	1.32	10	4
Sarcoplasmic/endoplasmic reticulum calcium ATPase 2	Atp2a2	1.32	10	4
Aconitate hydratase, mitochondrial	Aco2	1.28	17	7
Inter-alpha trypsin inhibitor, heavy chain 2	Itih2	1.1	15	7
Alpha-enolase	Eno1	1.09	17	8
Stress-70 protein, mitochondrial	Hspa9	1	10	5
Myelin proteolipid protein	Plp1	1	8	4

Table I-2. Potential GPR37L1 Interacting Partners

Proteins immunoprecipitated with GPR37L1 in wild-type (WT) and double knockout (DKO) mice lacking GPR37 and GPR37L1 as identified with mass spectrometry. Specific protein interactions were determined as having a log2 ratio score of ≥ 1 and at least 8 peptide spectrum matches (PSMs) in WT mice. Common contaminant, keratin, was removed from results.

Table I-3. Differentially Expressed Proteins in Brain of Mice Lacking GPR37 and GPR37L1

Protein Name	Gene Name	p-value	% Change (DKO/WT)
Isoform 4 of Protein enabled homolog	Enah	7.1E-10	2441%
Protein S100-A5	S100a5	7.5E-08	-2580%
3-beta-hydroxysteroid-Delta(8),Delta(7)-isomerase (Fragment)	Ebp	1.9E-06	-2396%
Myeloma-overexpressed gene 2 protein homolog	Myeov2	2.0E-06	2428%
Isoform 2 of Cyclin-dependent kinase 13 O	Cdk13	4.3E-06	2248%
D-2-hydroxyglutarate dehydrogenase, mitochondrial	D2hgdh	1.2E-05	2536%
BAG family molecular chaperone regulator 5	Bag5	2.0E-05	21%
Apolipoprotein A-II	Apoa2	2.7E-05	275%
Protein 0610011F06Rik	0610011F06Rik	2.8E-05	2521%
Peroxiredoxin 6	Prdx6	4.3E-05	-2806%
Syntaxin-16	Stx16	5.0E-05	33%
Prosaposin receptor	Gpr37l1	9.4E-05	-2704%
Pyridoxine-5-phosphate oxidase	Pnpo	1.1E-04	65%
Guanine nucleotide-binding protein-like 1	Gnl1	1.5E-04	21%
Ester hydrolase C11orf54 homolog	c11orf54	1.5E-04	48%
Protein MEMO1	Memo1	1.8E-04	2385%
Apolipoprotein C-III	Apoc3	2.1E-04	2368%
Murinoglobulin-1	Mug1	2.4E-04	187%
Isoform 2 of Protein NDRG2	Ndrg2	2.6E-04	-34%
Adenylate cyclase type 3	Adcy3	2.9E-04	2360%
Complement C1q subcomponent subunit C	C1qc	3.2E-04	-34%
Sodium/potassium-transporting ATPase subunit beta-3	Atp1b3	3.2E-04	28%
Protein 2010107G23Rik (Fragment)	2010107G23Rik	3.2E-04	2410%
ER membrane protein complex subunit 4	Emc4	3.5E-04	-2370%

Table I-3. Differentially Expressed Proteins in Brain of Mice Lacking GPR37 and GPR37L1 contd.

Protein Name	Gene Name	p-value	% Change (DKO/WT)
TBC1 domain family member 23	Tbc1d23	3.8E-04	2347%
Myelin-associated glycoprotein	Mag	4.2E-04	-69%
Protein FAM45A	Fam45a	5.3E-04	2346%
Disco-interacting protein 2 homolog A	Dip2a	6.1E-04	20%
Isoform 2 of Histone-lysine N-methyltransferase SETD1B	Setd1b	6.5E-04	-2432%
Apolipoprotein A-I	Apoa1	7.4E-04	82%
Protein Gm5901	Gm5901	8.5E-04	2485%
Transducin beta-like protein 2	Tbl2	8.8E-04	2382%
Abhydrolase domain-containing protein 4	Abhd4	9.2E-04	-2406%
Quinone oxidoreductase	Cryz	9.6E-04	-44%
Catenin alpha-3	Ctnna3	1.0E-03	54%
Parathymosin	Ptms	1.1E-03	21%
Ribonuclease UK114	Hrsp12	1.1E-03	-53%
Isoform 2 of Peroxisomal acyl-coenzyme A oxidase 1	Acox1	1.1E-03	-32%
Cystatin-C	Cst3	1.1E-03	-46%
Lon protease homolog, mitochondrial	Lonp1	1.2E-03	-30%
Inositol polyphosphate 1-phosphatase	Inpp1	1.2E-03	21%
D-beta-hydroxybutyrate dehydrogenase, mitochondrial	Bdh1	1.2E-03	18%
Synapse-associated protein 1	Syap1	1.3E-03	2359%
Creatine kinase U-type, mitochondrial	Ckmt1	1.3E-03	21%
Glycerol-3-phosphate dehydrogenase, mitochondrial	Gpd2	1.3E-03	-10%

Table I-3. Differentially Expressed Proteins in Brain of Mice Lacking GPR37 and GPR37L1 contd.

Protein Name	Gene Name	p-value	% Change (DKO/WT)
Isoform 2 of Nitrilase homolog 1	Nit1	1.3E-03	-40%
Alpha-1-antitrypsin 1-4	Serpina1d	1.4E-03	63%
39S ribosomal protein L12, mitochondrial	Mrpl12	1.4E-03	73%
Secernin-3	Scrn3	1.6E-03	-16%
Contactin-associated protein-like 2	Cntnap2	1.7E-03	7%
5-AMP-activated protein kinase subunit beta-2	Prkab2	1.8E-03	29%
Inactive dipeptidyl peptidase 10	Dpp10	1.8E-03	-46%
Quinone oxidoreductase-like protein 2	BC026585	2.1E-03	-29%
3-hydroxyisobutyryl-CoA hydrolase, mitochondrial	Hibch	2.2E-03	-16%
Fumarylacetoacetate hydrolase domain-containing protein 2A	Fahd2	2.3E-03	17%
Gap junction alpha-1 protein	Gja1	2.4E-03	-22%
2,4-dienoyl-CoA reductase, mitochondrial	Decr1	2.4E-03	-28%
Unconventional myosin-Va	Myo5a	2.4E-03	-12%
Dual specificity protein phosphatase 3	Dusp3	2.5E-03	26%
Vacuolar protein sorting-associated protein 33B	Vps33b	2.5E-03	81%
Proteasome subunit alpha type-5	Psma5	2.5E-03	-8%
Extended synaptotagmin-1	Esyt1	2.5E-03	32%
Electron transfer flavoprotein subunit alpha, mitochondrial	Etfa	2.5E-03	-22%
Enoyl-CoA hydratase, mitochondrial	Echs1	2.8E-03	18%
Protein bassoon	Bsn	3.0E-03	8%

Table I-3. Differentially Expressed Proteins in Brain of Mice Lacking GPR37 and GPR37L1 contd.

Protein Name	Gene Name	p-value	% Change (DKO/WT)
Type I inositol 3,4-bisphosphate 4-phosphatase	Inpp4a	3.1E-03	11%
Ectonucleotide pyrophosphatase/phosphodiesterase family member 6	Enpp6	3.1E-03	31%
Proton myo-inositol cotransporter	Slc2a13	3.2E-03	37%
Putative transferase CAF17 homolog, mitochondrial	Iba57	3.2E-03	-33%
Ubiquitin-conjugating enzyme E2 N	Ube2n	3.2E-03	-18%
Aldehyde dehydrogenase, mitochondrial	Aldh2	3.3E-03	-25%
Ras-related protein Rab-2A	Rab2a	3.3E-03	26%
5(3)-deoxyribonucleotidase, cytosolic type	Nt5c	3.3E-03	43%
Small integral membrane protein 1 (Fragment)	Smim1	3.5E-03	38%
cAMP-dependent protein kinase type II-beta regulatory subunit	Prkar2b	3.5E-03	7%
Stress-induced-phosphoprotein 1	Stip1	3.5E-03	-5%
4-trimethylaminobutyraldehyde dehydrogenase	Aldh9a1	3.6E-03	-31%
Amine oxidase [flavin-containing] B	Maob	3.6E-03	-31%
Aspartate--tRNA ligase, cytoplasmic	Dars	3.6E-03	-48%
Hematological and neurological expressed 1 protein	Hn1	3.6E-03	39%
Ganglioside-induced differentiation-associated protein 1-like 1	Gdap1l1	3.8E-03	28%
Tropomyosin alpha-4 chain	Tpm4	4.0E-03	28%

Table I-3. Differentially Expressed Proteins in Brain of Mice Lacking GPR37 and GPR37L1 contd.

Protein Name	Gene Name	p-value	% Change (DKO/WT)
Elongation factor 1-alpha 2	Eef1a2	4.0E-03	10%
Leucine-rich repeat-containing protein 27	Lrrc27	4.1E-03	-2488%
Sideroflexin-5	Sfxn5	4.3E-03	-31%
Glycogen phosphorylase, muscle form	Pygm	4.4E-03	16%
Protein NipSnap homolog 1	Nipsnap1	4.5E-03	24%
High mobility group protein B3 (Fragment)	Hmgb3	4.7E-03	-53%
N(G),N(G)-dimethylarginine dimethylaminohydrolase 1	Ddah1	4.7E-03	-13%
Isoform 2 of PH and SEC7 domain-containing protein 2	Psd2	5.1E-03	2405%
Calnexin	Canx	5.2E-03	18%
Syntaxin-1B	Stx1b	5.3E-03	-8%
Transgelin-2	Tagln2	5.3E-03	38%
NCK associated protein 1 like	Nckap1l	5.4E-03	2324%
Ubiquitin-conjugating enzyme E2 L3	Ube2l3	5.4E-03	12%
Isoform 2 of Prolyl endopeptidase-like	Prepl	5.4E-03	16%
Glutamate--cysteine ligase regulatory subunit	Gclm	5.6E-03	-16%
NADH-ubiquinone oxidoreductase 75 kDa subunit, mitochondrial	Ndufs1	5.6E-03	-8%
DnaJ homolog subfamily C member 17	Dnajc17	5.7E-03	2252%
Heat shock 70 kDa protein 4L	Hspa4l	5.9E-03	9%
WASH complex subunit 7	Kiaa1033	6.0E-03	56%
Isovaleryl-CoA dehydrogenase, mitochondrial	Ivd	6.1E-03	-27%

Table I-3. Differentially Expressed Proteins in Brain of Mice Lacking GPR37 and GPR37L1 contd.

Protein Name	Gene Name	p-value	% Change (DKO/WT)
Microtubule-associated protein RP/EB family member 2	Mapre2	6.1E-03	6%
Abhydrolase domain-containing protein 16A	Abhd16a	6.3E-03	-22%
CD200 antigen	Cd200	6.4E-03	-28%
Acyl-coenzyme A thioesterase 9, mitochondrial	Acot9	6.4E-03	-16%
26S proteasome non-ATPase regulatory subunit 4	Psmd4	6.4E-03	2341%
Bifunctional epoxide hydrolase 2	phx2	6.6E-03	-31%
Phosphatidylinositide phosphatase SAC1	Sacm1l	6.6E-03	-22%
Cytochrome c oxidase subunit 6A1, mitochondrial	Cox6a1	6.6E-03	-16%
Protein Ighg2b (Fragment)	Ighg2b	6.7E-03	315%
Peroxiredoxin-1	Prdx1	6.7E-03	-17%
Guanine nucleotide-binding protein G(i) subunit alpha-2	Gnai2	6.8E-03	-9%
Androgen-induced gene 1 protein	Aig1	7.0E-03	346%
Olfactory marker protein	Omp	7.0E-03	-215%
Histidine triad nucleotide-binding protein 2, mitochondrial	Hint2	7.0E-03	-44%
Neurocan core protein	Ncan	7.0E-03	-20%
NADH dehydrogenase [ubiquinone] 1 beta subcomplex subunit 5, mitochondrial	Ndufb5	7.0E-03	-21%

Table I-3. Differentially Expressed Proteins in Brain of Mice Lacking GPR37 and GPR37L1 contd.

Protein Name	Gene Name	p-value	% Change (DKO/WT)
ELKS/Rab6-interacting/CAST family member 1	Erc1	7.1E-03	21%
Protein flightless-1 homolog	Flii	7.2E-03	60%
Hyaluronan and proteoglycan link protein 4	Hapln4	7.2E-03	-30%
Perilipin-3	Plin3	7.3E-03	-41%
Mitochondrial carnitine/acylcarnitine carrier protein	Slc25a20	7.3E-03	-27%
Hydroxymethylglutaryl-CoA synthase, cytoplasmic	Hmgcs1	7.4E-03	-42%
Bromodomain and WD repeat domain containing 2, isoform CRA_a	Wdr11	7.6E-03	-23%
Thioredoxin-like protein 1	Txnl1	7.9E-03	22%
Plexin-C1	Plxnc1	8.0E-03	-125%
Mitogen-activated protein kinase 1	Mapk1	8.1E-03	-5%
Thioredoxin-dependent peroxide reductase, mitochondrial	Prdx3	8.5E-03	25%
Adenosine kinase	Adk	8.5E-03	-4%
Dynamin-3	Dnm3	8.6E-03	-15%
Glutamate receptor 3	Gria3	8.6E-03	20%
Alpha-centractin	Actr1a	8.6E-03	9%
Galectin-1	Lgals1	8.7E-03	-21%
Nucleosome assembly protein 1-like 1	Nap1l1	8.7E-03	22%
Isoform 2 of Elongator complex protein 3	Elp3	8.9E-03	41%
Rho guanine nucleotide exchange factor 9	Arhgef9	8.9E-03	-23%
Vesicle-fusing ATPase	Nsf	9.1E-03	7%

Table I-3. Differentially Expressed Proteins in Brain of Mice Lacking GPR37 and GPR37L1 contd.

Protein Name	Gene Name	p-value	% Change (DKO/WT)
Methylmalonate-semialdehyde dehydrogenase [acylating], mitochondrial	Aldh6a1	9.1E-03	-14%
Transthyretin	Ttr	9.2E-03	49%
Heat shock 70 kDa protein 4	Hspa4	9.4E-03	-9%
GDP-Man:Man(3)GlcNAc(2)-PP-Dol alpha-1,2-mannosyltransferase	Alg11	9.4E-03	-40%
Isoform A of Fragile X mental retardation syndrome-related protein 1	Fxr1	9.5E-03	31%
14 kDa phosphohistidine phosphatase	Phpt1	9.6E-03	20%
Isoform 2 of Calcium/calmodulin-dependent protein kinase type II subunit gamma	Camk2g;	9.6E-03	14%
Mycophenolic acid acyl-glucuronide esterase, mitochondrial	Abhd10	9.7E-03	-28%
Mitochondrial 2-oxoglutarate/malate carrier protein	Slc25a11	9.8E-03	-9%
Small nuclear ribonucleoprotein Sm D1	Snrpd1	9.9E-03	18%

Table I-3. Differentially Expressed Proteins in Brain of Mice Lacking GPR37 and GPR37L1

Proteins significantly up or down regulated in double knockout (DKO) mice lacking GPR37 and GPR37L1 compared with wild-type (WT) aged matched controls as identified with mass spectrometry. Specific protein interactions were determined as having a p value of ≤ 0.01.

Section I.4 Conclusions and Discussion

The studies described in this chapter have provided several interesting avenues for further study. However, it is important to acknowledge that this proteomic approach is limited, protein interactions are dynamic and change in respect to location, time and cellular context. This is evidenced by the fact that a number of established interaction partners of GPR37 and GPR37L1 were not observed in our studies. For example, both GPR37 and GPR37L1 contain a consensus PDZ binding motif (G-T-X-C) at their extreme C-terminus (Dunham et al. 2009) and have been reported to interact with syntenin-1 (Dunham et al. 2009; Dutta et al. 2014), multi-PDZ domain protein 1 (MUPP1) (Tanabe et al. 2015), protein interacting with C-kinase (PICK1) and GRIP4/5 (Dutta et al. 2014). In addition to association with PDZ containing proteins, GPR37 and GPR37L1 have been shown to physically interact with the dopamine transporter (DAT) and dopaminergic receptors, D1 and D2 (Dunham et al. 2009; Meyer 2014; Marazziti et al. 2007). It is possible that these interactions do not occur *in vivo* or that they are limited to a small subset of cells, for example interactions with DAT occurring in a subset of dopaminergic neurons, and thus not robust enough to emerge as significant within our stringent parameters. Therefore, while the results in this chapter provide exciting new avenues for future studies, the data are by no means a complete description of interaction partners for GPR37 and GPR37L1. Future studies will be required to elucidate the relevance of the proteins identified in our analyses.